Genetic Etiology and Clinical Consequences of Cone Disorders

Alberta Thiadens

ACKNOWLEDGMENTS

Cover: Alberta Thiadens
Red cone: Devaraju Market in Mysore, India, 2002
Green cone: A castle garden in Reims, France, 2010
Blue cone: Reinier in Consthum, Luxembourg, 2011

Genetic Etiology and Clinical Consequences of Cone Disorders

Genetische oorzaken en klinische gevolgen van kegelaandoeningen

PROEFSCHRIFT

ter verkrijging van de graad van doctor aan de
Erasmus Universiteit Rotterdam
op gezag van de
rector magnificus

Prof.dr. H.G. Schmidt

en volgens besluit van het College voor Promoties.
De openbare verdediging zal plaatsvinden op

woensdag 18 mei 2011 om 15.30 uur

door

Alberta Aaffina Huberta Johanna Thiadens
geboren te Utrecht

ERASMUS UNIVERSITEIT ROTTERDAM

PROMOTIECOMMISSIE

In herinnering aan mijn ouders, Ab Thiadens en Aafje Goedings

Voor Josephine & Reinier

CONTENTS

PUBLICATIONS AND MANUSCRIPTS ON WHICH THIS THESIS IS BASED

1. **Thiadens AA**, Hoyng CB, Simonsz HJ, Polling J, Bernaerts-Biskop R, van den Born LI, Klaver CCW. Accuracy of four commonly used color vision tests in individuals with cone disorders. (*Under review*)

2. **Thiadens AA**, Slingerland NWR, Roosing S, van Schooneveld MJ, van Lith-Verhoeven JJC, van Moll-Ramirez N, van den Born LI, Hoyng CB, Cremers FPM, Klaver CCW. Genetic etiology and clinical consequences of complete and incomplete achroma-topsia. *Ophthalmology 2009;116:1984-9.*

3. **Thiadens AA**, Somervuo V, van den Born LI, Roosing S, van Schooneveld MJ, Kuijpers RWAM, van Moll-Ramirez N, Cremers FPM, Hoyng CB, Klaver CCW. Progressive cone cell loss in achromatopsia. An imaging study using Spectral-Domain Optical Coher-ence Tomography. *Invest Ophthalmol Vis Sci. 2010;51:5952-7.*

4. **Thiadens AA**, Roosing S, Collin RWJ, van Moll-Ramirez N, van Lith Verhoeven JJC, van Schooneveld MJ, den Hollander AI, van den Born LI, Hoyng CB, Cremers FPM, Klaver CCW. Comprehensive analysis of the achromatopsia genes *CNGA3* and *CNGB3* in progressive cone dystrophy. *Ophthalmology 2010;117:825-30.*

5. **Thiadens AA**, den Hollander AI, Roosing S, Nabuurs SB, Zekveld-Vroon R, Collin RWJ, de Baere E, Koenekoop RK, van Schooneveld MJ, Strom TM, van Lith-Verhoeven JJC, Lotery AJ, van Moll-Ramirez N, Leroy BP, van den Born LI, Hoyng CB, Cremers FPM, Klaver CCW. Homozygosity mapping reveals *PDE6C* mutations in patients with early-onset cone photoreceptor disorders. *Am J Hum Genet. 2009;85:240-7.*

6. **Thiadens AA**, Soerjoesing GG, Florijn RJ, Tjiam AG, ten Brink JB, Buitendijk GHS, den Hollander AI, Bergen AAB, Klaver CCW. Clinical course of cone dystrophy caused by mutations in the *RPGR* gene. *(Under review)*

7. **Thiadens AA**, Phan TML, Zekveld-Vroon RC, Roosing S, Pott JR, van Schooneveld MJ, Lotery AJ, van Moll-Ramirez N, van Genderen MM, Boon CJF, den Hollander AI, Bergen AAB, de Baere E, Cremers FPM, van den Born LI, Leroy BP, Hoyng CB, Klaver CCW. Clinical course, etiology, and visual outcome in cone and cone-rod dystrophy. (*Under review*)

8. **Thiadens AA**, Slingerland NWR, Polling J, Visser GH, Klaver CCW. Cone-rod dystrophy can be a manifestation of Danon disease. (*Accepted*)

9. **Thiadens AA**, Klaver CCW. Genetic testing and clinical characterization of patients with cone-rod dystrophy. *Invest Ophthalmol Vis Sci. 2010;51:6904-5.*

* This publication is not part of the manuscript, but has been referred to in the General Discussion.
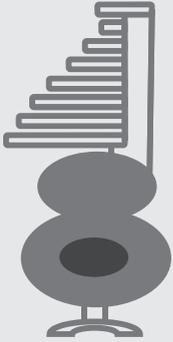
General Introduction

GENERAL INTRODUCTION

Cones give color to a person's life. The retina contains 3-6 million of these photoreceptor cells, enabling one to see details, to read, to recognize faces, and to, indeed, see colors. Cone photoreceptor cells account for only 5% of the total number of photoreceptors; the other 95% consists of rods. The fovea contains no rods but only cones and supporting Müller cells. Rods and cones can be distinguished by shape, type of photopigment, light sensitivity, retinal distribution, and synaptic connections. These characteristics are required for their specialization in different aspects of vision. Cone cells have a low sensitivity and a high spatial resolution, which make them particularly suitable for visual acuity and color discrimination. Rod cells are extremely sensitive to light with a low spatial resolution and thus are more appropriate for mesopic light conditions. Cones and rods differ in their visual pigment (red, green and blue opsins versus rhodopsin) and in their spatial arrangement. Each rod bipolar cell receives input from a number of rods, while each cone bipolar cell is connected with only one cone. The one-to-one relationship enhances signal transduction and resolution of the image. A rod produces a reliable response to a single photon of light, whereas more than 100 photons are required to produce a comparable response in a cone. Morphologically, the largest difference is the structure of the outer segments; rods segments are long, thin, and have a cylindrical shape, while cones have shorter segments with a conical shape. The rod outer segment contains a stack of discs which are separated from the plasma membrane. Cone cells

Table 1. Comparison of cone and rod photoreceptor properties of the human retina.

Features	Cones	Rods
Total number in the retina (N)	3-6 million	120 million
Visual pigment	Red, green and blue opsin	Rhodopsin
Localization and density (mm^2)	Fovea: 150.000	Periphery: 30.000
Contact with Müller cell	Fovea 1:1	>1 rods:1
Contact with bipolar cell	1:1	50-100:1
Photons needed for depolarization (N)	>100	1
Spatial resolution	High	Low
Vitamin A recycling	In Müller cells and RPE	In the RPE
Discs	Open and attached to cell membrane	Closed and not attached to cell membrane
Open discs (N)	>15	5-7
ERG A-wave (max. nm)	360	500
OS length mice (μm)	13.4 (SD 0.7)	23.6 (SD 0.7)
OS width mice (μm)	1.2 (SD 0.03)	1.4 (SD 1.4)
OS volume mice (μm^3)	14	36

do not have these discrete discs; their outer segment plasma membrane is highly invaginated, and is continuously connected to the membrane of the cilium. This results in a greater cone outer segment surface area, and a faster exchange of proteins.[1,2] The most important function of rod and cone outer segments is the conversion of light into an electrical signal. A cell layer which supports this process is the retinal pigment epithelium (RPE). In rods, discs are constantly removed and renewed by the RPE, but how exchange of membrane material works in cones is still unclear.[1,2,3] (Table 1). Although the above illustrates the many morphological and functional differences between rods and cones, a large overlap exists at the biochemical level (Figure 1).
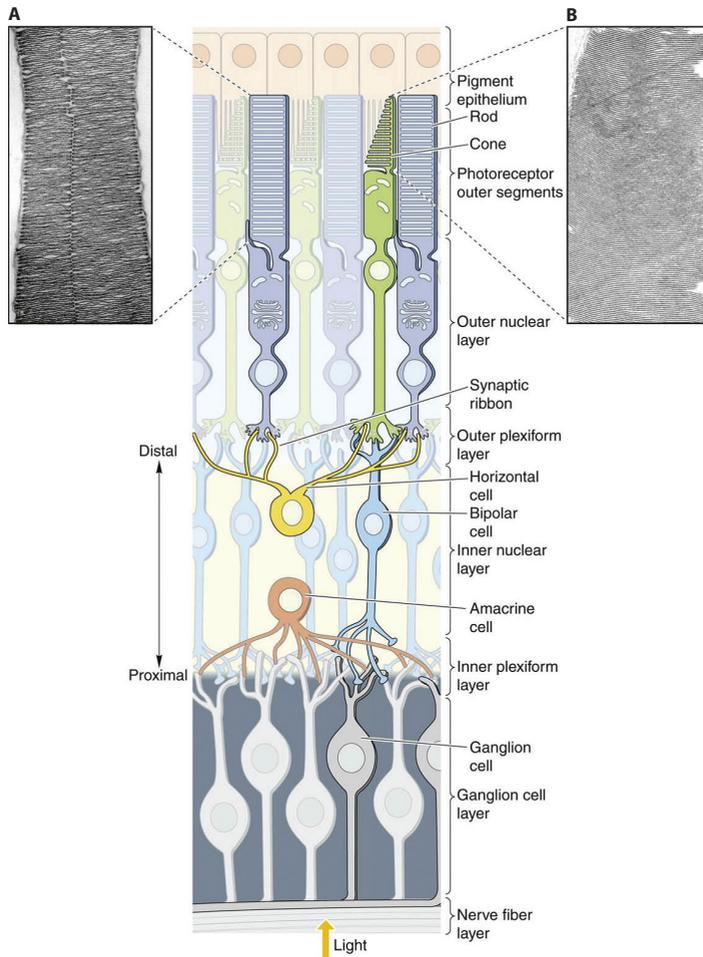
Figure 1. Differences in photoreceptors and their arrangement in the retina. Rod (A) and cone (B) photoreceptors are displayed in a cross-sectional depiction of the retina also showing connections of these photoreceptors to the retinal pigment epithelium and inner nuclear layer. Electron microscopic images show rod and cone outer segments. *(Figure derived from Mustafi, 2009 and published with permission)*

Cone cell function

Phototransduction cascade - Phototransduction is the process of conversing light into an electric neural signal, which takes place in the outer segments of photoreceptors, and is translated in the visual cortex of the brain. The photo-capturing molecule in photoreceptors is the visual pigment, which consists of light-sensing chromophore 11-cis-retinal attached to an opsin protein. The first step in the phototransduction cascade is the activation of opsin by a photon, which induces the isomerization of 11-cis-retinal to all-trans-retinal, and a subsequent conformational change in the structure of the opsin protein molecule.[4,5] This change allows the opsin to bind to transducin, thereby activating the α-subunit which then dissociates to activate phosphodiesterase (PDE). The activated α- and β-subunits of PDE hydrolyze cyclic guanosine monophosphate (cGMP) to 5'-GMP. In daylight, this results in the closure of the cGMP gated ion channel (or CNG-channel) in the cone outer segment membrane, and hyperpolarization of the cell. Accordingly, this induces inhibition of the release of neurotransmitters at the synaptic terminal of the photoreceptor cell, leading to a stimulus for the adjacent neurons.[6] In the dark, the CNG-channels are open, allowing free influx of Na^+ and Ca^{2+} ions (Figure 2).

Figure 2. Schematic overview of the activation and recovery of the phototransduction cascade. *(Figure designed by and published with permission of B.P. Leroy)*

Visual cycle - The process of recycling the chromophore all-trans-retinal to 11-cis-retinal, required for the phototransduction, is known as the visual cycle. All-trans retinal dissociates from the opsin into the discs of the outer segment, and is transferred to the cytoplasmic space by the ABCA4 protein in the disc membrane. In all photoreceptors, all-trans-retinal is then converted to all-trans-retinol (i.e. vitamin A), and taken up by the RPE cell. In the RPE cells, vitamin A is converted to all-cis-retinal and transferred back to the photoreceptors to rejoin the phototransduction cascade.[7] Cones function under light conditions and require a more rapid supply of recycled vitamin A than rods. Mata et al. discovered in the cone-dominated retinae of chickens and ground squirrels a second, independent cone visual cycle that takes place in the retinal Müller cells[8-10] (Figure 3). The ratio of cones and Müller cells in the fovea is 1:1, which helps to facilitate a quick recycling of vitamin A.

Figure 3. Schematic representation of the cone visual cycle. The cone visual cycle takes place in the outer segments, retinal pigment epithelium and Müller cells.
'Sun' symbol: photon; RAL: retinal; RDH: retinol dehydrogenase; RE: retinyl ester; REH: retinyl ester hydrolase; ROL: retinol; palm CoA: palmitoyl coenzyme A. Proteins are presented in grey and are encoded by the following genes (in italic). 11-cis RDH: *RDH5.* All-trans RDH: *RDH12.* CRALP: *RLBP1.* IRBP*: IRBP. (Figure designed by and published with permission of K.W. Littink)*

Testing of cone function

The gold standard for the diagnosis of cone disorders is based on the electro- and psychophysical evidence of cone dysfunction, and is tested by full-field electroretinogram (ERG) and color vision testing. Age of onset, presence or absence of a nystagmus, visual course, family history, and macular appearance are other important clues to diagnose these patients. A kinetic visual field measurement (e.g. by Goldmann perimetry) complements the test results.

Color vision testing - The human retina contains three cone types: red (protan), green (deutan) and blue (tritan) cones which are distinguished mainly by the portion of the visible spectrum to which each is maximally sensitive. The red cones are most sensi-

tive to low-frequency photons (555–565 nm), the green cones to middle-frequencies (530–537 nm), and the blue cones to high-frequencies (415–430 nm). Mixing the three primary colors will produce any secondary color or hue. The genes coding for the red and green cone opsins lie in tandem array on the X-chromosome, and there are one to six copies of the red and green opsins. Color blindness (protan- and deutanomaly) with normal visual acuity is caused by unequal crossing over between the red and green opsins. This condition occurs in 5-8% of males and in 0.5% of females. The gene encoding the blue cone opsin is located on chromosome 7.[11,12] Blue cones constitute only about 5% of the total cone population; they are absent in the fovea and located only in the peripheral part of the retina.[3] In contrast to X-linked (XL) color blindness, patients with cone disorders have defects in all three color axes.

In 1913, a committee was established to create a reference system for designers of color vision tests (Committee Internationale de l'Eclairage, CIE). This committee designed a color spaced chromaticity diagram, which shows the spectrum of colors from 400 nm (purple) to 700 nm (red) for individuals with normal color vision. Color test designers used the information on color space, and lines of confusion within this space, to design tests that identified color deficiencies. A variety of color vision tests currently exists in clinical practice. Tests can be subdivided into four main categories based on their design: the pseudoisochromatic plates (eg. Ishihara, and Hardy-Rand-Rittler test), arrangements tests (eg. Panel-D15, FM 100-Hue test), anomaloscopes (eg. Nagel), and lanterns. All tests are designed for specific purposes, and each has its own advantages; however, which test best identifies cone disorders is as yet unknown.[13]

ERG - A full-field ERG measures a mass electrical response of action potentials produced by all photoreceptors when stimulated by illumination. The ERG can be executed in light-adapted (photopic) as well as dark-adapted (scotopic) conditions. Photopic measurements represent exclusively cone responses, while scotopic measurements represent either isolated rod responses or a mixed rod-cone response. A normal ERG consists of an A-wave and a B-wave. The negative A-wave is caused by hyperpolarization of the photoreceptors. The positive B- wave results from activity of bipolar cells, the inner plexiform layer, and the Müller cells. The amplitude and latency of these waves changes with stimulus intensity. The International Society for Clinical Electrophysiology of Vision (ISCEV) has developed standard protocols for the performance of ERGs. In this thesis, we performed all ERGs according to this protocol (www.iscev.org).[14-16]

Classification of cone disorders

Hereditary photoreceptor disorders form a large heterogeneous group in which the cones and/or the rods are affected. In this thesis, we focused on the most common cone

disorders, i.e. achromatopsia (ACHM), cone dystrophy (CD), and cone-rod dystrophy (CRD). Other, rare cone disorders include blue cone monochromacy (BCM), oligocone trichromacy and Bornholm eye disease.[17] The clinical presentation of all cone disorders will be discussed in more detail below.

Achromatopsia - ACHM is a congenital cone photoreceptor disorder with an estimated prevalence of 1:40,000 individuals. Patients present shortly after birth with severe photophobia, a pendular nystagmus, color vision defects, and a low Snellen visual acuity of ~0.10. High refractive errors are common in these patients. The macula can have a variable appearance ranging from no abnormalities to atrophic lesions. ERG shows absent or residual cone responses with normal rod responses. The inheritance pattern is autosomal recessive, and the literature up to 2008 reported three genes to be involved in this disease, *CNGA3, CNGB3*, and *GNAT2*, explaining ~70% of the genetic etiology.[18-20]

Oligocone trichromacy - This disease is a rare condition which was first described in 1973. It is characterized by a reduced visual acuity, nearly normal color vision, and reduced cone responses on multifocal ERG. It was proposed that these patients have a reduced number of central cones. Genetically, there is considerable overlap with ACHM, as mutations in the *GNAT2, CNGB3,* and *CNGA3* genes have also been associated with this form of cone dysfunction.[21-23]

Blue cone monochromacy - While ACHM affects all three cone types, BCM is a congenital XL disease that affects only the red and green cones, leaving the blue cones intact. Its prevalence is 1:100,000 individuals, and patients have the same presentation as ACHM patients: photophobia, nystagmus, severe color vision disturbances, and a low visual acuity of ~0.10. To distinguish BCM from ACHM, it is necessary to use color vision tests that test for the blue axis, for instance the Berson plates.[24] The disease is characterized by absence of red and green cone opsins, which are located on the X-chromosome. Transcription of these genes is regulated by a region called the locus control region (LCR). Almost 40% of BCM can be explained by mutations in this region.[17,25]

Bornholm eye disease - This XL disease has been reported in a large Danish family originating from the Danish island Bornholm. In that family, the disease was characterized by a low visual acuity, a reduced photopic ERG, moderate to high myopia, and deuteropia. Linkage analysis mapped the defect to the red and green opsin gene array, suggesting overlap with congenital color blindness (deuteropia).[26,27]

Cone dystrophy - CD is a progressive cone disorder with an estimated prevalence of 1:30,000-40,000. All Mendelian inheritance patterns are observed. Patients have normal

cone function initially, but present with visual loss and color vision disturbances in the first or second decade. Macular abnormalities can be present, ranging from no abnormalities to a bull's eye maculopathy or RPE atrophy; the optic nerve may show a variable degree of temporal pallor. Goldmann perimetry shows a reduced central sensitivity or (relative) scotoma with intact peripheral fields. ERG exhibits progressively deteriorating cone responses, with normal rod responses, at least in early stages. Although the course of disease may vary, the visual acuity generally worsens to legal blindness before 50 years of age. The current knowledge on genes that cause CD is scarce; several genes have been identified for the autosomal dominant (AD)[28-30] and XL forms[31,32] but little is known about the genetic causes of the most prevalent autosomal recessive (AR) form. Until now, four genes and some additional loci have been implicated in this form (*ABCA4, KCNV2, CNGB3, CACNA2D4*)[33-37] These genes explain only a minority of all patients.

Cone-rod dystrophy - CRD can be distinguished from CD by early rod involvement or concomitant loss of both cones and rods. The prevalence of the disease is 1:30,000-40,000 and can be inherited in an AR, AD, or XL manner. Symptoms resemble those of CD, but patients may also experience nyctalopia due to rod involvement. Macular and peripheral abnormalities can be observed, with a variable degree of vascular attenuation and peripheral intraretinal pigment deposits. Goldmann perimetry shows a (relative) central scotoma with a variable degree of peripheral involvement. The ERG shows reduced cone and rod responses, with the cone responses the more severely affected. The course of the disease is more severe than CD, and may lead to legal blindness at a younger age. Currently, ~17 genes and some additional loci are known to be involved in CRD.[38-40] Of all these genes, the *ABCA4* gene is the most prevalent causative gene for AR-CRD in the literature (24-65%).[41-48] CD and CRD can be part of a syndrome like Bardet-Biedl syndrome, spinocerebellar ataxia type 2, or amelogenesis imperfecta.[39]

Incentives

Retinal disorders affect approximately 1 in 2,000 individuals, which equal more than two million people worldwide, and account for ~5% of legal blindness.[38] Although the contribution of cone disorders is limited, they have a great impact on the individual and on society, as the blindness is lifelong and currently irreversible.[49] The consequences on daily life for patients with cone disorders are tremendous. These patients who have only scotopic responses need to survive in a world which is dominated by photopic triggers. Currently, little is known about the causes of cone disorders and therapeutic options are not available. This calls for thorough investigations into the etiology and consequences of this devastating disease.

Scope of this thesis

Main goals for this thesis were to unravel the genetic etiology of cone disorders and to investigate the clinical course.

Setting

This research was imbedded in a multicenter study including the Department of Oph-thalmology at the Erasmus Medical Center in Rotterdam, the Departments of Human Genetics and Ophthalmology at the Radboud University Nijmegen Medical Center, the Rotterdam Eye Hospital, the University Medical Center Utrecht, the Netherlands Institute for Neuroscience in Amsterdam, the Royal Dutch Visio, Center of Expertise for blind and partially sighted people, in Grave, the University Medical Center Groningen, Bartiméus Institute for the Visually Impaired in Zeist, the University Hospital of Ghent (Belgium), the University of Southampton (United Kingdom), and McGill University Health Center, Montreal (Canada).

This work is stratified into four sections:

Chapter 1   **Diagnostic challenges in cone disorders**
Chapter 2   **Achromatopsia**
Chapter 3   **Cone and Cone-rod dystrophy**
Chapter 4   **Cone disorders as part of a syndrome**
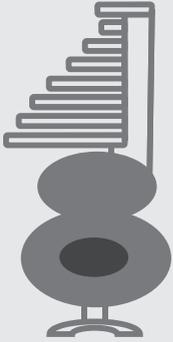
Chapter 1

Diagnostic challenges in cone disorders
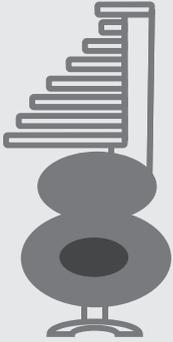
Chapter 1a

Accuracy of four commonly used color vision tests in individuals with cone disorders

ABSTRACT

Purpose: To determine which color vision tests are most appropriate for the identification of cone disorders.

Methods: Patients with cone dystrophy (N=37) were compared to controls with normal visual acuity (N=35), and to controls with low vision (N=39). We evaluated the specificity, sensitivity, positive predictive value and discriminative accuracy of four different commonly used color vision tests: Ishihara and Hardy-Rand-Rittler pseudoisochromatic tests (HRR), (de)saturated Panel-D15 tests and the Nagel anomaloscope.

Results: All tests had a better discriminative accuracy when cone disorders were compared to controls with normal vision than to controls with low vision. For the latter, the discriminative accuracy was highest for the HRR test (c-statistic for protan-deutan (PD) axes 0.900; for tritan (T) axis 0.766), followed by the Panel D-15 desaturated test (c-statistic for PD axes 0.880, for T axis 0.500) and Ishihara test (c-statistic 0.886), the Nagel anomaloscope (c-statistic 0.860) and the saturated Panel D-15 test (c-statistic for PD axes 0.756; for T axis 0.516). For legally blind patients, discriminative accuracies of all tests remained stable.

Conclusions: The HRR and the desaturated Panel D-15 tests are most appropriate for the identification of cone disorders since these tests have a high discriminative accuracy, allow evaluation of all three color axes, and quantification of the color defects. Visual acuity did not affect the discriminative accuracy of these tests.

INTRODUCTION

Cone disorders are a group of hereditary retinal disorders in which the cones are primarily affected. Cone disorders can be subdivided into achromatopsia (ACHM), progressive cone dystrophy (CD) and cone-rod dystrophy (CRD).[1-3] Typical symptoms of cone disorders are poor visual acuity, photophobia, and severe color vision disturbances. Standard ophthalmologic examination can reveal macular changes such as RPE alterations or a bull's eye maculopathy, and a temporal pallor of the optic disc. However, often no retinal abnormalities are observed, making cone disorders difficult to identify. To make a definite diagnosis, it is essential to perform a full-field electroretinogram (ERG). Patients with cone disorder will show reduced or absent cone responses with normal or diminished rod responses. The execution of an ERG requires specifically trained personnel, is rather time-consuming, and often requires an extra visit for the patient. To optimize the selection of patients who must undergo the ERG, it would be helpful to perform a simple and quick psychophysical test to identify patients most likely to have a cone disorder.

All patients with cone disorders present with disturbances in the three color axes protan, deutan and tritan (red, green, and blue, respectively). Testing for color vision is generally conceived as easy and agreeable. In a general ophthalmologic practice, the commonly utilized and easy accessible color vision tests are the pseudoisochromatic color vision tests Hardy-Rand-Rittler (HRR) and Ishihara's test, arrangement tests such as the (de) saturated Lanthony or Farnsworth D-15 hue discrimination test or FM 100 hue test, or the anomaloscope (Nagel). In practice, clinicians use any of these tests to evaluate color vision. Their reliability has been investigated in subjects with low vision,[4] however, performance in patients with primary cone disorders has never been investigated.

The purpose of this study was to determine which test is most suitable as a first step to diagnose cone disorders in a general clinical setting. We first compared cone disorder patients to controls with normal vision. Subsequently, we made a comparison with controls having low vision since they more closely resemble cone disorder patients. We evaluated the discriminative accuracy of the HRR, Ishihara, Panel D-15, and Nagel anomaloscope.

MATERIAL AND METHODS

Study Population
All persons were ascertained from Erasmus Medical Center in Rotterdam, the Rotterdam Eye Hospital, and the University Medical Center Nijmegen St Radboud. We included 37

patients with cone disorders (mean age 32 years, 24 male). Criteria for the diagnosis cone disorder were poor visual acuity (Snellen visual acuity < 0.50), color vision disturbances, (relative) central scotoma, and significantly reduced or absent cone responses with normal or diminished rod responses on a full-field ERG. We compared patients to two reference groups. The first group (N=35; mean age 42 years, 12 male) consisted of persons with a best corrected visual acuity of ≥1.0 with no ophthalmic abnormalities. The second group consisted of 39 persons (mean age 40 years, 19 male) with a low (uncorrected) visual acuity (<0.50), but with a normal cone ERG. Causes of decreased visual acuity were cataract (N=5), maculopathy (N=4), uncorrected refractive error (N=13), amblyopia (N=6), cornea pathology (N=2), macula edema due to a vascular problem (N=6), and glaucoma (N=3). Males with congenital color vision defects were excluded. The study was approved by the Medical Ethics Committee of Erasmus Medical Center and adhered to the tenets of the Declaration of Helsinki. All participants provided signed, informed consent for participation in the study, and retrieval of medical records.

Clinical Examination

All patients were invited for the study examination at the Department of Ophthalmology from Erasmus Medical Center. Medical history and family pedigree data were obtained by a questionnaire. We determined visual acuity with a Snellen chart under standard conditions, and examined the eye by regular slitlamp examination and ophthalmoscopy. Visual fields were determined by Goldmann perimetry. ERGs were performed in all persons with low visual acuity according to the International Society for Clinical Electrophysiology of Vision (ISCEV) standard.[5]

Color vision tests were performed consecutively by a single observer; the American Optical Company Hardy-Rand-Rittler Test (HRR), edition 1957; the Ishihara Test for Color Blindness, 38 plates, edition 1994; the saturated and desaturated version of the Lanthony Panel D-15 Test, and the Nagel anomaloscope, Model 1, manufactured by Schmidt & Haensch (Figure 1). The HRR, Ishihara and the Panel D-15 plates were illuminated with the MacBeth Easel Lamp (providing 350 lux). The tests were performed per eye as well as binocularly.

A

B

C

D
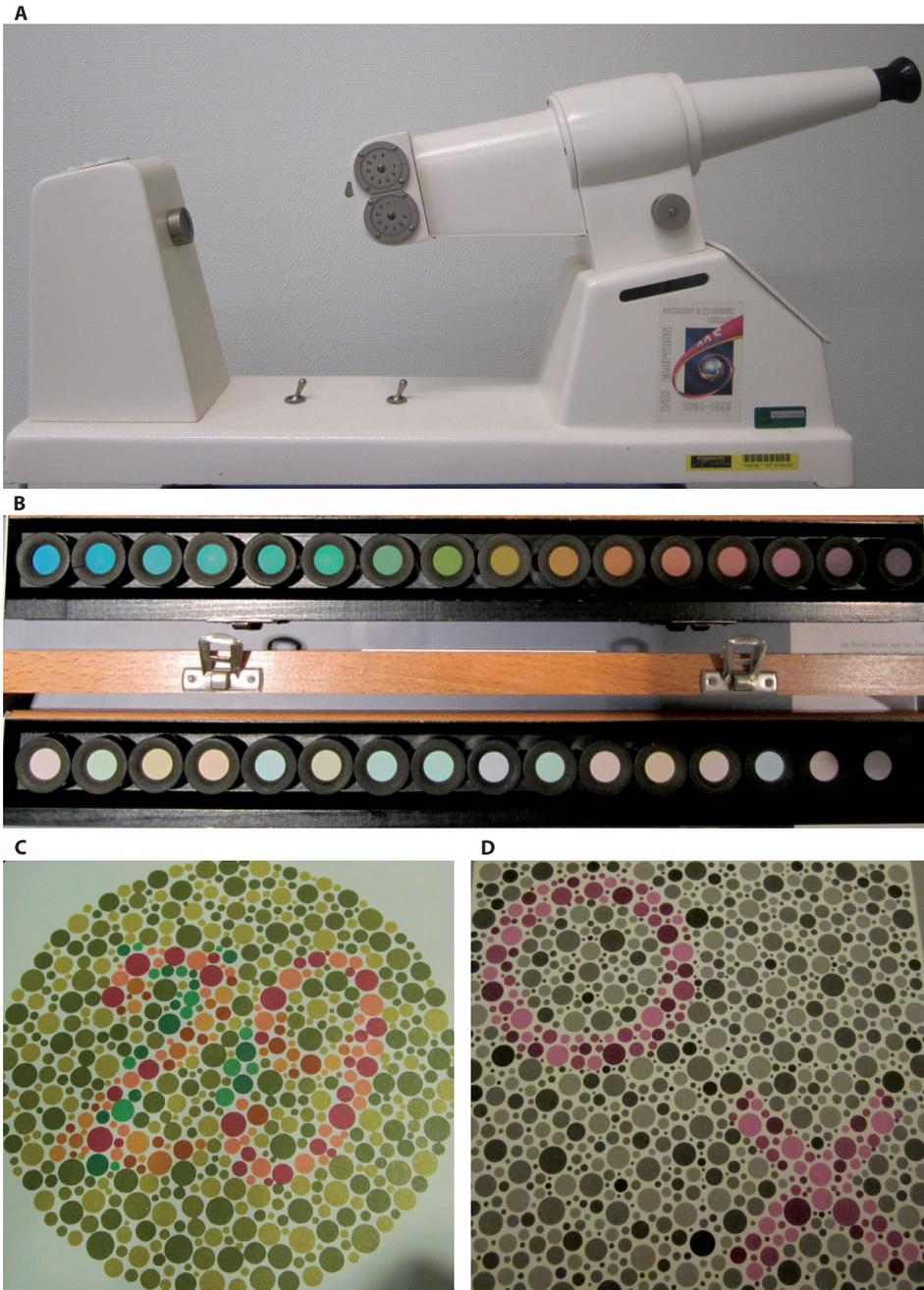
Figure 1. Color vision tests used in this study.
(a) The Model 1 Nagel Anomaloscope.
(b) The Lanthony saturated and desaturated Panel D-15 arrangement color vision tests.
(c) The pseudoisochromatic Ishihara color vision test.
(d) The pseudoisochromatic Hardy-Rand-Rittler (HRR) color vision test.

Pseudoisochromatic HRR and Ishihara test
Subjects were given 2-3 seconds to respond to each page. Each symbol or number missed was counted as an error. The HRR test was scored as normal when no errors were made. The HRR test started with 6 screening plates; if no errors were made the test ended, if any error was made, the examiner continued with plate 7-20. We classified color defects as: mild (1 or more errors in plate 7-11); moderate (1 or more errors in plate 12-14, or in 17-18 for tritan/tetartan defects), and severe (1 or more errors in plate 15 and 16, or in 19-20 for tritan/tetartan defects).[6] The first control plate of the Ishihara test had to be identified as '12' by all subjects. The test was classified as abnormal if 4 or more errors were made in the first 21 plates.[7]

Arrangement tests Lanthony Panel D-15 (de)saturated
The Panel D-15 tests were performed without restriction for time. The patient was asked to arrange the 16 randomly placed colored caps in natural order, beginning with the reference cap. Scoring was accomplished by comparing the patient's arrangement with the sequence of numbers printed on the back of the caps. The arrangement of caps was plotted on a score sheet. Correct arrangements formed a continuous circle following numerical order. For incorrect arrangements, we considered the following outcomes: 1. Few (1-2) or many (>2) crossed lines; or 2. any skips in the numbering.[8] The axis of these lines reflected which type of cone was most affected.

Nagel anomaloscope
The anomaloscope is based on the principle of color matching. The lower half of the field of the device is filled with spectral yellow, fixed at 589 nm. The upper half of the field is filled with a combination of spectral red (670 nm) and spectral green (545 nm). Our anomaloscope was calibrated at 41 (scale 0-73) for the protan-deutan (PD) mixture and at 15 (scale 0-80) for brightness. At the beginning of the test, both halves matched at scale unit 41. Subjects were asked to look at the lighted screen on the front panel of the instrument for three minutes, and subsequently asked whether both halves were the same color. If the answer was affirmative, the test result was considered normal. If the answer was negative, the examiner moved the scale in one-unit steps, each time asking the subject if the fields matched. The test was repeated three times. The normal matching range is 0 to 5 scale units; we therefore considered the test as failure when the scale unit of the PD-mixture was <36 or >46.[9,10]

Statistical Analysis
Since all test outcomes were highly correlated between right and left eyes ($R^2 \geq 0.90$), we used the right eye for all analyses. Reliability was evaluated by standard measures[11] using two reference groups: low vision controls and controls with normal visual acuity.

Sensitivity of each test was calculated as those with cone disorder who scored positive on the test divided by all patients with cone disorder. Specificity was calculated as controls with a negative test result divided by all controls. Positive predictive value was calculated as patients with cone disorder with positive test result divided by all subjects (patients and controls) with positive test result.

We constructed a receiver operating characteristic (ROC) curve, which indicates the probability of a true-positive result (sensitivity) and the probability of a false-positive result (1-specificity) for each test. We assessed the area under the ROC curve (c-statistic) as a measure of the discriminative accuracy. The c-statistic indicates the degree to which the test can discriminate between cone disorder patients and controls. This value ranges from 0.50 (chance, as accurate as tossing a coin) to 1.00 (perfect agreement). A test with a c-statistic 0.70 is generally considered to have acceptable discriminative capacity.

RESULTS

Table 1 reports the distribution of clinical characteristics in the entire study group. The mean age ranged from 32-42 years in the three study groups. Most cone disorder patients and low vision controls had a visual acuity between 0.10 and 0.30. The majority of cone disorder patients had either RPE alterations or atrophy in the macula (27/37;73%). Ten controls had macular abnormalities. No differences were observed for severity of color defects in all four tests between patients with reduced cone responses (16/37; 43%) or absent cone responses (21/37; 57%) on ERG.

Table 1. Distribution of clinical characteristics of the study population.

Variable	Cone disorder patients (N = 37)	Controls Low vision‡ (N = 39)	Controls Normal vision‡ (N = 35)
Mean age (years, range)	32 (6-80)	40 (8-81)*	42 (10-76)*
Sexe (Male/Female)	24/13	19/18	12/23*
Visual acuity (%, n/N)			
1.0 - >0.50	0	0	100 (35/35)
≥ 0.30 - ≤ 0.50	30 (11/37)	59 (23/39)*	0
> 0.10 - <0.30	32 (12/37)	13 (5/39)*	0
0.10	38 (14/37)	28 (11/39)	0
Macular appearance (%, n/N)			
Normal	27 (10/37)	75 (29/39)	100 (35/35)
RPE alterations	54 (20/37)	25 (10/39)	0
RPE atrophy	19 (7/37)	0	0

Table 1. Continued

Variable	Cone disorder patients (N = 37)	Controls Low vision‡ (N = 39)	Controls Normal vision‡ (N = 35)
ERG† (%, n/N)			
Normal	0	100 (39/39)	NA
Reduced photopic responses	43 (16/37)	0	NA
Absent photopic responses	57 (21/37)	0	NA
Perimetry of central retina (%, n/N)			
Reduced sensitivity	54 (14/26)	NA	NA
Relative scotoma	19 (5/26)	NA	NA
Absolute scotoma	27 (7/26)	NA	NA

‡: Low vision: <0.50 Snellen visual acuity; Normal vision: ≥1.0 Snellen visual acuity.
†: ERG: Full-field electroretinogram.
* $P < 0.05$ for the difference between cone disorder patients and controls.

Table 2 shows the color vision test results in the study population per axis. Controls with normal visual acuity did not make any mistakes on the HRR test, made only a few mistakes on Ishihara, but made many mistakes on the T axis of the Panel D-15 tests. They ranged from 31-46 for the PD-mix on the Nagel anomaloscope, with a mean (41) matching the expected unit number for individuals with normal color vision. Controls with low vision made considerably more mistakes, predominantly on the HRR and Ishihara tests and on the T axis of the Panel D-15 tests. The range and mean of the Nagel anomaloscope was relatively unaffected by low vision. All cone disorder patients made mistakes on HRR and Ishihara tests for the PD axes. With respect to the Panel D-15 tests, 31/37 (84%) of the patients had 2 or more crossings on the desaturated test, while only half (54%) of the patients showed two or more crossing lines at the saturated Panel D-15 test. When we graded any skips in the test result of the Panel D-15 tests as abnormal, 2 additional patients scored as abnormal as well as many controls (17/39 (44%) on PD axes of desaturated test; 16/39 (41%) on saturated test). Controls with normal vision made less mistakes on these tests than those with low vision (5/35 (14%) on PD axes of desaturated test; 2/35 (6%) on saturated test).

Table 2. Color vision test outcomes in patients with cone disorder and controls, stratified for protan-deutan (PD), and tritan (T) axis.

Color test	Test outcome	Cone disorder patients (N = 37) % (n/N)	Controls Low vision‡ (N = 39) % (n/N)	Controls Normal vision‡ (N = 35) % (n/N)
Ishihara				
Protan/Deutan	Normal	0 (0/37)	79 (31/39)	97 (34/35)
	Defects	100 (37/37)	21 (8/39)	3 (1/35)
Panel D-15 desaturated				
Protan/Deutan	Normal	16 (6/37)	92 (36/39)	94 (33/35)
	1-2 Crossings	0 (0/37)	8 (3/39)	6 (2/35)
	>2 Crossings	84 (31/37)	0 (0/39)	0 (0/35)
Tritan	Normal	49 (18/37)	49 (19/39)	77 (27/35)
	1-2 Crossings	0 (0/37)	14 (5/39)	17 (6/35)
	>2 Crossings	51 (19/37)	37 (15/39)	6 (2/35)
Panel D-15 saturated				
Protan/Deutan	Normal	46 (17/37)	97 (38/39)	97 (34/35)
	1-2 Crossings	0 (0/37)	3 (1/39)	3 (1/35)
	>2 Crossings	54 (20/37)	0 (0/39)	0 (0/35)
Tritan	Normal	57 (21/37)	62 (24/39)	83 (29/35)
	1-2 Crossings	0 (0/37)	21 (8/39)	14 (5/35)
	>2 Crossings	43 (16/37)	17 (7/39)	3 (1/35)
HRR				
Protan/Deutan	Normal	0 (0/37)	79 (31/39)	100 (35/35)
	Mild defects	5 (2/37)	18 (7/39)	0 (0/35)
	Medium defects	14 (5/37)	0 (0/39)	0 (0/35)
	Severe defects	81 (30/37)	3 (1/39)	0 (0/35)
Tritan	Normal	30 (11/37)	82 (32/39)	100 (35/35)
	Mild defects	8 (3/37)	10 (4/39)	0 (0/35)
	Medium defects	59 (22/37)	8 (3/39)	0 (0/35)
	Severe defects	3 (1/37)	0 (0/39)	0 (0/35)
Nagel				
	Mean PD-mix (range;SD†)	57 (27-74;15)	40 (30-46;4)	41 (31-46;4)

‡: Low vision: <0.50 Snellen visual acuity; Normal vision: ≥1.0 Snellen visual acuity.

†: SD: Standard Deviation.

Table 3 reports the sensitivity, specificity, positive predictive value, and discriminative accuracy per axis for all tests in three strata of visual acuity. When comparing patients to both normal and low vision controls, the HRR had the best values for the PD axes, followed by the Ishihara test, desaturated Panel D-15 test, and Nagel anomaloscope. The saturated Panel D-15 test had the lowest values. The Panel D-15 tests as well as HRR all had low scores for the T axis. These scores were lowest for the Panel D-15, and did not reach statistical significance for discriminative accuracy. Low visual acuity decreased the reliability measures of all tests, in particular of the T axis. Legal blindess (visual acuity ≤ 0.10) did not further decrease these measures.

Table 3. Reliability of color vision testing for cone disorders using a reference group with normal visual acuity (A), low visual acuity (B), and legal blindness (C) stratified for protan-deutan (PD) and tritan (T) axis.

	Sensitivity	Specificity	Positive predictive value	Discriminative accuracy
A. Patients (N=37) and Controls Normal vision‡ (N=35)				
Ishihara				
Protan/Deutan	1.0	0.97	0.97	0.985*
Panel D-15 desaturated				
Protan/Deutan	0.84	0.94	0.94	0.890*
Tritan	0.51	0.77	0.70	0.639
Panel D-15 saturated				
Protan/Deutan	0.54	0.97	0.95	0.756*
Tritan	0.43	0.83	0.73	0.628
HRR				
Protan/Deutan	1	1	1	1*
Tritan	0.70	1	1	0.851*
Nagel anomaloscope				
Protan/Deutan-mix	0.89	0.74	0.79	0.814*
B. Patients (N=37) and Controls Low vision‡ (N=39)				
Ishihara				
Protan/Deutan	1	0.79	0.82	0.886*
Panel D-15 desaturated				
Protan/Deutan	0.84	0.92	0.91	0.880*
Tritan	0.51	0.49	0.49	0.500
Panel D-15 saturated				
Protan/Deutan	0.54	0.97	0.95	0.756*
Tritan	0.43	0.62	0.52	0.516

Table 3. Continued

	Sensitivity	Specificity	Positive predictive value	Discriminative accuracy
HRR				
Protan/Deutan	1	0.79	0.82	0.900*
Tritan	0.70	0.82	0.79	0.766*
Nagel anomaloscope				
Protan/Deutan-mix	0.89	0.83	0.85	0.860*
C. Patients (N=14) and Controls Legal blindness‡ (N=11)				
Ishihara				
Protan/Deutan	1	0.82	0.88	0.900*
Panel D-15 desaturated				
Protan/Deutan	0.86	1	1	0.929*
Tritan	0.29	0.64	0.50	0.443
Panel D-15 saturated				
Protan/Deutan	0.57	0.91	0.89	0.736*
Tritan	0.50	0.64	0.64	0.550
HRR				
Protan/Deutan	1	0.82	0.88	0.950*
Tritan	0.78	0.91	0.92	0.843*
Nagel anomaloscope				
Protan/Deutan-mix	1	0.80	0.85	0.950*

‡: Normal vision: ≥1.0 Snellen visual acuity; Low vision: <0.50 Snellen visual acuity; Legal blindness ≤0.10 Snellen visual acuity.

* $P < 0.01$ for the difference in discriminative accuracy per test between cone disorder patients and controls.

DISCUSSION

Our study shows that all four tests have a good discriminative accuracy for the detection of cone disorders. The HRR and desaturated Panel D-15 tests were the most reliable color vision tests, and the most appropriate since they allow for evaluation of all three color axes and quantification of the color defect. HRR excelled in discriminating between cases and controls for both PD axes as well as the T axis. Low visual acuity decreased the discriminative accuracy of all color vision tests. Nevertheless, the HRR remained the most reliable test in these subjects. Least reliable was testing of the T axis of the Panel D-15 tests, which scored not much better than tossing a coin in the low vision strata.

The type of color vision test used in the diagnosis of cone disorders often varies per clinic. Each test has its advantage and disadvantage, and has unique requirements for administration and settings to achieve the best test results. Factors that affect performance of all tests are illumination, the angle under which the test figure is viewed, and the cognitive abilities of the test person.[12]

The Nagel anomaloscope (Figure 1a), developed in 1907, is considered the definitive clinical instrument for classifying phenotypic variation in congenital X-linked PD color blindness.[10] The use and maintenance of the Nagel can be challenging; the test is time-consuming, may be difficult to perform, and the instrument is rather bulky. Nevertheless, the test performed rather well in the diagnosis of cone disorders, and had consistent high values for discriminative accuracy in all visual acuity strata. A disadvantage in the diagnosis of cone disorders is that the model of the Nagel used in this study does not evaluate the T axis. Other, less commonly used, models such as the Heidelberg Multi Color (HMC) Anomaloscope (Oculus) do have this possibility.

The Lanthony saturated and desaturated Panel D-15 tests are arrangement tests which were developed in 1973 to test color discrimination ability for occupational purposes (Figure 1b). The tests have a fixed saturation at different levels; the colored caps are paler and lighter in the desaturated version. Advantages of Panel D-15 are the ability to categorize defects according to P, D and T axis, and to diagnose the type of defect by visual recognition of the pattern.[13] The saturated Panel D-15 test performed considerably worse than the desaturated version in the discrimination between cases and controls. The hues and chroma (saturation) of the caps are more distinguishable in the saturated version, making the test easier for cone disorder patients and thereby increasing false negatives. The advantage of the Panel D-15 test is the rather large diameter of the caps (>1.0 cm). Patients do not have to identify numbers or symbols and this makes the test less dependent on visual acuity.[4] We did not observe a decrease in discriminative accuracy in legally blind patients. When we graded the test result of the Panel D-15 tests for any skips as abnormal, the number of false positives raised in all controls groups. The increase in number of skips was particularly high in the desaturated Panel D-15 test, leading to a lower specificity and discriminative accuracy of this test. These findings indicate that one should only consider true crossings as a positive test result in these tests, and not just any skips.

The pseudoisochromatic color vision tests, Ishihara and HRR, have the ability to test differences in hue and chroma of colors which lie close to the confusion axes. The Ishihara test, first published in 1917 by Shinobu Ishihara in Tokyo, uses ten different numbers in small colored dots varying in size, hue and saturation (Figure 1c). The test was designed

for a quick and accurate assessment of congenital X-linked PD color blindness. The test is inexpensive, durable, as well as readily available. A disadvantage is the absence of quantification of the color defect. In addition, the test is somewhat complex because it tests 10 different characters, and, importantly for the diagnosis of cone disorders, the test does not evaluate the T axis. Nevertheless, the discriminative accuracy for the PD axes was consistently high, even in the low vision strata.

The HRR test, first published by the American Optical Company in 1955, has been developed to quantify the type and extent of the color defect (Figure 1d). It uses three symbols and has a background of small circular dots varying in size, hue, and saturation. Advantages of the test are the easy application, the ability to use the test in children and illiterate adults, the ability to differentiate the three color axes, and the possibility to quantify the extent of the color defect.[14,15] The HRR test had the best discriminative accuracy in all three color axes, and remained the most reliable test in the low vision strata.[14,16]

The T axis could only be tested with the HRR and Panel D-15 tests. Testing this axis can help to differentiate between congenital X-linked PD colorblindness and cone pathology. Moreover, if the T axis is normal while the PD axes are severely disturbed in subjects with low vision, a diagnosis of X-linked blue cone monochromacy can be suspected. A Berson test should then follow; this test has test plates which differ from one another only with respect to the chroma of the purple-blue arrow.[17] For all tests, the discriminative accuracy was lower for the T axis than for the PD axes. This may be due to the lower frequency of blue cones in the retina; the ratio of all three cone types is approximately 20 protan: 40 deutan: 1 tritan.[12] Another factor of importance may be the ability of the human crystalline lens to absorb blue light (short wavelength of ~420 nm). As the lens density increases with age, its capacity to absorb short wavelength light increases even more, and this may further affect blue sensitivity and hue discrimination.[12]

The purpose of our study was to determine which color vision test would be most appropriate to identify color vision defects in patients with cone disorders. We selected a control group with a variety of diseases affecting vision, and acknowledge that some of these can influence color vision. Recently, Almog et al.[18] explored the correlation between low visual acuity and color vision disturbances, and found that in particular patients with optic neuropathy experienced severe color vision defects, while patients with macular diseases or media opacities experienced milder color vision losses. Our study shows that patients with primary cone disorders have a more profound loss of color vision than patients with disorders affecting cone function as a secondary event.

Limitations of our study are the relatively low number of patients and controls, and the selection of only a few tests for comparison. Newly developed computer-based color tests (Portal color sort test, Seohan computerized hue test) are available now; these tests are more complex, expensive and less suitable for daily practice in a general clinical setting.[19,20] The accuracy of these tests in the identification of patients with cone disorders has not been investigated.

In conclusion, we investigated which color vision test should be used as a first step in the diagnosis of cone disorders. We found that the HRR and Ishihara test were the most reliable tests. However, we consider the HRR and desaturated Panel D-15 test the most appropriate tests due to the possibility of T axis testing and quantification of the defect. We recommend to use these tests in patients in whom a primary cone disorder is suspected.

REFERENCES

1. Michaelides M, Hardcastle AJ, Hunt DM, Moore AT. Progressive cone and cone-rod dystrophies: phenotypes and underlying molecular genetic basis. Surv Ophthalmol. 2006;51:232-58.

2. Michaelides M, Hunt DM, Moore AT. The cone dysfunction syndromes. Br J Ophthalmol. 2004;88:291-7.

3. Thiadens AA, Slingerland NW, Roosing S, et al. Genetic etiology and clinical consequences of complete and incomplete achromatopsia. Ophthalmology. 2009;116:1984-9.

4. McCulley TJ, Golnik KC, Lam BL, Feuer WJ. The effect of decreased visual acuity on clinical color vision testing. Am J Ophthalmol. 2006;141:194-6.

5. Marmor MF, Fulton AB, Holder GE, et al. International Society for Clinical Electrophysiology of Vision (2009) ISCEV Standard for full-field clinical electroretinography (2008 update). Doc Ophthalmol. 118:69-77.

6. Manual: Hardy LH, Rand G, Rittler MC. A Manual of the American Optical Company H-R-R pseudo-isochromatic plates, edition 2002.

7. Manual: Ishihara S. The Series of Plates Designed as a Test for Colour-Deficiency, edition 1994.

8. Manual: saturated and desaturated version of the Lanthony Panel D15 Test, edition 1978.

9. Manual: Nagel anomaloskop, Model 1, manufactured by Schmidt & Haensch.

10. Jägle H, Pirzer M, Sharpe LT. The Nagel anomaloscope: its calibration and recommendations for diagnosis and research. Graefes Arch Clin Exp Ophthalmol. 2005;243:26-32.

11. Altman DG. Practical statistics for medical research. First ed. London. Chapman & Hall. 1991:417-419

12. Melamud A, Hagstrom S, Traboulsi EI. Color vision testing. Ophthalmic Genet. 2004;25:159-87.

13. Good GW, Schepler A, Nichols JJ. The reliability of the Lanthony Desaturated D-15 test. Optom Vis Sci. 2005;82:1054-9.

14. Cole BL, Lian KY, Lakkis C. The new Richmond HRR pseudoisochromatic test for colour vision is better than the Ishihara test. Clin Exp Optom. 2006;89:73-80.

15. Birch J. Clinical use of the American Optical Company (Hardy, Rand and Rittler) pseudoisochromatic plates for red-green colour deficiency. Ophthalmic Physiol Opt. 1997;17:248-54.

16. Bailey JE, Neitz M, Tait DM, Neitz J. Evaluation of an updated HRR color vision test. Vis Neurosci. 2004;21:431-6.

17. Berson EL, Sandberg MA, Rosner B, Sullivan PL. Color plates to help identify patients with blue cone monochromatism. Am J Ophthalmol. 1983;95:741-7.

18. Almog Y, Nemett A. The Correlation Between Visual Acuity and Color Vision as an Indicator of the Cause of Visual Loss. Am J Ophthalmol 2010;149:1000–1004.

19. Melamud A, Simpson E, Traboulsi EI. Introducing a new computer-based test for the clinical evaluation of color discrimination. Am J Ophthalmol. 2006;142:953-60.

20. Shin YJ, Park KH, Hwang JM, et al. A new color vision test to differentiate congenital and acquired color vision defects. Ophthalmology. 2007;114:1341-7.
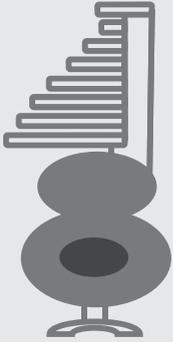
Chapter 2

Achromatopsia
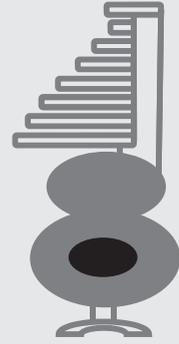
Chapter 2a

**Genetic etiology and clinical consequences
of complete and incomplete achromatopsia**

ABSTRACT

Objective: To investigate the genetic causes of complete and incomplete achromatopsia (ACHM) and assess the association between disease-causing mutations, phenotype at diagnosis, and visual prognosis.

Design: Clinic-based, longitudinal, multicenter study.

Participants: Probands with complete ACHM (N=35), incomplete ACHM (N=26), or non-specific ACHM (N=2) and their affected relatives (N=18) from various ophthalmogenetic clinics in The Netherlands.

Methods: Ophthalmologic clinical data were assessed over a life time and were registered from medical charts and updated by ophthalmologic examination. Mutations in the *CNGB3*, *CNGA3*, and *GNAT2* genes were analyzed by direct sequencing.

Main Outcome Measures: Genetic mutations and clinical course of ACHM.

Results: *CNGB3* mutations were identified in 55 of 63 (87%) of probands and all caused premature truncation of the protein. The most common mutation was p.T383IfsX13 (80%); among the four other mutations was the novel frameshift mutation p.G548VfsX35. *CNGA3* mutations were detected in 3 of 63 (5%) probands; all caused an amino acid change of the protein. No mutations were found in the *GNAT2* gene. The ACHM subtype, visual acuity, color vision, and macular appearance were equally distributed among the *CNGB3* genotypes, but were more severely affected among *CNGA3* genotypes. Visual acuity deteriorated from infancy to adulthood in 12% of patients, leading to 0.10 in 61%, and even lower than 0.10 in 20% of patients.

Conclusions: In this well-defined cohort of ACHM patients, the disease seemed much more genetically homogeneous than previously described. The *CNGB3* gene was by far the most important causal gene, and T383IfsX13 the most frequent mutation. The ACHM subtype did not associate with a distinct genetic etiology, nor were any other genotype–phenotype correlations apparent. The distinction between complete and incomplete subtypes of ACHM has no clinical value, and the assumption of a stationary nature is misleading.

INTRODUCTION

Achromatopsia (ACHM), or rod monochromatism, is a rare, autosomal-recessive cone dysfunction disorder with an estimated prevalence of 1:30,000 to 1:50,000.[1–3] Affected patients present with a congenital pendular nystagmus, photophobia, poor visual acuity, and severe defects in the protan, deutan, and tritan color axes. The disease has been divided into complete and incomplete ACHM subtypes. Patients with the complete subtype have no recordable cone function on electroretinogram (ERG), whereas those with incomplete ACHM retain some residual cone function on ERG, and presumably have better color vision and a higher visual acuity (up to 0.20).[4,5] Funduscopy is usually normal in both subtypes, although macular pigmentary changes and atrophy have been described. Rod function can be slightly abnormal on ERG.[6]

The genetic basis of ACHM has been elucidated to a large extent during the past decade. Three genes have been associated: *CNGA3*, *CNGB3*, and *GNAT2*.[7–9] *CNGA3* and *CNGB3* encode for the α- and β-subunits, respectively, of the cyclic nucleotide gated channel type 3 located on the outer membrane segment of cones and play an important role during the cone phototransduction cascade. The third gene, *GNAT2*, encodes for the α-subunit of cone transducin, which plays a role in the hydrolyzation of cyclic guanosine monophosphate (cGMP), thereby reducing its intracellular concentration and leading to closure of the channel.[8–10]

Previous studies have reported many mutations in these genes. The most frequent mutations were found in the *CNGB3* gene, explaining up to 50% of all ACHM. Mutations in *CNGA3* seemed to account for approximately 20% of cases, whereas mutations in *GNAT2* were found in <2% of ACHM.[8,11–13] Thus, the genetic etiology of ACHM remains unknown in about 30% of patients. The consequences of the observed mutations vary widely per gene, ranging from amino acid changes to truncated or absent proteins. Little is known about the effect of these mutations on clinical phenotype and course of disease.[14–16]

Herein, we have reported the genetic findings of 63 independent ACHM probands and their affected relatives from The Netherlands. We investigated incomplete and complete ACHM, and assessed the correlation between disease-causing mutations, color vision, visual acuity, macular appearance, and prognosis.

PATIENTS AND METHODS

Study Population

Patients (N=63 probands; 36 male; mean age, 40 years) and affected family relatives (N=18) who had been diagnosed with complete or incomplete ACHM were ascertained from various university hospitals, low vision institutes, and from the Rotterdam Eye Hospital in The Netherlands. We defined complete ACHM as the presence of poor visual acuity, congenital nystagmus, photophobia, color vision disturbances, and absent cone responses with normal rod responses on a full-field ERG. Experienced electrophysiologists performed ERGs according to the International Society for Clinical Electrophysiology of Vision standard.[17] We diagnosed patients with incomplete ACHM when a residual cone response was still present on the first ERG performed at diagnosis.

The study was approved by the Medical Ethics Committee of Erasmus Medical Center and adhered to the tenets of the Declaration of Helsinki. All participants provided signed, informed consent for participation in the study, retrieval of medical records, and use of blood and DNA for research. The genotype of a fraction of probands (31/63) had been part of an earlier ACHM consortium study by Kohl et al.[11] Clinical Examination All patients received a questionnaire that addressed their medical history and family pedigree. Medical charts were retrieved from their ophthalmologists, and all available data on Snellen visual acuity, color vision (American Optical Hardy-Rand-Rittler Test, Ishihara Test for Color Blindness, or Lanthony Panel D-15 Test), slit-lamp and fundus examinations, and ERGs were collected. Patients with incomplete or no available data from the last five years were invited for an additional ophthalmologic examination, ERG, and fundus photography. The clinical data were registered per decade. Findings at presentation in childhood (0–20 years) were compared with those in adulthood (≥20 years).

Molecular Genetic Analysis

Blood samples were obtained from probands, affected relatives, and parents. DNA was isolated from peripheral blood lymphocytes by standard procedures. The coding region and intron/exon boundaries of the *CNGB3*, *CNGA3*, and *GNAT2* genes were amplified by polymerase chain reaction using the conditions and primer sequences provided in Supplemental Table 1. Segregation analysis was performed when mutations were detected.

RESULTS

Mutation Analysis

The frequency and relative contributions of all mutations that were detected in our study group are provided in Table 2. *CNGB3* mutations were identified in 55/63 (87%) probands with ACHM (Figure 1). The most common mutation was p.T383IfsX13, a null mutation in exon 10. Probands homozygous for this mutation originated from different areas in The Netherlands and were not known to have parental consanguinity. Four probands carried other mutations in the *CNGB3* gene. One of these probands carried the novel homozygous frameshift mutation p.G548VfsX35, leading to a premature stop codon in exon 14. Mutations in the *CNGA3* gene were detected in 3 probands who all had compound heterozygous missense mutations. No mutations were detected in the *GNAT2* gene. Five (8%) probands did not reveal any mutations in the investigated genes. Segregation analysis showed that affected siblings shared the same mutant alleles as the proband, whereas unaffected relatives did not have these allele combinations.

Table 2. Overview of *CNGB3* and *CNGA3* mutations detected in the present study

|		Allele 1				Allele 2			
Gene	Exon	Alteration nucleotide	Alteration polypeptide	Ref.	Exon	Alteration nucleotide	Alteration polypeptide	Ref.	N
CNGB3	10	c.1148delC	p.T383IfsX13	25	10	c.1148delC	p.T383IfsX13	25	37
CNGB3	10	c.1148delC	p.T383IfsX13	25	9	c.991-3T>G	Splice defect	10	8
CNGB3	10	c.1148delC	p.T383IfsX13	25	7	c.886_896del11insT	p.R296YfsX9	10	4
CNGB3	10	c.1148delC	p.T383IfsX13	25	6	c.819_826del8	p.R274VfsX12	25	2
CNGB3	14	c.1642delG	p.G548VfsX35	-	14	c.1642delG	p.G548VfsX35	-	1
CNGB3	9	c.991-3T>G	splice defect	1	9	c.991-3T>G	Splice defect	1	1
CNGB3	9	c.991-3T>G	splice defect	1	7	c.886_896del11insT	p.R296YfsX9	1	1
CNGB3	9	c.991-3T>G	splice defect	1	6	c.819_826del8	p.R274VfsX12	1	1
CNGA3	7	c.1565T>C	p.I522T	8	7	c.1641C>A	p.F547L	8	1
CNGA3	8	c.829C>T	p.R277C	8	8	c.1718A>G	p.Y573C	8	1
CNGA3	8	c.778G>A	p.D260N	8	6	c.485A>T	p.D162V	8	1
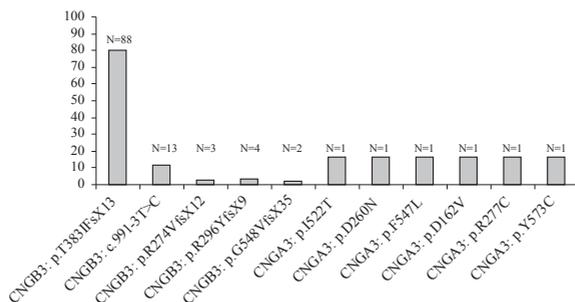
Figure 1. Frequency of the mutations in the *CNGA3* and *CNGB3* genes in probands with complete and incomplete achromatopsia.

Clinical Findings

Clinical charts were collected of all probands and affected relatives (N=81) during a mean follow-up of 15 years (range, 5–25 years). The number of clinical examinations ranged from 2 to 8 with a mean of 6. Of all probands and affected relatives, 47 were diagnosed with complete ACHM, 32 with incomplete ACHM, and 2 patients could not be classified into either category. Age at diagnosis did not differ between the subtypes (mean age complete ACHM, 6.5 years [SD 3.4]; mean age incomplete ACHM, 6.9 years [SD 3.7]). Tables 3 and 4 show that genotype frequencies, color vision, and visual acuity were similar in the two subtypes.

Tables 3 and 4 present a summary of the clinical findings per genotype. *CNGB3* genotypes did not seem to correlate with specific phenotypes: Outcomes in ACHM subtype, visual acuity, color vision, refractive error, and macular appearance were equally distributed among the different mutations. Visual acuity and macular appearance were slightly more affected among the five subjects with *CNGA3* genotypes. Other clinical observations consisted of deterioration of residual cone function in patients with incomplete ACHM leading to an extinguished photopic ERG. This occurred in various *CNGB3* genotypes, making a genotype–phenotype relationship unlikely. In addition, deterioration of rod function occurred in three other patients with *CNGB3* mutations (homozygous p.T383IfsX13 mutations; compound heterozygous c.991-3T>G / p.T383IfsX13, and p.R274VfsX12 / c.991-3T>G mutations). One of these patients was diagnosed with complete ACHM, whereas the other two showed incomplete ACHM. The reduction of rod responses was mild and occurred during a follow-up period of ≥10 years. One quarter of the patients already presented with macular changes during childhood; this augmented to 36% in adulthood. Visual acuity progressively worsened below 0.10 in 12% of patients (N=81) in adulthood. Color vision was severely affected in all but one patient, although substantial refractive errors were present in approximately half of all patients. These consisted of hyperopia >2 diopters (31%) as well as myopia <-2 diopters (25%).

Table 3. Clinical findings stratified per genotype in probands and affected relatives.

Mutations (N=76)	Diagnoses (N=79)*		Visual Acuity Childhood			Visual Acuity Adulthood			Refractive error			Color vision		Electroretinogram	
	Incom† (N=32)	Comp† (N=47)	0.16-0.20	0.10	<0.10	0.16-0.20	0.10	<0.10	-2 to +2	<-2	>+2	Mild/Medium	Severe	Stable	Progressive
CNGB3 p.T383lfsX13-/- (N=46)	17/46 (37%)	29/46 (63%)	15/46 (33%)	26/46 (57%)	5/46 (10%)	10/46 (22%)	26/46 (56%)	10/46 (22%)	21/39 (54%)	8/39 (20%)	10/39 (26%)	0	46/46 (100%)	42/46 (91%)	4/46 (9%)
CNGB3 compound heterozygous mutations (N=23)	9/23 (39%)	14/23 (61%)	6/23 (26%)	14/23 (61%)	3/23 (13%)	5/23 (22%)	15/23 (65%)	3/23 (13%)	8/21 (38%)	4/21 (19%)	9/21 (43%)	1/21 (5%)	20/21 (95%)	20/23 (87%)	3/23 (13%)
CNGA3 missense mutations (N=5)	1/5 (20%)	4/5 (80%)	0	5/5 (100%)	0	0	3/5 (60%)	2/5 (40%)	1/5 (20%)	4/5 (80%)	0	0	5/5 (100%)	5/5 (100%)	0
No mutations (N=5)	5/5 (100%)	0	1/5 (20%)	3/5 (60%)	1/5 (20%)	0	4/5 (80%)	1/5 (20%)	2/4 (50%)	1/4 (25%)	1/4 (25%)	0	5/5 (100%)	5/5 (100%)	0
Total	32/79 (41%)	47/74 (64%)	22/74 (30%)	48/79 (61%)	9/74 (12%)	15/69 (22%)	48/79 (61%)	16/79 (20%)	32/69 (46%)	17/69 (25%)	20/64 (31%)	1/21 (5%)	76/77 (99%)		8/77 (10%)

Mutations	Macular appearance Childhood				Macular appearance Adulthood			
	Normal	No foveal reflex	Pigmentary changes	Bulls eye/Atrophy	No foveal reflex	Normal	Pigmentary changes	Bulls eye/Atrophy
CNGB3 p.T383lfsX13 -/- (N=48)	30/45 (67%)	6/45 (13%)	6/45 (13%)	3/45 (7%)	5/45 (11%)	27/45 (60%)	8/45 (18%)	5/45 (11%)
CNGB3 compound heterozygous mutations (N=23)	15/22 (68%)	0	6/22 (27%)	1/22 (5%)	3/22 (14%)	11/22 (50%)	7/22 (32%)	1/22 (4%)
CNGA3 missense mutations (N=5)	3/5 (60%)	0	1/5 (20%)	1/5 (20%)	0	1/5 (20%)	3/5 (60%)	1/5 (20%)
No mutations (N=5)	3/5 (60%)	0	1/5 (20%)	1/5 (20%)	0	2/5 (40%)	2/5 (40%)	1/5 (20%)
Total	51/77 (66%)	6/45 (13%)	14/77 (18%)	6/77 (8%)	8/67 (12%)	41/77 (53%)	20/77 (26%)	8/77 (10%)

*Not included two patients with diagnosis achromatopsia not otherwise specified
†Incom: incomplete achromatopsia, Comp: Complete achromatopsia

Table 4. Distribution of genotype, color vision and course of visual acuity as a function of subtype

Diagnosis†	Allele frequency*						Color vision defects		Visual acuity childhood‡			Visual acuity adulthood‡		
	p.T383IfsX13	c.991-3T>G	p.R296YfsX9	p.R274VfsX12	p.G548VfsX35	CNGA3 missense mutations	Mild/Medium	Severe	0.16-0.20	0.10	<0.10	0.16-0.20	0.10	<0.10
Complete achromatopsia (N=35)	52/70 (74%)	7/70 (10%)	3/70 (4%)	2/70 (3%)	0	6/70 (9%)	0	35 (100%)	10/35 (29%)	21/35 (60%)	4/35 (11%)	7/35 (20%)	20/35 (57%)	8/35 (23%)
Incomplete achromatopsia (N=26)	32/42 (76%)	6/42 (14%)	1/42 (2.5%)	1/42 (2.5%)	2/42 (5%)	0	1/26 (4%)	25/26 (96%)	8/26 (31%)	14/26 (54%)	4/26 (15%)	6/26 (23%)	12/26 (46%)	8/26 (31%)

*Not included: five patients without mutations in the CNGA3 or CNGB3 gene

†Not included two patients with diagnosis achromatopsia not otherwise specified

‡Childhood has been defined as 0-20 years. Adulthood has been defined as ≥20 years

Five probands did not carry any mutations in the *CNGA3*, *CNGB3*, or *GNAT2* genes (Tables 3 and 4). The diagnosis of these probands had been incomplete ACHM. Three of them were male and had severely affected color vision in the protan and deutan axes. Two had no evidence of tritan axis involvement on the Panel D-15 test, although this could not be excluded in the third male because he had only undergone Ishihara color vision testing.

DISCUSSION

In this Dutch cohort study, we found that mutations in the *CNGB3* gene are the most important causes of incomplete and complete ACHM. In the majority of the probands (55/63; 87%), we identified two affected alleles in this gene. No probands with one affected allele were detected. We found five different mutations, including the common p.T383IfsX13 and a novel mutation p.G348VfsX35; all mutations caused premature truncation of the protein. In only three probands we detected mutations in the *CNGA3* gene (3/63; 5%), which consisted of six different missense mutations. We did not identify any mutations in the *GNAT2* gene. Irrespective of the genetic cause, a large proportion of ACHM patients showed progression of cone dysfunction, worsening of macular appearance, and deterioration of central vision.

Previous reports claimed that a high proportion (25–30%) of patients still have an unknown cause of disease.[4,11,12] In our study, we used very strict criteria for diagnosis and thereby created a well-characterized ACHM study group. We found mutations in 92% (58/63) of probands in only two genes, indicating that only a small number of genes is involved in ACHM. The three male probands without a mutation were retested for color vision defects and seemed to have an intact tritan color axis. This may point to the diagnosis blue cone monochromacy, which is characterized by only 5% functional cones, and therefore closely resembles the rod-monochromatic disorder ACHM.[18,19] Excluding these three probands from the analysis would indicate that 92% of ACHM can be explained by mutations in *CNGB3*.

Previous reports had estimated that mutations in *CNGB3* caused ACHM in approximately 36% to 50% of cases.[4,11,12] In contrast to our study, which consisted mostly of Caucasians, these reports had included probands of various ethnic backgrounds. We suspect that *CNGB3* is more important in probands of Northern European descent, and *CNGA3* mutations are more prevalent among probands from the Middle East.[20] The most common *CNGB3* mutation in our study was p.T383IfsX13, which occurred in 80% (88/110) of affected *CNGB3* alleles (Figure 1). This is comparable to the study of Johnson et al,[12] who found that this allele was responsible for 78% of all *CNGB3* mutations. It is now well-

established that the cone nucleotide gated channels are tetrameric proteins composed of two α-subunits and two β-subunits in the cone cell.[21] Each channel subunit contains six transmembrane helices, a cytoplasmic NH2 and COOH terminus, a conserved pore domain, and a cGMP-binding domain.[21–23] In the dark state, cGMP binds to this domain, thereby keeping the gate open, and enabling a free flow of ions through the channel. However, illumination hydrolyses and decreases intracellular cGMP, and causes closure of the gate and hyperpolarization of the cone membrane. Our observed mutations in *CNGB3* were located either in the transmembrane helices or in the cGMP binding domain (Figure 2), and all caused truncation of the protein. We hypothesize that this leads to defective pore formation, which hampers hyperpolarization of the cone cell membrane and may ultimately lead to apoptosis by the continuous influx of Ca^{2+} ions.[24]
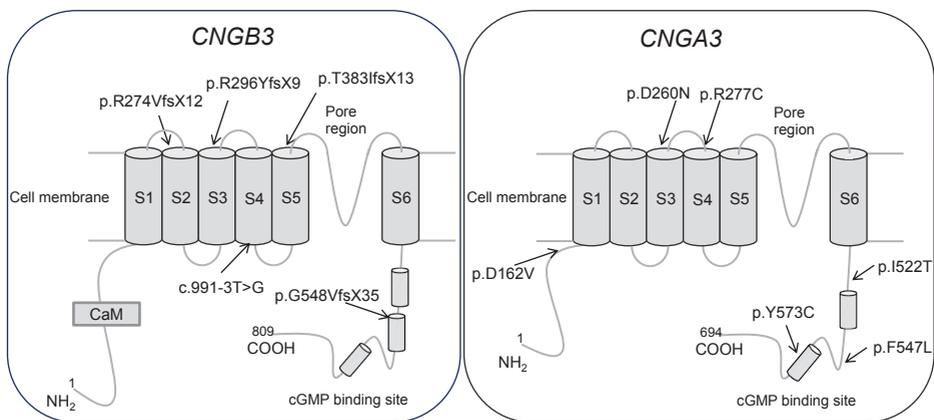
Figure 2. Localization of the mutations with respect to the proposed topological model of the *CNGA3* and *CNGB3* polypeptide. CaM: Ca^{2+} calmodulin domains; COOH: carboxylic acids; cGMP: cyclic guanosine monophosphate.

The mutations in the *CNGA3* gene were localized in the cytoplasmic NH2 terminus, the transmembrane helices, and the cGMP binding domain of the CNGA3 protein, and all caused an amino acid change (Figure 2). The phenotypic consequences were similar or even more severe than the truncating mutations in *CNGB3*. Cone nucleotide gated α-subunits indeed are highly conserved and have little tolerance for substitutional changes in the protein.[11,12,22] In vitro experiments have shown that α-subunits can function as a channel in the absence of β-subunits; the latter cannot conduct ion currents by themselves.[25]

Phenotypically, we distinguished ACHM in the two classical disease subtypes, complete and incomplete ACHM. We questioned the etiologic background and prognostic consequences of this clinical subclassification, and compared genotypes as well as visual

acuity, color vision, and macular appearance in both groups. The distribution of muta-tions was not skewed toward either diagnosis in our study, suggesting a similar genetic etiology. Likewise, visual acuity, color vision, and macular appearance showed a similar distribution at onset as well as in adulthood, indicating no differences in phenotypic variation (Tables 3 and 4). Remarkably, a proportion of patients of both groups deterio-rated in visual function, macular appearance, and cone function on ERG, contradicting the presumable stationary nature of ACHM. This corresponds with findings in *CNGA3* knock-out mice, which showed progressive loss of cones from the second postnatal week to the third postnatal month.[26] Thus, our data do not validate a clinical subclas-sification of ACHM, and demonstrate that the disease can be progressive in at least some patients.

To summarize, in our clinically well-characterized group of patients, ACHM seemed to be much more genetically homogeneous than previously described. The *CNGB3* gene was by far the most important causal gene, and p.T383IfsX13 the most frequent mutation. The ACHM subtype did not predispose to a distinct genetic background, nor were any other apparent genotype–phenotype correlations. A fraction of patients showed evi-dence of progressive cone cell death in adult life. If gene therapy becomes a possibility for this disease in the future, we recommend implementation in early childhood.

SUPPLEMENTAL TABLE 1

Supplemental Table 1. Primers used for sequencing of the *CNGB3*, *CNGA3* and *GNAT2* genes.

Gene and exon	Forward	Reverse	Product size (basepairs)	Annealing temp.(°C)
	Sequence (5'→3')			
CNGB3				
Exon 1	ggcacagtcataaatacagaggg	ggagactatactaggatttgg	393	58
Exon 2	agtacatcataaacagtcaattt	gcattttcatcacctgacatg	425	58
Exon 3	ttggcctgaaggtgtctacc	gctcaaatatccactctcccc	400	62
Exon 4	tgccccaccatctgtagc	ccaaaagcagaccctgagaa	561	62
Exon 5	cggtgtttggttaagaaattc	ccctgtgactcaaagtcacag	309	58
Exon 6	acagtccagaggcagaatgg	caattatccatgcagatagcc	481	62
Exon 7	gagattggaaggaaccaacc	ttgagaggcagaaacttcagg	298	62
Exon 8	gccttaaaaagccccatgc	ccatctttctgccctcatca	397	62
Exon 9	ctataactacagggtagcaat	tcatatccctgccaaattcc	388	55
Exon 10	cagtcaagacattgccatcag	gcatttaccagccattgaatgg	430	60
Exon 11	cccaagaatagtggtctttcg	gatcaacagtgcttttccatt	385	58
Exon 12	cagggcattagaaggaagta	ctgtaaggtagcagagactag	340	58
Exon 13	aggtatggaggtccaataga	cctagagaaattatgtgga	405	56
Exon 14	cacacccaagtctatctgagc	actctgagagcacgttattgc	468	58
Exon 15	ggaggcaaacagtactcacg	ggtttgattgtgctgagagc	472	58
Exon 16	aatcacctggaccctcacc	ctctgagatagggagaaccg	357	58
Exon 17	cttgatcacagtgagatatg	acgcccactctaattccatt	410	58
Exon 18	tcttggtggtgatcttagcc	ccttgagaaacgaaaggcaa	543	58
CNGA3				
Exon 2	cttgatgagctggggtttgc	cccccacagtctagatcagc	283	60
Exon 3	tctcactcctggctgtgtcc	ccccatctagcactttttcc	279	60
Exon 4	agggaaagactggggtttgg	caaacaggatggagcaaagc	335	60
Exon 5	gtaatccctggtgaaatgg	gggagcaggagcactaagg	228	60
Exon 6	gccctaggctctctaaaacc	gggagaggtggagctctgg	274	60
Exon 7	ttacatgatccagcgtcttcc	taatgtcccatccaccatgc	294	60
Exon 8.1	gcatactgtgtagccgtgagg	ggttttgggacagactcctg	655	60
Exon 8.2	gttcaggattgggaacttgg	ccgtgaggcattcatattcg	331	60
Exon 8.3	gtgggtgttctgattttgc	cccaatatctcccttcttgc	390	60
Exon 8.4	gacacgctgaagaaggttcg	gctgcttcatcttcatctgg	559	60
Exon 8.5	ctggacaccctgcagacc	ttcaaccctgaccaagttcc	271	60

Supplemental Table 1. Continued

Gene and exon	Sequence (5'→3')		Product size (basepairs)	Annealing temp.(°C)
	Forward	Reverse		
GNAT2				
Exon 1	agttgaagtagggagtctca	tctctggctcatcttcccat	350	57
Exon 2	gtggaaatcgaaagcataag	tcttcaccctatcttgtctt	120	57
Exon 3	tcttcaccctatcttgtctt	ctgcttccacccttaaccac	210	57
Exon 4	tgtgaagttcttaaccaggt	ctagaagattgcttaagcat	240	57
Exon 5	gtctcttagcctcgtctgtg	tgtatccgagatgccctagg	220	57
Exon 6	gtatgttgggcatacctatg	tgttctaccaaagctgcttg	210	57
Exon 7	attctataagccaaatctga	agtctctactaaaaggcatt	250	57
Exon 8	tcagcaactaacaagggttc	atacctgaggaatggtgagg	270	57

Primers were designed using Primer3 software (http://frodo.wi.mit.edu/cgi-bin/primer3/primer3_www.cgi, April 2007) or using Exon Primer from the Genome Browser (http://genome.ucsc.edu/). Exon 1 of the *CNGA3* gene is non-coding.

REFERENCES

1. Michaelides M, Hardcastle AJ, Hunt DM, Moore AT. Progressive cone and cone-rod dystrophies: phenotypes and underlying molecular genetic basis. Surv Ophthalmol. 2006;51:232-58.

2. Michaelides M, Hunt DM, Moore AT. The cone dysfunction syndromes. Br J Ophthalmol. 2004;88:291-7.

3. Simunovic MP, Moore AT. The cone dystrophies. Eye. 1998;12:553-65.

4. Nishiguchi KM, Sandberg MA, Gorji N, et al. Cone cGMP-gated channel mutations and clinical findings in patients with achromatopsia, macular degeneration, and other hereditary cone diseases. Hum Mutat. 2005;25:248-58.

5. Pokorny J, Smith VC, Pinckers AJ, Cozijnsen M. Classification of complete and incomplete autosomal recessive achromatopsia. Graefes Arch Clin Exp Ophthalmol. 1982;219:121-30.

6. Khan NW, Wissinger B, Kohl S, Sieving PA. CNGB3 achromatopsia with progressive loss of residual cone function and impaired rod-mediated function. Invest Ophthalmol Vis Sci. 2007;48:3864-71.

7. Kohl S, Baumann B, Broghammer M, et al. Mutations in the CNGB3 gene encoding the beta-subunit of the cone photoreceptor cGMP-gated channel are responsible for achromatopsia (ACHM3) linked to chromosome 8q21. Hum Mol Genet. 2000;9:2107-16.

8. Kohl S, Baumann B, Rosenberg T, et al. Mutations in the cone photoreceptor G-protein alpha-subunit gene GNAT2 in patients with achromatopsia. Am J Hum Genet. 2002;71:422-5.

9. Wissinger B, Gamer D, Jagle H, et al. CNGA3 mutations in hereditary cone photoreceptor disorders. Am J Hum Genet. 2001;69:722-37.

10. Sundin OH, Yang JM, Li Y, et al. Genetic basis of total colourblindness among the Pingelapese islanders. Nat Genet. 2000;25:289-93.

11. Kohl S, Varsanyi B, Antunes GA, et al. CNGB3 mutations account for 50% of all cases with autosomal recessive achromatopsia. Eur J Hum Genet. 2005;13:302-8.

12. Johnson S, Michaelides M, Aligianis IA, et al. Achromatopsia caused by novel mutations in both CNGA3 and CNGB3. J Med Genet. 2004;41.

13. Rosenberg T, Baumann B, Kohl S, et al. Variant phenotypes of incomplete achromatopsia in two cousins with GNAT2 gene mutations. Invest Ophthalmol Vis Sci. 2004;45:4256-62.

14. Michaelides M, Aligianis IA, Ainsworth JR, et al. Progressive cone dystrophy associated with mutation in CNGB3. Invest Ophthalmol Vis Sci. 2004;45:1975-82.

15. Liu C, Varnum MD. Functional consequences of progressive cone dystrophy-associated mutations in the human cone photoreceptor cyclic nucleotide-gated channel CNGA3 subunit. Am J Physiol Cell Physiol. 2005;289:C187-98.

16. Bright SR, Brown TE, Varnum MD. Disease-associated mutations in CNGB3 produce gain of function alterations in cone cyclic nucleotide-gated channels. Mol Vis. 2005;11:1141-50.

17. Marmor MF. An international standard for electroretinography. Doc Ophthalmol. 1989;73:299-302.

18. Nathans J, Davenport CM, Maumenee IH, et al. Molecular genetics of human blue cone monochromacy. Science. 1989;245:831-8.

19. Nathans J, Maumenee IH, Zrenner E, et al. Genetic heterogeneity among blue-cone monochromats. Am J Hum Genet. 1993;53:987-1000.

20. Ahuja Y, Kohl S, Traboulsi EI. CNGA3 mutations in two United Arab Emirates families with achromatopsia. Mol Vis. 2008;14:1293-7.

21. Peng C, Rich ED, Varnum MD. Subunit configuration of heteromeric cone cyclic nucleotide-gated channels. Neuron. 2004;42:401-10.

22. Kaupp UB, Seifert R. Cyclic nucleotide-gated ion channels. Physiol Rev. 2002;82:769-824.

23. Ottschytsch N, Raes A, Van HD, Snyders DJ. Obligatory heterotetramerization of three previously uncharacterized Kv channel alpha-subunits identified in the human genome. Proc Natl Acad Sci U S A. 2002;99:7986-91.

24. Biel M, Seeliger M, Pfeifer A, et al. Selective loss of cone function in mice lacking the cyclic nucleotide-gated channel CNG3. Proc Natl Acad Sci U S A. 1999;96:7553-7.

25. Wissinger B, Muller F, Weyand I, et al. Cloning, chromosomal localization and functional expression of the gene encoding the alpha-subunit of the cGMP-gated channel in human cone photoreceptors. Eur J Neurosci. 1997;9:2512-21.

26. Michalakis S, Geiger H, Haverkamp S, et al. Impaired opsin targeting and cone photoreceptor migration in the retina of mice lacking the cyclic nucleotide-gated channel CNGA3. Invest Ophthalmol Vis Sci. 2005;46:1516-24.

Chapter 2b

**Progressive cone cell loss in achromatopsia.
An imaging study using
Spectral-Domain Optical Coherence Tomography**

ABSTRACT

Purpose: Achromatopsia (ACHM) is a congenital autosomal recessive cone disorder with a presumed stationary nature and only a few causative genes. Animal studies suggest that ACHM may be a good candidate for corrective gene therapy. Future implementation of this therapy in humans requires the presence of viable cone cells in the retina. In this study the presence of cone cells in ACHM was determined, as a function of age.

Methods: The appearance and thickness of all retinal layers were evaluated by spectral-domain optical coherence tomography (SD-OCT) in 40 ACHM patients (age range, 4–70 years) with known mutations in the *CNGB3*, *CNGA3*, and *PDE6C* genes. A comparison was made with 55 healthy age-matched control subjects.

Results: The initial feature of cone cell decay was loss of inner and outer segments with disruption of the ciliary layer on OCT, which was observed as early as 8 years of age. Cone cell loss further progressed with age and occurred in 8 (42%) of 19 patients below 30 years and in 20 (95%) of 21 of those aged 30+ years. Retinal thickness was significantly thinner in the fovea of all patients (126 μm in ACHM vs. 225 μm in the control; P <0.001) and correlated with age ($\beta = 0.065$; $P = 0.011$). Foveal hypoplasia was present in 24 (80%) of 30 patients and in 1 of 55 control subjects.

Conclusions: ACHM is not a stationary disease. The first signs of cone cell loss occur in early childhood. If intervention becomes available in the future, the present results imply that it should be applied in the first decade.

INTRODUCTION

Achromatopsia (ACHM) is a congenital cone photoreceptor disorder with a presumed stationary course. The estimated prevalence is 1 in 30,000. ACHM is characterized by low visual acuity, photophobia, nystagmus, severe color vision defects, and a presumably normal macular appearance.[1] The inheritance is autosomal recessive, and the known responsible genes are *CNGA3*, *CNGB3*, *GNAT2,* and *PDE6C*.[2–5] Together, these genes explain the majority (>90%) of all ACHM cases. Although it is known that these genes code for essential proteins in the cone phototransduction cascade, repair of the gene defects is not feasible as yet.

A promising therapy that is currently under investigation is cone-targeted gene therapy. The first results of animal studies showed that *CNGB3, CNGA3*, or *GNAT2* knockout mice and dogs responded well to adenoassociated virus gene therapy. In these rescued animals, cone ERG amplitudes recovered to nearly normal levels.[6,7] The next step in this development will be gene therapy in humans with cone dysfunction. For that purpose, it is crucial to know whether the nonfunctional cones are present and still viable in the macula.[8]

The purpose of this study was to investigate the presence of cone cells as a function of age in ACHM. We compared foveal morphology in 40 ACHM patients of various ages with that in 55 healthy age-matched control subjects using a new spectral domain optical coherence tomography system (SD-OCT; Spectralis; Heidelberg Engineering, Heidelberg, Germany). This device has high reproducibility[9] and better resolution than conventional OCT, and its images correlate well with histopathology in vivo.[10]

METHODS

Study Population

ACHM patients (N=40; N=77 eyes) were ascertained from the Dutch ACHM patient organization (AchroNed) as well as from various ophthalmogenetic centers in The Netherlands (Erasmus Medical Center, Rotterdam; The Rotterdam Eye Hospital, Radboud; Nijmegen Medical Center, Nijmegen; and Sensis Institute, Grave). Diagnostic criteria were poor visual acuity since birth, congenital nystagmus, photophobia, color vision disturbances in three axes, and absent or residual cone responses with normal rod responses on full-field electroretinogram (ERG). All patients were screened for mutations in the *CNGA3*, *CNGB3, GNAT2*, and *PDE6C* genes. Control subjects (N=55; N=110 eyes) were unrelated persons accompanying patients or healthcare workers derived from

the Erasmus Medical Center who had best corrected visual acuity (BCVA) of 0.8 (20/25) or higher and no eye diseases. Control subjects were age-matched with patients per decade. The study was approved by the Medical Ethics Committee of Erasmus Medical Center and adhered to the tenets of the Declaration of Helsinki. All patients provided signed, informed consent for participation in the study, retrieval of medical records, and use of blood and DNA for research.

Clinical Examination and OCT

All ACHM patients underwent a complete ophthalmic examination, including best corrected Snellen visual acuity, refractive error, color vision testing (HRR, Ishihara), ERG, and 35° fundus photography centered on the macula (TRC 50IX; Topcon, Tokyo, Japan). We performed SD-OCT on all eyes with the Heidelberg Spectralis (HRA+OCT ver. 4.0, with TruTrack eye tracking and Heidelberg Noise Reduction; Heidelberg Engineering) according to published procedures.[11] Allied software (Eye Explorer, ver. 1.61; Heidelberg Engineering) was used for all measurements. We performed a single-section scan (one B-scan, 30°, 768 pixels) to obtain a longitudinal section across the center of the macula, and we performed a volume scan (19 B-scans, 20° x 15°, 512 pixels, 12 frames per B-scan) to ensure capturing the center of the fovea. When the nystagmus in the ACHM patients was so severe that it impaired the tracking system of the OCT, settings for resolution, speed, the number of B-scans, and the number of frames per B-scan were adjusted.

Retinal thickness measurements in the fovea included the following structures: outer nuclear layer (ONL), inner and outer segments of the cone cells, and retinal pigment epithelium (RPE). Measurements were determined per ETDRS area12 using the automated measurements from the software. We calculated retinal thickness in the fovea manually by searching the thinnest point in the fovea (Eye Explorer tool; Heidelberg Engineering). We placed points to outline the boundaries of the foveal pit and then used the system's measurement tool to calculate depth and width of the fovea. In subjects with foveal hypoplasia or a hypodense area (bubble), measurements were performed manually as well. In these cases, we placed points to outline the boundaries of the extra retinal layers or the bubble, measured these with the system's measurement tool, and then subtracted the results from the total retinal thickness given by the automated measurements.

Statistical Analysis

Frequency differences between ACHM patients and control subjects were compared by using Student's *t*-test for continuous variables and one-way ANOVA for categorical variables. First, we calculated between- eye correlations for the OCT measurements. Correlations between continuous variables (e.g., foveal thickness and disease status; ACHM and control) were calculated with a bivariate Pearson's correlation test; correla-

tions between categorical variables (e.g., macular appearance) were analyzed with the Spearman correlation analysis. Differences in the presence of cone and RPE cell disruptions were analyzed with the chi-square test. In the cases, we further examined, by linear regression analysis, whether age, visual acuity, and/or macular appearance influences foveal thickness.

RESULTS

Clinical Features

Baseline characteristics of the study population are presented in Table 1. We examined 77 eyes of 40 patients with ACHM and all 110 eyes of 55 control subjects. All patients showed pendular nystagmus, were photophobic, and had BCVA of 0.05 to 0.20. Refractive errors (<2 D or >2 D) were significantly more present among the patients (24/16 vs. 18/37; P = 0.004). Gene defects in the patients were mostly present in the *CNGB3* gene (83%; 33/40). We did not find a genotype–phenotype correlation (i.e., the genes were equally distributed among those with and without OCT abnormalities).

Table 1. Clinical characteristics of patients with achromatopsia and age-matched controls

Variable	Achromatopsia (N total = 40)	Controls (N total = 55)
Mean age (SD) ‡	34 (19)	32 (18)
0-9 years	6	6
10-19 years	6	7
20-29 years	4	13
30-39 years	8	9
40-49 years	8	9
50-59 years	5	7
60-70 years	3	4
Male	21	23
Female	19	32
Nystagmus	40	0*
BCVA < 0.10 †	4	0*
BCVA ≥ 0.10 †	36	55*
Emmetropia	16	37*
Myopia	11	14*
Hypermetropia	13	4*

Table 1. Continued

	Achromatopsia	Controls
	(*N total* = 40)	(*N total* = 55)
Molecular defect		
CNGB3 mutations	33	
CNGA3 mutations	2	
PDE6C mutations	5	
No mutations	0	55*

*$P<0.05$ for the difference between achromatopsia patients and controls
† BCVA: Best Corrected Visual Acuity
‡ SD: Standard Deviation

OCT Findings

All OCT parameters correlated highly between the right and left eyes ($R^2 \geq 0.90$). To ensure the best images for analysis, we used the eye that was least affected by congenital nystagmus for all subsequent measurements. Observations on OCT and macular appearance are summarized in Table 2.

Table 2: Measurements of the macular appearance on fundus photographs and on OCT in achromatopsia patients and controls

	Achromatopsia N total=40	Controls N total=55	*P*
Macular appearance on fundus photographs, N			
No aberrations	15	38	
Foveal reflex absent	6	17	
(Subtle) RPE alterations	13	0	<0.001
Bull's eye with RPE degeneration	3	0	
Area of RPE atrophy	3	0	
Macular appearance on OCT*, N			
Retinal thickness of ETDRS† area 1 (fovea), mean (µm)			

Age stratum	N total			
0-9 yrs	6	163 (SD‡ 22)	215 (SD 17)	
10-19 yrs	6	176 (SD 37)	217 (SD 6)	
20-29 yrs	5	113 (SD 16)	222 (SD 13)	
30-39 yrs	7	116 (SD 55)	229 (SD 12)	
40-49 yrs	8	91 (SD 82)	230 (SD 22)	<0.001
50-59 yrs	5	103 (SD 53)	223 (SD 19)	
60-70 yrs	3	126 (SD 28)	218 (SD 7)	
Total	40	127 (SD 59)	222 (SD 14)	

Table 2. Continued

		Achromatopsia N total=40	Controls N total=55	*P*
Retinal thickness of ETDRS area 2-9 (parafovea), mean (µm)				
0-9 yrs	6	301 (SD 8)	354 (SD 7)	
10-19 yrs	6	305 (SD 14)	352 (SD 13)	
20-29 yrs	5	290 (SD 22)	354 (SD 15)	
30-39 yrs	7	289 (SD 25)	363 (SD 27)	
40-49 yrs	8	301 (SD 17)	367 (SD 17)	<0.001
50-59 yrs	5	287 (SD 23)	368 (SD 6)	
60-70 yrs	3	308 (SD 8)	356 (SD 7)	
Total	40	297 (SD 19)	359 (SD 16)	
Foveal hypoplasia , N				
0-9 yrs	6	2	0	
10-19 yrs	6	3	0	
20-29 yrs	5	2	0	
30-39 yrs	7	5	0	
40-49 yrs	8	5	1	<0.001
50-59 yrs	5	4	0	
60-70 yrs	3	3	0	
Total	40	24	1	
Loss of cone inner- and outer segments, N				
0-9 yrs	6	1	0	
10-19 yrs	6	1	0	
20-29 yrs	5	4	0	
30-39 yrs	7	8	0	
40-49 yrs	8	6	0	<0.001
50-59 yrs	5	5	0	
60-70 yrs	3	3	0	
Total	40	28	0	
Intraretinal bubble, N				
0-9 yrs	6	1	0	
10-19 yrs	6	1	0	
20-29 yrs	5	3	0	
30-39 yrs	7	7	0	
40-49 yrs	8	4	0	<0.001
50-59 yrs	5	5	0	
60-70 yrs	3	3	0	
Total	40	24	0	

Table 2. Continued

		Achromatopsia N total=40	Controls N total=55	*P*
RPE atrophy, N				
0-9 yrs	6	0	0	
10-19 yrs	6	0	0	
20-29 yrs	5	0	0	
30-39 yrs	7	0	0	
40-49 yrs	8	2	0	<0.001
50-59 yrs	5	2	0	
60-70 yrs	3	3	0	
Total	40	7	0	

*OCT: Optical Coherence Tomography
†ETDRS: Early Treatment Diabetic Retinopathy Study
‡SD: Standard Deviation

Loss of cone inner and outer segments (IS and OS) with interruption of the ciliary layer (the connecting cilium of the photoreceptors) was the most frequent retinal abnormality among the patients (Figures 1a, 1b). This feature was present in 28 (70%) of 40 of the ACHM patients and showed a strong association with age. In the age group 0 to 10 years, only one (1/7; 14%) child had this feature, whereas in the oldest age group, all patients (7/7, 100%) showed this characteristic (Figure 2). Fundus photographs of patients with only loss of IS and OS (N=2) showed no abnormalities.

A bubble, an optical empty cavity, was visible in the cone cell layer in 24 (60%) of 40 of the ACHM patients (Figures 1c, 1d). Smaller bubbles coincided with loss of OS, whereas bigger bubbles also involved the IS of cone photoreceptor cells. Fundus photographs of patients with a bubble and intact RPE layer on OCT (N=19) showed RPE mottling (N=11), no foveal reflexes (N=2), or no abnormalities (N=6). The presence of a bubble on OCT was not significantly related to BCVA.

Disruption of the RPE cell layer was visible in 7 (18%) of 40 of the ACHM patients (Figures 1e, 1f) and was present only in those beyond 40 years of age. Fundus photographs evidenced the RPE disruption in the majority of cases (6/7; 86%). BCVA was not significantly reduced.

We determined the total thickness of the ONL, IS, and OS of the cone photoreceptors and the RPE layer in the fovea and of all retinal layers in the nine ETDRS areas. These layers were significantly thinner in the patients (mean thickness of 126 μm in foveas of the patients; 225 μm in foveas of the control subjects, $P < 0.001$), and the reduction correlated significantly with age (1.2 μm [SE 0.33]) decrease per year; $β = 0.065$; $P = 0.011$).

Figure 1. Fundus photographs and OCT images showing progressive loss of cones in patients with ACHM.

(a) Normal OCT in a 9-year-old patient with mutations in the *CNGA3* gene (c.847C>T / c.1709G>T).

(b) Loss of cone photoreceptor inner and outer segments with disruption of the ciliary layer on OCT and normal macular appearance on the fundus photograph in an 8-year-old patient. Mutations were detected in the *CNGB3* gene (c.1148delC / c.991-3T>G).

(c) Small bubble with absent cone photoreceptors in the fovea on OCT and normal macular appearance on the fundus photograph in a 15-year-old patient with mutations in the *CNGB3* gene (c.1148delC / c.1148delC).

(d) Large bubble with absent cone photoreceptors in the fovea on OCT and normal macular appearance on the fundus photograph in a 21-year-old patient with mutations in the *CNGB3* gene (c.1148delC / c.1148delC).

(e) Foveal bubble and moderate RPE cell layer disruption on OCT and macular RPE atrophy on the fundus photograph in a 49-year-old patient with mutations in the *CNGA3* gene (p.D260N / p.D162V).

(f) Complete cone and RPE cell layer disruption in the fovea on OCT and macular RPE atrophy on the fundus photograph in a 56-year-old patient with mutations in the *CNGB3* gene (c.1148delC / c.886–896del11insT).

NFL, nerve fiber layer; GCL, ganglion cell layer; IPL, inner plexiform layer; INL, inner nuclear layer; OPL, outer plexiform layer; ONL, outer nuclear layer; IS/OS, inner segments and outer segments of the cones; CC, ciliary layer (connecting cilium); RPE, retinal pigment epithelium.

The patients without any signs of retinal degeneration (all layers intact on OCT; N=12) also had thinner layers (mean thickness, 179 μm in foveas of the patients; 225 μm in foveas of the control subjects; $P = 0.05$). The control subjects all had a foveal thickness of at least 215 μm and showed no reduction with age. Refractive error did not correlate with foveal thickness ($P = 0.822$).
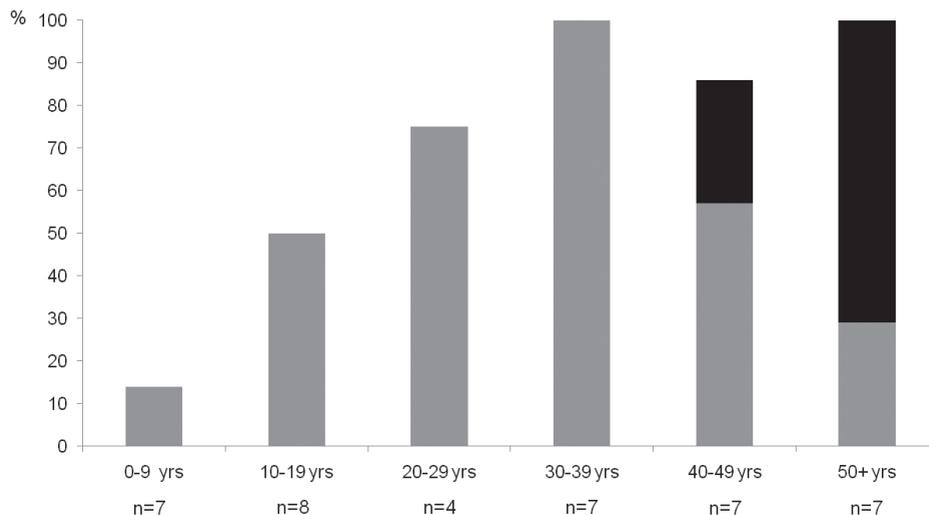
Figure 2. The proportion of ACHM patients with cone cell degeneration (*gray*) and RPE atrophy (*black*) per age group in percentages. The total number of patients per stratum is given below the age range. The youngest patient with signs of cone cell decay was 8 years old.

Foveal Hypoplasia

In the fovea of 80% (24/30) of the ACHM patients, we noted multiple ganglion cell layers. These extra layers indicate a lack of formation of the foveal pit (i.e., foveal hypoplasia). This phenomenon was always present bilaterally. It occurred in all age groups of patients and in one 51-year-old control subject with a Snellen visual acuity of 1.25 in both eyes, no color vision defects, and a normal macular appearance. Those with foveal hypoplasia had a less steep foveal slope than those with a normal fovea (92 μm vs. 133 μm; $P = 0.02$), but had no differences in foveal width (2004 μm vs. 2126 μm; $P = 0.20$) (Figure 3). Fundus photographs showed absent foveal reflexes in only 50% of patients with hypoplasia and revealed normal macular appearance in the remaining half.
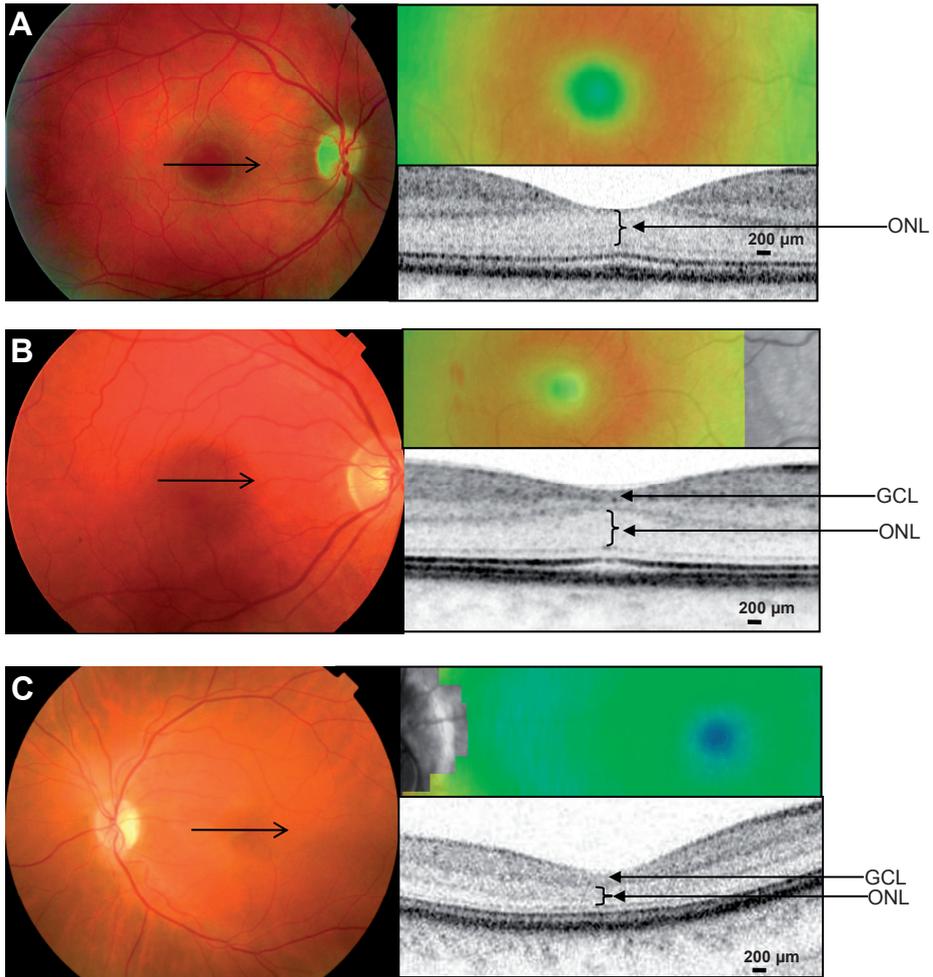
Figure 3. Fundus photographs and OCT images showing foveal hypoplasia.

(a) Normal OCT and macula appearance in a 26-year-old control subject; outer nuclear layer (ONL) thickness, 100 μm.

(b) Foveal dip hypoplasia on OCT and no abnormalities on fundus photograph in a 51-year-old control subject with normal (103 μm) ONL thickness.

(c) Foveal hypoplasia on OCT and no abnormalities on fundus photograph in a 27-year-old patient with ACHM and mutations in the *CNGB3* gene (c.1148delC / c.1148delC). Note the decreased thickness of the ONL (70 μm).

DISCUSSION

Our study provides evidence that cone cells die progressively in ACHM. The first signs of decay were loss of IS and OS with a disruption of the ciliary layer on OCT, followed by appearance of an evolving bubble with cell loss in the cone photoreceptor layer. The end stage was characterized by atrophy of the RPE. This cascade of events had its onset predominantly in the second decade and showed a strong association with age thereafter. Before any signs of decay were visible, the foveal and parafoveal regions were already significantly thinner in the ACHM patients than in the age-matched control subjects. With the appearance of cone cell degeneration, thinning of the retina became more pronounced.

A strength of this study was the use of the recently developed Spectralis SD-OCT (Heidelberg Engineering). The resolution of this device is 50 times higher than that of the conventional Stratus OCT (Carl Zeiss Meditec, Oberkochen, Germany), making it possible to distinguish the different retinal layers and to analyze changes on a cellular level.[13] Moreover, the SD-OCT has settings that are adjustable for the individual patient, facilitating measurements in patients with congenital nystagmus and in young children.[9] A limitation of the study was the relatively small sample size and its cross-sectional design. Only larger studies with longer follow-up can overcome the problems. Nevertheless, to our knowledge, the current investigation is the largest imaging study of ACHM to date. The wide age range in subjects who were otherwise homogeneous in genotype and disease onset enabled interpretation of the clinical course over time.

Investigations of retinal morphology in ACHM have been scarce. Former histopathology studies of individual patients contradict each other on the presence and number of cones in the fovea.[14,15] Falls et al.[14] described a normal number of foveal cones with aberrant morphology in one ACHM patient. In contrast, Glickstein and Heath[15] reported a patient who had no detectable foveal cones. Two in vivo imaging studies in which the Stratus OCT was used had disparate results, as well. One reported a normal macular thickness, whereas the other showed a significant decrease.[16,17] We believe that these contradictory findings may result from differences in the age of the patients. In favor of this view are the results from a study of knock-out mice that had no CNG3 channels. Cones were present at the age of two months, but no cones were detected at eight months.[18,19]

Foveal hypoplasia was a frequent phenomenon in the ACHM patients in our study (24/30; 80%). It has been reported in histology studies, but not yet confirmed in in vivo imaging studies.[15,20] Foveal hypoplasia is not specific for ACHM, but is present in other

congenital eye disorders, such as ocular albinism and aniridia.[21,22] In the healthy eye, foveal development takes place at 24 to 36 weeks of gestation by thinning of the ganglion cell layers and thickening of the ONL. The final relocation of the inner nuclear and ganglion cell layers to the periphery takes places at four months after birth, resulting in uncovered foveal cone nuclei thereafter.[23] Our ACHM patients with foveal hypoplasia appeared not to have had these early foveal developments. They showed no thickening of the ONL, persistent ganglion cell layers, and a significantly less steep foveal slope (Figure 3). Remarkably, one control subject also had foveal hypoplasia with extra ganglion cell layers. The difference from the ACHM patients was that this person had a normal thickness of the ONL. We do not know the exact mechanism behind this aberrant retinal development. However, the range in the measurements of the width (range, 1665–2629 µm; SD: 257) and the slope of the fovea (range, 91–173 µm; SD: 20) was large in our healthy control subjects, indicating that normal foveal development varies considerably among subjects with normal visual acuity. The diagnosis of foveal hypoplasia was by far more sensitive on OCT than on fundus photographs, suggesting that aberrant foveal development may be more common than presumed. Half of the ACHM patients with foveal hypoplasia on OCT showed a normal macular appearance. In these patients, a minor slope was often present, giving the impression of a normal foveal reflex (Figure 3). What do our results indicate for the application of future therapies? They imply that the foveal cones of ACHM patients, although reduced in number, are morphologically intact at birth. However, after the first decade, cone cell loss occurs progressively in a relatively short time. Therefore, our results suggest that if gene therapy becomes available in the future, earlier application may be preferable to later application.

In conclusion, our study provides profound evidence that ACHM is not a stationary disease, but a disorder that shows progressive loss of cone photoreceptors. SD-OCT is a valuable, noninvasive tool for visualizing the severity of cone decay and a helpful means of giving insight to the cellular changes present in ACHM.

REFERENCES

1. Michaelides M, Hardcastle AJ, Hunt DM, Moore AT. Progressive cone and cone-rod dystrophies: phenotypes and underlying molecular genetic basis. Surv Ophthalmol. 2006;51:232-58.

2. Kohl S, Baumann B, Broghammer M, et al. Mutations in the CNGB3 gene encoding the beta-subunit of the cone photoreceptor cGMP-gated channel are responsible for achromatopsia (ACHM3) linked to chromosome 8q21. Hum Mol Genet. 2000;9:2107-16.

3. Wissinger B, Gamer D, Jagle H, et al. CNGA3 mutations in hereditary cone photoreceptor disorders. Am J Hum Genet. 2001;69:722-37.

4. Kohl S, Baumann B, Rosenberg T, et al. Mutations in the cone photoreceptor G-protein alpha-subunit gene GNAT2 in patients with achromatopsia. Am J Hum Genet. 2002;71:422-5.

5. Thiadens AAHJ, den Hollander AI, Roosing S, et al. Homozygosity mapping reveals PDE6C mutations in patients with early-onset cone photoreceptor disorders. Am J Hum Genet. 2009; 85:240-7.

6. Alexander JJ, Umino Y, Everhart D, et al. Restoration of cone vision in a mouse model of achromatopsia. Nat Med. 2007;13:685-7.

7. Pang JJ, Alexander JJ, Lei B, et al. Achromatopsia as a potential candidate for gene therapy. Adv Exp Med Biol. 2010;664:639-46.

8. Buch PK, Bainbridge JW, Ali RR. AAV-mediated gene therapy for retinal disorders: from mouse to man. Gene Ther. 2008;15:849-57.

9. Menke MN, Dabov S, Knecht P, Sturm V. Reproducibility of retinal thickness measurements in healthy subjects using spectralis optical coherence tomography. Am J Ophthalmol. 2009;147:467-72.

10. Grover S, Murthy RK, Brar VS, Chalam KV. Normative data for macular thickness by high-definition spectral-domain optical coherence tomography (spectralis). Am J Ophthalmol. 2009;148:266-71.

11. Nassif N, Cense B, Park BH, et al. In vivo human retinal imaging by ultrahigh-speed spectral domain optical coherence tomography. Opt Lett. 2004;29:480-2.

12. Photocoagulation for diabetic macular edema. Early Treatment Diabetic Retinopathy Study report number 1. Early Treatment Diabetic Retinopathy Study research group. Arch Ophthalmol. 1985;103:1796-806.

13. Drexler W, Morgner U, Ghanta RK, Kärtner FX, Schuman JS, Fujimoto JG. Ultrahigh-resolution ophthalmic optical coherence tomography. Nat Med. 2001;7:502.

14. Falls HF, Reimer Wolter J, Alpern M, Arbor A. Typical total monochromacy. A histological and psychophysical study. Arch Opthalmol. 1965;74:610-616.

15. Glickstein M, Heath GG. Receptors in the monochromat eye. Vision Res. 1975;15:633-636.

16. Barthelmes D, Sutter FK, Kurz-Levin MM, et al. Quantitative analysis of OCT characteristics in patients with achromatopsia and blue-cone monochromatism. Invest Ophthalmol Vis Sci. 2006;47:1161-6.

17. Varsányi B, Somfai GM, Lesch B, Vámos R, Farkas A. Optical coherence tomography of the macula in congenital achromatopsia. Invest Ophthalmol Vis Sci. 2007;48:2249-53.

18. Michalakis S, Geiger H, Haverkamp S, et al. Impaired opsin targeting and cone photoreceptor migration in the retina of mice lacking the cyclic nucleotide-gated channel CNGA3. Invest Ophthalmol Vis Sci. 2005;46:1516-24.

19. Biel M, Seeliger M, Pfeifer A, et al. Selective loss of cone function in mice lacking the cyclic nucleotide-gated channel CNG3. Proc Natl Acad Sci U S A. 1999;96:7553-7.

20. Harrison K, Hoefnagel D, Hayward JN.Congenital total color blindness: a clinic pathological report. Arch Ophthalmol. 1960;64:685-692.

21. Holmström G, Eriksson U, Hellgren K, Larsson E. Optical coherence tomography is helpful in the diagnosis of foveal hypoplasia. Acta Ophthalmol. 2009;2:1-4.

22. Chong GT, Farsiu S, Freedman SF, et al. Abnormal foveal morphology in ocular albinism imaged with spectral-domain optical coherence tomography. Arch Ophthalmol. 2009;127:37-44.

23. Provis JM, Hendrickson AE. The foveal avascular region of developing human retina. Arch Ophthalmol. 2008;126:507-11.
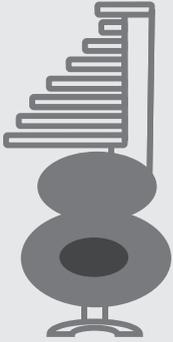
Chapter 3

Cone and Cone-rod dystrophy
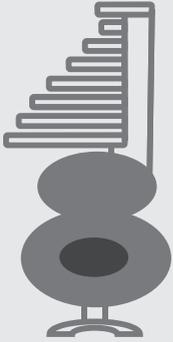
Chapter 3a

**Comprehensive analysis of the achromatopsia genes
CNGA3 and *CNGB3* in progressive cone dystrophy**

ABSTRACT

Objective: To investigate whether the major achromatopsia genes (*CNGA3* and *CNGB3*) play a role in the cause of progressive cone dystrophy (CD).

Design: Prospective multicenter study.

Participants: Probands (N=60) with autosomal recessive (ar) CD from various ophthalmogenetic clinics in the Netherlands.

Methods: All available ophthalmologic data from the arCD probands were registered from medical charts and updated by an additional ophthalmologic examination. Mutations in the *CNGA3* and *CNGB3* genes were analyzed by direct sequencing.

Main Outcome Measures: *CNGA3* and *CNGB3* mutations and clinical course in arCD probands.

Results: In three arCD probands (3/60; 5%) we found two mutations in the *CNGB3* gene. Two of these probands had compound heterozygous mutations (p.R296YfsX9/p.R274VfsX12 and p.R296YfsX9/c.991-3T>G). The third proband revealed homozygous missense mutations (p.R403Q) with two additional variants in the *CNGA3* gene (p.E228K and p.V266M). These probands did not have a congenital nystagmus, but had a progressive deterioration of visual acuity, color vision, and photopic electroretinogram, with onset in the second decade. In six other unrelated probands, we found six different heterozygous amino acid changes in the *CNGA3* (N=4) and *CNGB3* (N=2) gene.

Conclusions: The *CNGB3* gene accounts for a small fraction of the later onset progressive form of cone photoreceptor disorders, and *CNGA3* may have an additive causative effect. Our data indicate that these genes are involved in a broader spectrum of cone dysfunction, and it remains intriguing why initial cone function can be spared despite similar gene defects.

INTRODUCTION

Cone dystrophy (CD) is a progressive cone disorder with an estimated prevalence of 1:30,000 to 1:40,000. Patients have normal cone function initially, but present with visual loss and color vision disturbances in the first or second decade.[1–3] Macular abnormalities can be present, and the optic nerve may show a variable degree of temporal pallor. On electroretinogram (ERG), cone responses progressively deteriorate and rod responses are initially normal, but can diminish slightly over time. Although the course of disease may vary, the visual acuity generally worsens to legal blindness before middle age.

For CD, several genes have been identified for the autosomal dominant[4–6] and X-linked forms,[7,8] but little is known about the genetic causes of the most prevalent autosomal recessive (arCD) form. Three genes have been implicated in this form: the *ABCA4*, *CAC-NA2D4,* and *KCNV2* genes.[9–12] They play a role in only a fraction of patients; thus, most patients with arCD have an unknown genetic cause.

In contrast with the progressive nature of CD, achromatopsia is a congenital cone disorder. The estimated prevalence is 1:30,000, and the inheritance is autosomal recessive.[13,14] The clinical course is characterized by low visual acuity, nystagmus, photophobia, severe color vision defects, and no recordable or only residual cone function on ERG. The genetic basis of achromatopsia has been elucidated to a large extent during the last decade. Three genes have been implicated: *CNGA3, CNGB3*, and *GNAT2*.[15–18] The contribution of the *CNGB3* gene in achromatopsia varies per population, but it explains the majority of achromatopsia cases (50-80%) in The Netherlands and Germany.[19,20]

The *CNGA3* and *CNGB3* genes are cone-specific and code for the α and β subunits of the cyclic nucleotide gated channel type 3 (CNG3), respectively. They are located on the membrane of cone outer segments and play an important role during the phototransduction cascade. In the dark, high levels of cGMP open the channel, facilitate free flow of ions, and prohibit formation of an action potential. In the presence of light, cGMP levels decrease, resulting in closure of the channel, hyperpolarization of the cell, and initiation of phototransduction.[21] We hypothesize that genes with such a vital role for cone function also may be involved in other disorders in which cones are primarily affected. On this subject, only one study reported mutations in *CNGB3* in three relatives with arCD[22]; and one study described a heterozygous *CNGA3* mutation in one patient with CD.[16] In our study, we expanded the possible role of *CNGA3* and *CNGB3* in cone photoreceptor disorder by investigating a large series of patients with arCD for mutations in these genes.

PATIENTS AND METHODS

Study Population

Patients (N=60; 65% were male, age range 10-79 years, mean age 39 years, standard deviation 16 years) who had been diagnosed with arCD were ascertained from various ophthalmogenetic centers in The Netherlands. Inclusion criteria for the study were progressively deteriorating visual acuity, color vision disturbances in three axes, decreasing cone responses over time with normal or only slightly reduced rod responses on ERG, and no presence of nystagmus. The study was approved by the Medical Ethics Committee of Erasmus Medical Center and adhered to the tenets of the Declaration of Helsinki. All participants provided signed, informed consent for participation in the study, retrieval of medical records, and use of blood and DNA for research.

Clinical Examination

All patients received a questionnaire that addressed the medical history and family pedigree. Medical charts were retrieved from their ophthalmologists, and all available data on Snellen visual acuity, color vision (American Optical Hardy-Rand-Rittler Test, Ishihara Test for Color Blindness, or Lanthony Panel D-15 Test), slit-lamp and fundus examination, and ERGs were collected. Color vision defects were classified as mild, moderate, or severe in the three color axes (red, green, and blue). Patients with incomplete or unavailable data from the last five years were invited for an additional ophthalmologic examination, ERG, and fundus photography. Electroretinograms incorporated the recommendations of the International Society for Clinical Electrophysiology of Vision.[23]

Molecular Genetic Analysis

Blood samples were obtained from probands, affected relatives, and parents. DNA was isolated from peripheral blood lymphocytes by standard procedures. The coding region and intron/exon boundaries of the *CNGA3* and *CNGB3* genes were amplified by polymerase chain reaction using the conditions and primer sequences provided in Supplemental Table 1. Direct sequencing was performed on sequence analyzer 3730 (Applied Biosystems, Inc., Foster City, CA) with sequence analysis software (Vector NTI Advance, version 10; Invitrogen Corp., Carlsbad, CA). Segregation analysis was performed when mutations were detected.

RESULTS

Mutation Analysis

Table 2 shows the mutations that were detected. We found two variants in the *CNGB3* gene in 3 of 60 patients (5%) and confirmed their independent segregation in the families (Figure 1). In two patients, the mutations affected exonic splicing and caused a frameshift; and in one patient the mutation caused an amino acid change mutation, p.R403Q. This variant could not be detected in 100 ethnically matched control subjects. One patient had two additional variants in the *CNGA3* gene. Segregation analysis in this family (Figure 1) showed that the unaffected sister of the proband had the two *CNGA3* variants without a *CNGB3* variant, whereas the unaffected children were heterozygous for the *CNGB3* variant and one *CNGA3* variant. This suggests that the pathogenicity was predominantly caused by the *CNGB3* variants. One missense variant, p.V266M, was novel. Neither *CNGA3* variant could be detected in 100 ethnically matched control subjects. In two other unrelated probands, we found two different heterozygous mutations in the *CNGB3* gene: c.1148delC (p.T383IfsX13) and c.1208G>A (p.R403Q). In four other unrelated probands we detected four different *CNGA3* variants: c.1856C>T (p.A619V); c.284C>T (p.P95L); c.1618G>A (p.V540I); and c.1694C>T (p.T565M). In these patients, we did not find a second variant on the other allele in the coding region of the *CNGA3, CNGB3,* and *GNAT2* genes, despite complete sequencing (Table 2).
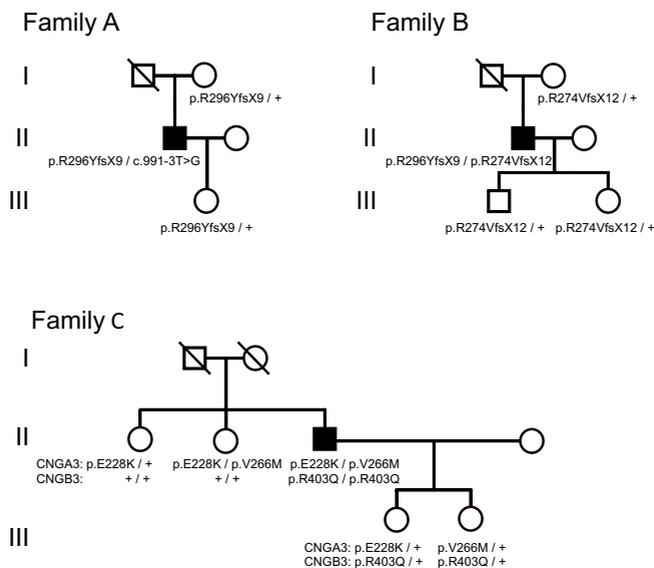

Figure 1. Pedigrees of three families with progressive autosomal recessive cone dystrophy showing segregation of *CNGA3* and *CNGB3* gene mutations. Unaffected men and women (*open square* and *circle*); affected men and women (*black square* and *circle*); deceased individuals (*dashed symbols*).

Table 2. Mutations in the *CNGA3* and *CNGB3* genes in three probands with autosomal recessive progressive cone dystrophy and in the six unrelated probands with a heterozygous variant in these genes.

Nr. Patient	CNGB3 allele 1			CNGB3 allele 2			CNGA3 allele 1			CNGA3 allele 2		
	Exon	DNA variant	Protein change	Exon	DNA variant	Protein change	Exon	DNA variant	Protein change	Exon	DNA variant	Protein change
A-II-1	7	c.886_896del11insT	p.R296YfsX9	9	c.991-3T>G	splice defect						
B-II-1	7	c.886_896del11insT	p.R296YfsX9	6	c.819_826del8	p.R274VfsX12						
C-II-3	11	c.1208G>A	p.R403Q	11	c.1208G>A	p.R403Q	8	c.682G>A	p.E228K	8	c.796G>A	p.V266M
1	10	c.1148delC	p.T383IfsX13									
2	11	c.1208G>A	p.R403Q									
3							8	c.1856C>T	p.A619V			
4							4	c.284C>T	p.P95L			
5							8	c.1618G>A	p.V540I			
6							8	c.1694C>T	p.T565M			

Clinical Findings

Clinical findings are summarized in Table 3. The three probands with two variants had a progressive deterioration of visual acuity, color vision, and photopic ERG since their teens. Two patients had passed their driving examination at age 18 years, with a best-corrected visual acuity of at least 0.50 decimals Snellen. In all three patients, the best corrected visual acuity deteriorated rapidly in the second decade. They did not have a congenital nystagmus. The macular appearance varied in each patient. Two patients showed degeneration of the macula over time, one patient had progressive pigmentary changes since age 10 years, one patient developed a bull's eye maculopathy in the second decade, and one patient still had a normal macular appearance at the age of 45 years. The optic discs did not show any abnormalities in the three probands; no temporal pallor was apparent (Figure 2).
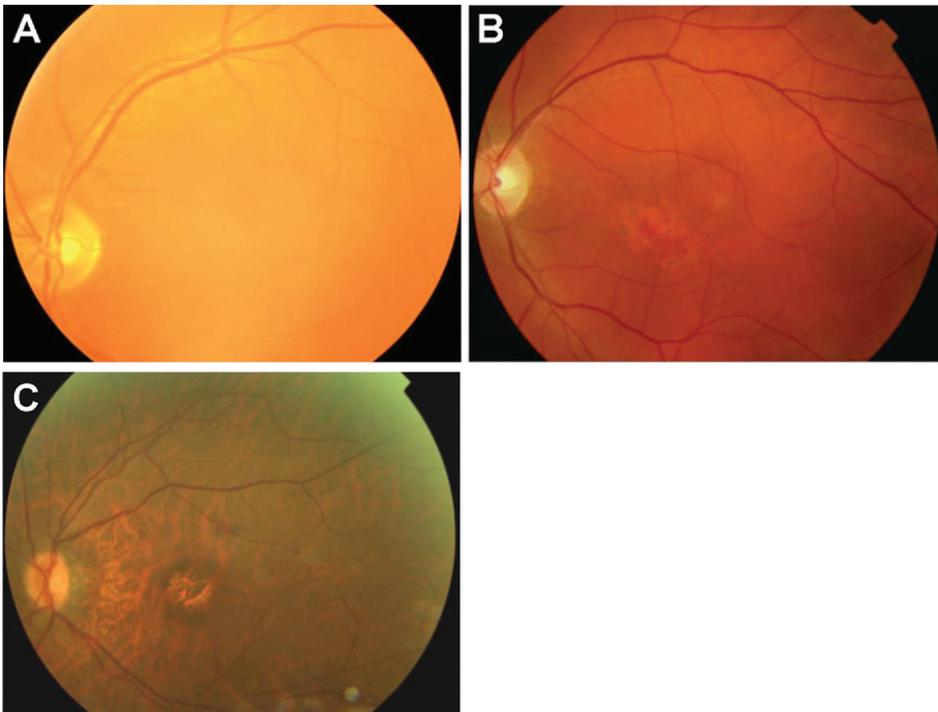

Figure 2. Fundus appearance of probands with cone dystrophy and mutations in the *CNGA3* and *CNGB3* genes.
(a) Fundus photograph of the left eye of proband A-II-1, performed at age 45 years. No macular abnormalities are apparent.
(b) Fundus photograph of the left eye of proband B-II-1, performed at age 57 years, showing pigmentary changes in the macular region.
(c) Fundus photograph of the left eye of proband C-II-3, performed at age 47 years, showing a bull's eye maculopathy with atrophy of retinal pigment epithelium.

Table 3 Clinical findings at first and last exam of three probands with autosomal recessive progressive cone dystrophy and mutations in the *CNGA3* and *CNGB3* genes.

Patient No.	Age		Best Corrected Visual Acuity: better eye		Best Corrected Visual Acuity: worse eye		Color vision test		Involved color axis		Macular appearance		Photopic Electroretinogram		Scotopic Electroretinogram	
	First exam	Last exam	First exam	Last exam	First exam	Last exam	First exam	Last exam	First exam	Last exam	First exam	Last exam	First exam	Last exam	First exam	Last exam
A-II-1	10	45	0.50	0.20	0.40	0.20	Severe	Severe	All axes	All axes	Normal	Normal	Reduced	Absent	Normal	Normal
B-II-1	18	57	0.50	0.20	0.50	0.16	Severe	Severe	All axes	All axes	No foveal reflex	Pigmentary changes	Reduced	Severely reduced	Normal	Normal
C-II-3	12	47	0.70	0.20	0.70	0.16	Mild	Medium	All axes	All axes	Pigmentary changes	Bulls eye maculopathy	Reduced	Absent	Normal	Normal

DISCUSSION

It has been well established that mutations in the *CNGA3* and *CNGB3* genes are a common cause of achromatopsia. We now report that mutations in these genes can also cause a progressive cone disorder. In contrast with achromatopsia, the patients with arCD with these mutations had no clinical signs of cone dysfunction at birth, but developed progressive loss of cone function during the first two decades of life.

The truncating mutations in *CNGB3* were described earlier in patients with achromatopsia, as was the combination of the splice defect in exon 9 and the frameshift mutation p.R296YfsX9.[19] The combination of p.R296YfsX9 and p.R274VfsX12 has not been reported earlier. Our observed mutations in the *CNGB3* gene were all located in the transmembrane helices (Figure 3). This is likely to lead to defective pore formation and may ultimately lead to apoptosis by the continuous influx of Ca^{2+} ions.[24] The question remains why the severe mutations in these patients did not disturb initial cone function but caused deterioration only after the first decade. There are no functional studies of absent β-subunits of the CNG3 channel, but mice lacking the α-subunits because of *CNGA3* deficiency have been described.[25] These mice never had recordable cone responses on ERG. However, histology showed presence of cones at birth and progressive cone cell loss only after the second postnatal week. Residual cones could still be identified after 22 months.[25] Apparently, there is functional redundancy of an unidentified cGMP-dependent protein, particularly early in development, which is also capable of ion transport and initiation of an action potential. Another explanation could be that the CNGA3 protein can compensate initially for some function of CNGB3.
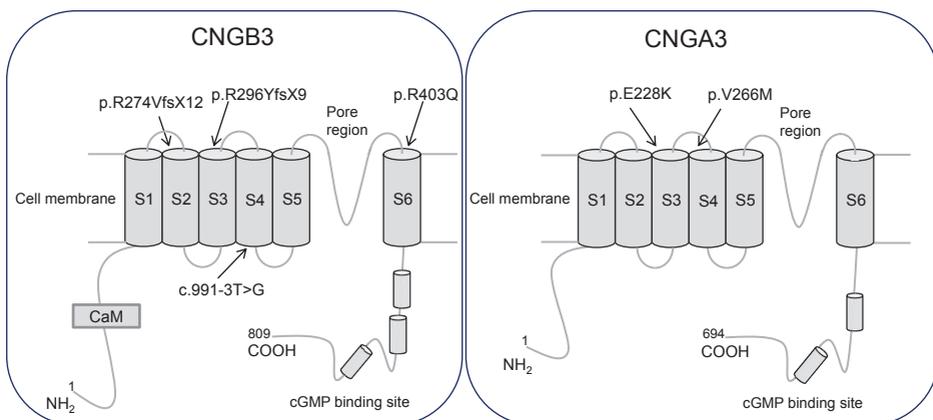

Figure 3. Localization of the mutations with respect to the topological model of the CNGB3 and CNGA3 polypeptides (http://smart.embl-heidelberg.de, accessed October 2008). CaM: Ca^{2+} calmodulin domains; COOH: carboxylic acids; cGMP: cyclic guanosine monophosphate.

The third patient had a homozygous missense mutation in *CNGB3 (*p.R403Q) in combination with a compound heterozygous variant in *CNGA3* (p.E228K; p.V266M). In a previous report, Nishiguchi et al.[26] found a homozygous p.R403Q mutation without *CNGA3* mutations in a 31-year old patient with few macular drusen, a slightly decreased visual acuity, normal color vision, and normal cone responses on full-field ERG. p.R403Q has also been described in a patient with CD in a compound heterozygous genotype with p.T383IfsX13.[22] Although this combination is more pathogenic, the phenotype was comparable to that of our patient. p.R403Q is located in a well-conserved domain of the cone β-subunit in the middle of the pore domain of the CNG channel (Figure 3). This mutation replaces the positively charged residue arginine by a neutral glutamine. The substitution may directly affect ion transfer through the channel pore[27] or change the electrostatic environment of the pore region and influence Ca^{2+} binding.[27] Both will result in dysfunction of the channel. Evidence for channelopathy was provided by an in vitro study that investigated the effect of p.R403Q in recombinant cone CNG-channels.[27] p.R403Q appeared to increase sensitivity for cGMP. This will sustain the opening of the channel, cause increased Ca^{2+} entry, and eventually cause cell dysfunction and apoptosis.[24] Remarkably, cGMP affinity of CNGB3 containing the p.R403Q variant was more comparable to the wild-type protein than cGMP affinity of CNGB3 containing p.F525N, a variant associated with achromatopsia.[27]

Whether the heterozygous *CNGA3* mutations have an additional pathogenic effect in the third patient is unclear. p.E228K is located in a fully conserved site in the transmembrane region of the cone α-subunit (Figure 3) and was found homozygously without *CNGB3* mutations in a proband with achromatopsia.[28] This observation indicates that the p.E228K variant can be pathogenic and suggests that this variant could have an additive effect to the arCD phenotype in our proband. The eldest daughter of this proband, who is a heterozygous carrier of this *CNGA3* variant and of a *CNGB3* variant, is still unaffected at the age of 9 years. The next decade will show whether she will develop any cone dysfunction and provide further proof of a true digenic disease model. The newly identified p.V266M variant seems to be well tolerated and is unlikely to affect protein function. What may be the consequences of mutations in both *CNGB3* and *CNGA3*? The CNG channels in the cone are heterotetramers with two α- and two β-subunits. In a mouse model, inter-subunit interaction between CNGA3 and CNGB3 was identified with immunolabeling. Matveev et al.[29] concluded that this interaction was necessary to obtain a heterotetrameric complex in the cone CNG-channels. Our hypothesis is that a missense mutation in the *CNGA3* gene in the presence of two missense mutations in *CNGB3* further deteriorates an already compromised CNG3 channel.

The single *CNGA3* and *CNGB3* variants that we found in six probands all reside in evolutionary conserved areas.[30] If a second mutation is present, it could be located in an area of the *CNGA3*, *CNGB3,* or *GNAT2* gene that was not analyzed (deep intronic, promotor), or it may have been a large deletion that was missed because of the nature of our polymerase chain reaction-based analysis. However, a second mutation may not be present. In this scenario, the heterozygous variant does not contribute to the CD phenotype. The *CNGB3* gene accounts for only a small fraction of the later onset progressive form of cone photoreceptor disorders, and *CNGA3* may have an additive causative effect. It is likely that the majority of arCD cases are due to other genetic causes. The finding that cone function can be maintained in the early years of life despite mutations coding for essential proteins of the cell suggests that protective mechanisms are present. Identification of these pathways may help develop strategies to prolong the life of the cone photoreceptor cell.

SUPPLEMENTAL TABLE 1

**Supplemental Table 1.** Primers used for sequencing of the *CNGB3* and *CNGA3* genes.

Gene and exon	Sequence (5'→3')		Product size (basepairs)	Annealing temp. (°C)
	Forward	Reverse		
CNGB3				
Exon 1	ggcacagtcataaatacagaggg	ggagactatactaggatttgg	393	58
Exon 2	agtacatcataaacagtcaattt	gcattttcatcacctgacatg	425	58
Exon 3	ttggcctgaaggtgtctacc	gctcaaatatccactctcccc	400	62
Exon 4	tgccccaccatctgtagc	ccaaaagcagaccctgagaa	561	62
Exon 5	cggtgtttggttaagaaattc	ccctgtgactcaaagtcacag	309	58
Exon 6	acagtccagaggcagaatgg	caattatccatgcagatagcc	481	62
Exon 7	gagattggaaggaaccaacc	ttgagaggcagaaacttcagg	298	62
Exon 8	gccttaaaaagccccatgc	ccatctttctgccctcatca	397	62
Exon 9	ctataactacagggtagcaat	tcatatccctgccaaattcc	388	55
Exon 10	cagtcaagacattgccatcag	gcatttaccagccattgaatgg	430	60
Exon 11	cccaagaatagtggtctttcg	gatcaacagtgcttttccatt	385	58
Exon 12	cagggcattagaaggaagta	ctgtaaggtagcagagactag	340	58
Exon 13	aggtatggaggtccaataga	cctagagaaattatgtggga	405	56
Exon 14	cacacccaagtctatctgagc	actctgagagcacgttattgc	468	58
Exon 15	ggaggcaaacagtactcacg	ggtttgattgtgctgagagc	472	58
Exon 16	aatcacctggaccctcacc	ctctgagatagggagaaccg	357	58
Exon 17	cttgatcacagtgagatatg	acgcccactctaattccatt	410	58
Exon 18	tcttggtggtgatcttagcc	ccttgagaaacgaaaggcaa	543	58
CNGA3				
Exon 2	cttgatgagctgggtttgc	cccccacagtctagatcagc	283	60
Exon 3	tctcactcctggctgtgtcc	ccccatctagcactttttcc	279	60
Exon 4	agggaaagactggggtttgg	caaacaggatggagcaaagc	335	60
Exon 5	gtaatcccctggtgaaatgg	gggagcaggagcactaagg	228	60
Exon 6	gccctaggctctctaaaacc	gggagaggtggagctctgg	274	60
Exon 7	ttacatgatccagcgtcttcc	taatgtcccatccaccatgc	294	60
Exon 8.1	gcatactgtgtagccgtgagg	ggttttgggacagactcctg	655	60
Exon 8.2	gttcaggattgggaacttgg	ccgtgaggcattcatattcg	331	60
Exon 8.3	gtgggtgttctgatttttgc	cccaatatctcccttcttgc	390	60
Exon 8.4	gacacgctgaagaaggttcg	gctgcttcatcttcatctgg	559	60
Exon 8.5	ctggacaccctgcagacc	ttcaaccctgaccaagttcc	271	60

Primers were designed using Primer3 software (http://frodo.wi.mit.edu/cgi-bin/primer3/primer3_www.cgi, April 2007) or using Exon Primer from the Genome Browser (http://genome.ucsc.edu, April 2007). Exon 1 of the *CNGA3* gene is non-coding.

REFERENCES

1. Michaelides M, Hunt DM, Moore AT. The cone dysfunction syndromes. Br J Ophthalmol. 2004;88:291–7.

2. Michaelides M, Hardcastle AJ, Hunt DM, Moore AT. Progressive cone and cone-rod dystrophies: phenotypes and underlying molecular genetic basis. Surv Ophthalmol. 2006;51:232–58.

3. Simunovic MP, Moore AT. The cone dystrophies. Eye. 1998;12:553– 65.

4. Jiang L, Katz BJ, Yang Z, et al. Autosomal dominant cone dystrophy caused by a novel mutation in the GCAP1 gene (GUCA1A). Mol Vis. 2005;11:143–51.

5. Nishiguchi KM, Sokal I, Yang L, et al. A novel mutation (I143NT) in guanylate cyclase-activating protein 1 (GCAP1) associated with autosomal dominant cone degeneration. Invest Ophthalmol Vis Sci. 2004;45:3863–70.

6. Kitiratschky VB, Wilke R, Renner AB, et al. Mutation analysis identifies GUCY2D as the major gene responsible for autosomal dominant progressive cone degeneration. Invest Ophthalmol Vis Sci. 2008;49:5015–23.

7. Yang Z, Peachey NS, Moshfeghi DM, et al. Mutations in the RPGR gene cause X-linked cone dystrophy. Hum Mol Genet. 2002;11:605–11.

8. Demirci FY, Rigatti BW, Wen G, et al. X-linked cone-rod dystrophy (locus COD1): identification of mutations in RPGR exon ORF15. Am J Hum Genet. 2002;70:1049 –53.

9. Wycisk KA, Zeitz C, Feil S, et al. Mutation in the auxiliary calcium-channel subunit CACNA2D4 causes autosomal recessive cone dystrophy. Am J Hum Genet. 2006;79:973–7.

10. Kitiratschky VB, Grau T, Bernd A, et al. ABCA4 gene analysis in patients with autosomal recessive cone and cone rod dystrophies. Eur J Hum Genet. 2008;16:812–9.

11. Wissinger B, Dangel S, Jagle H, et al. Cone dystrophy with supernormal rod response is strictly associated with mutations in KCNV2. Invest Ophthalmol Vis Sci. 2008;49:751–7.

12. Ben Salah S, Kamei S, Senechal A, et al. Novel KCNV2 mutations in cone dystrophy with supernormal rod electroretinogram. Am J Ophthalmol. 2008;145:1099–106.

13. Sundin OH, Yang JM, Li Y, et al. Genetic basis of total colourblindness among the Pingelapese islanders. Nat Genet. 2000;25:289 –93.

14. Pokorny J, Smith VC, Pinckers AJ, Cozijnsen M. Classification of complete and incomplete autosomal recessive achromatopsia. Graefes Arch Clin Exp Ophthalmol. 1982;219:121–30.

15. Kohl S, Baumann B, Broghammer M, et al. Mutations in the CNGB3 gene encoding the beta-subunit of the cone photoreceptor cGMP-gated channel are responsible for achromatopsia (ACHM3) linked to chromosome 8q21. Hum Mol Genet. 2000;9:2107–16.

16. Wissinger B, Gamer D, Jagle H, et al. CNGA3 mutations in hereditary cone photoreceptor disorders. Am J Hum Genet. 2001;69:722–37.

17. Kohl S, Baumann B, Rosenberg T, et al. Mutations in the cone photoreceptor G-protein alpha-subunit gene GNAT2 in patients with achromatopsia. Am J Hum Genet. 2002;71:422–5.

18. Sidjanin DJ, Lowe JK, McElwee JL, et al. Canine CNGB3 mutations establish cone degeneration as orthologous to thehuman achromatopsia locus ACHM3. Hum Mol Genet. 2002;11:1823–33.

19. Kohl S, Varsanyi B, Antunes GA, et al. CNGB3 mutations account for 50% of all cases with autosomal recessive achromatopsia. Eur J Hum Genet. 2005;13:302–8.

20. Thiadens AA, Slingerland NWR, Roosing S, et al. Genetic etiology and clinical consequences of complete and incomplete achromatopsia. Ophthalmology. 2009;116:1984–9.

21. Kaupp UB, Seifert R. Cyclic nucleotide-gated ion channels. Physiol Rev. 2002;82:769–824.

22. Michaelides M, Aligianis IA, Ainsworth JR, et al. Progressive cone dystrophy associated with mutation in CNGB3. Invest Ophthalmol Vis Sci. 2004;45:1975– 82.

23. Marmor MF. An international standard for electroretinography. Doc Ophthalmol. 1989;73:299 –302.

24. Biel M, Seeliger M, Pfeifer A, et al. Selective loss of cone function in mice lacking the cyclic nucleotide-gated channel CNG3. Proc Natl Acad Sci U S A. 1999;96:7553–7.

25. Michalakis S, Geiger H, Haverkamp S, et al. Impaired opsin targeting and cone photoreceptor migration in the retina of mice lacking the cyclic nucleotide-gated channel CNGA3. Invest Ophthalmol Vis Sci. 2005;46:1516 –24.

26. Nishiguchi KM, Sandberg MA, Gorji N, et al. Cone cGMPgated channel mutations and clinical findings in patients with achromatopsia, macular degeneration, and other hereditary cone diseases. Hum Mutat. 2005;25:248 –58.

27. Bright SR, Brown TE, Varnum MD. Disease-associated mutations in CNGB3 produce gain of function alterations in cone cyclic nucleotide-gated channels. Mol Vis. 2005;11:1141–50.

28. Reuter P, Koeppen K, Ladewig T, et al, Achromatopsia Clinical Study Group. Mutations in CNGA3 impair trafficking or function of cone cyclic nucleotide-gated channels, resulting in achromatopsia. Hum Mutat. 2008;29:1228 –36.

29. Matveev AV, Quiambao AB, Browning Fitzgerald J, Ding XQ. Native cone photoreceptor cyclic nucleotide-gated channel is a heterotetrameric complex comprising both CNGA3 and CNGB3: a study using the cone-dominant retina of Nrl -/- mice. J Neurochem. 2008;106:2042–55.

30. Muraki-Oda S, Toyoda F, Okada A, et al. Functional analysis of rod monochromacy-associated missense mutations in the CNGA3 subunit of the cone photoreceptor cGMP-gated channel. Biochem Biophys Res Commun. 2007;362:88 –93.
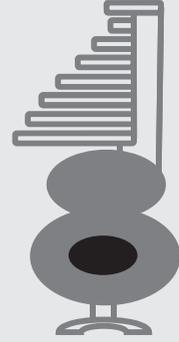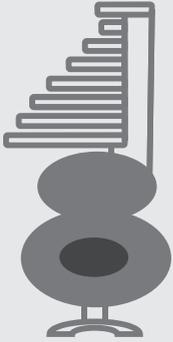
Chapter 3b

Homozygosity mapping reveals *PDE6C* mutations in patients with early-onset cone photoreceptor disorders

ABSTRACT

Cone photoreceptor disorders form a clinical spectrum of diseases that include cone dystrophy (CD) and complete and incomplete achromatopsia (ACHM). The underlying disease mechanisms of autosomal recessive (ar)CD are largely unknown. Our aim was to identify causative genes for these disorders by genome-wide homozygosity mapping. We investigated 75 ACHM, 97 arCD, and 20 early-onset arCD probands and excluded the involvement of known genes for ACHM and arCD. Subsequently, we performed high-resolution SNP analysis and identified large homozygous regions spanning the *PDE6C* gene in one sibling pair with early-onset arCD and one sibling pair with incomplete ACHM. The *PDE6C* gene encodes the cone a subunit of cyclic guanosine monophosphate (cGMP) phosphodiesterase, which converts cGMP to 5'-GMP, and thereby plays an essential role in cone phototransduction. Sequence analysis of the coding region of *PDE6C* revealed homozygous missense mutations (p.R29W, p.Y323N) in both sibling pairs. Sequence analysis of 104 probands with arCD and 10 probands with ACHM revealed compound heterozygous *PDE6C* mutations in three complete ACHM patients from two families. One patient had a frameshift mutation and a splice defect; the other two had a splice defect and a missense variant (p.M455V). Cross-sectional retinal imaging via optical coherence tomography revealed a more pronounced absence of cone photoreceptors in patients with ACHM compared to patients with early-onset arCD. Our findings identify *PDE6C* as a gene for cone photoreceptor disorders and show that arCD and ACHM constitute genetically and clinically overlapping phenotypes.

Impairment or death of the cone photoreceptor cells is the clinical hallmark of cone disorders, which have an estimated prevalence of 1:30,000–1:40,000.[1,2] Achromatopsia (ACHM) (MIM *600827) is a stationary congenital autosomal recessive cone disorder characterized by low visual acuity (0.10–0.20 decimal Snellen equivalent), photophobia, nystagmus, and severe color vision defects. Patients with the complete ACHM subtype have no cone function on electroretinogram (ERG), whereas those with incomplete ACHM have residual cone function. Cone dystrophy (CD) (MIM *600827) is a progressive cone disorder in which patients may initially have normal cone function but develop progressive visual acuity loss, increasing photophobia, color vision disturbances, and diminished cone responses on ERG, usually in the first or second decade of life. The visual acuity of these patients generally worsens to legal blindness before the fourth decade of life.[3]

The genetic basis of these disorders has been partly elucidated during the last decade. Three genes have been implicated in ACHM: *CNGA3* (MIM *600053), *CNGB3* (MIM *605080), and *GNAT2* (MIM +139340). Mutations in these genes explain a majority of cases of this disease, but a fraction of cases still remain unsolved.[4–7] Several genes have been identified for the autosomal dominant[3,8,9] and X-linked forms of CD,[10,11] but little is known about the genetic causes of the most prevalent autosomal recessive (arCD) form. Four genes have been implicated in this form: *ABCA4* (MIM *601691),[12] *CACNA2D4* (MIM *608171),[13] *CNGB3* (MIM *605080),[14] and *KCNV2* (MIM *607604),[15,16] which together explain only ~10% of all cases.

We aimed to identify disease genes for cone photoreceptor disorders and investigated patients with ACHM and arCD. Patients were ascertained from various ophthalmic centers in the Netherlands, Belgium, the United Kingdom, and Canada. This study was approved by the local and national medical ethics committees and adhered to the tenets of the Declaration of Helsinki. All participants provided signed, informed consent for participation in the study, retrieval of medical records, and use of blood and DNA for research.

All available data on visual acuity, color vision, fundus appearance, and ERGs were retrieved from medical charts and updated by additional examinations including optical coherence tomography (OCT) and fundus photography. Recent ERGs were performed according to the recommendations of the International Society for Clinical Electrophysiology of Vision.[17] Patients could be stratified into three clinical categories: ACHM (N=75 probands), arCD (N=97 probands), and a group who had clear documentation of progressive cone dysfunction but already had impaired visual acuity in early childhood (early-onset arCD; N=20 probands). We tested for the presence of known *ABCA4* muta-

tions in all probands (A.T.,unpublished data) and for the presence of *CNGB3* variants in all probands via sequence analysis.[5,7] When *CNGB3* variants were absent, all ACHM patients were analyzed for *CNGA3* and *GNAT2* variants via sequence analysis.[5,7] Finally, most of the arCD patients were analyzed for *KCNV2* variants via sequence analysis (A.T., unpublished data). These studies resulted in 116 probands- i.e., 11 ACHM, 85 arCD, and 20 early-onset arCD- with unknown etiology who formed the basis of the present genetic analyses.

We performed high-resolution SNP analysis (Affymetrix GeneChip Genome-Wide Human Array 5.0) on a subset of 76 patients from 64 families with autosomal recessive cone dysfunction from whom DNA was available. In 8 of these 64 families, the parents were consanguineous. Genotyping was performed with Genotype Console software (Affymetrix), and regions of homozygosity were calculated with Partek Genomics Solution software. Large identity by descent (IBD) regions (i.e., >5 Mb) were found in all consanguineous families and in 34 of the nonconsanguineous probands. In these 34 nonconsanguineous patients, we found a total of 57 IBD regions larger than 5 Mb, with an average size of 9 Mb (range 5–31 Mb).

In a sibling pair from a consanguineous marriage (family B) and in a sibling pair from a nonconsanguineous family (family A), we identified large homozygous regions on chromosome 10 (11 Mb and 26 Mb, respectively) (Figure 1a). The common 26 Mb homozygous region in the sibs from family A was the largest homozygous region (SNP boundaries SNP_A-2260521 and SNP_A-1892358); the second, third, and fourth largest regions measured 8, 4.3, and 4.2 Mb. The overlapping 11 Mb homozygous region in the affected sibs of family B was the second largest homozygous region (SNP boundaries SNP_A-2003359 and SNP_A-1804692). The largest region in this family spanned 25 Mb; the third and fourth largest regions measured 10 and 6 Mb. The overlapping homozygous region in both families spanned the *PDE6C* gene but no other obvious candidate genes (Figure 1a; see also Supplemental Table 1). These regions were not found in other patients.
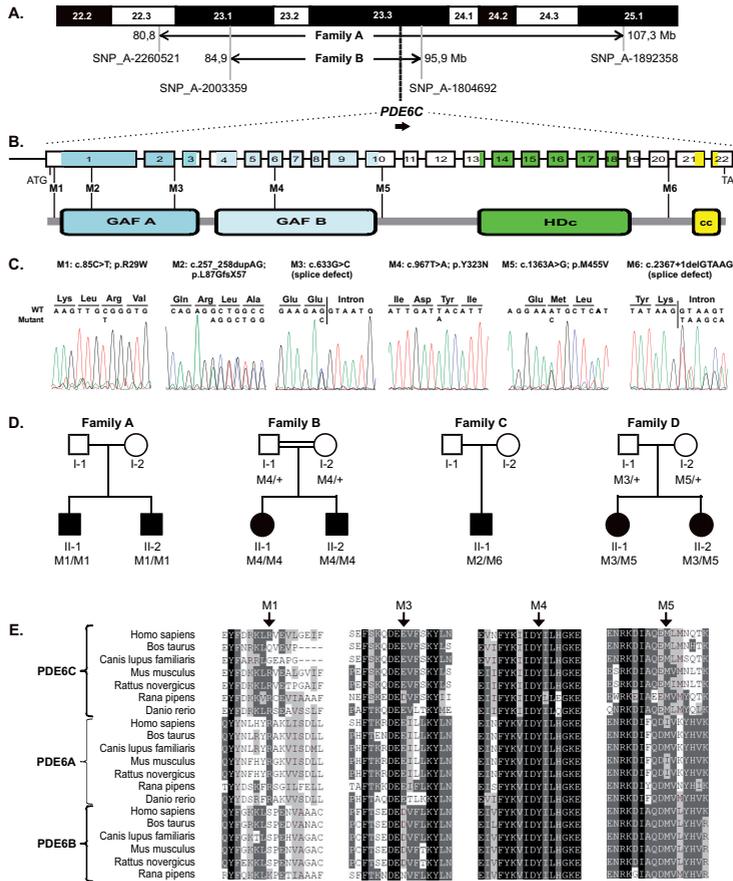
Figure 1. Molecular genetic characterization of the *PDE6C* gene in four families with autosomal recessive cone photoreceptor disorders.

(a) The 10q22-q25 region and the homozygous regions identified in patients of families A and B. The SNPs flanking the homozygous regions and their genomic positions, from the March 2006 UCSC genome build (hg18), are indicated.

(b) Protein and genomic structure of PDE6C. GAF, acronym derived from proteins in which these domains were initially identified (cGMP-regulated mammalian phosphodiesterases, cyanobacterial adenylyl cyclases, and a formate-hydrogen lyase transcriptional activator); HDc, domain with highly conserved histidines (H) and aspartic acids (D); cc, coiled-coil domain. The six mutations are labeled M1 through M6.

(c) Chromatograms showing the *PDE6C* mutations.

(d) Pedigrees of early-onset cone dystrophy (family A), incomplete achromatopsia (family B), and complete achromatopsia (families C and D) and segregation analysis of the respective *PDE6C* variants. The parents in family A are not related to each other in the last three generations. BI-1 and BI-2 are first cousins.

(e) Evolutionary conservation of the altered amino acid residues in three families. PDE6A and PDE6C are rod and cone a subunits respectively; PDE6B is the rod β subunit. Using the Swiss-Prot database, we searched for their orthologs in as many species as possible and included, with the exception of Danio rerio, those present in all species. White lettered residues on a black background are fully conserved between different species in all three subunits. White lettered residues on a gray background are conserved in most sequences. Black lettered residues with light gray background are similar to amino acid residues in other orthologs and homologs. The arginine residue at position 29 is fully conserved in all orthologs of both a subunits (PDE6C and PDE6A), except for bovine and canine PDE6C. The aspartic acid residue in the GAF-A domain at position 211 is conserved or replaced by a functionally conserved glutamic acid residue in 19 of 20 orthologs and homologs. This observation strongly suggests that the predicted p.E211D substitution in family D is neutral and that the effect of c.633G>C on the splice site is pathologic. The tyrosine residue located in the GAF-B domain at position 323 is completely conserved among all three PDE6 subunits. The methionine residue at position 455 is conserved or substituted by a functionally conserved isoleucine in all PDE6 molecules.

PDE6C encodes the cone α subunit of cyclic guanosine monophosphate (cGMP) phosphodiesterase, an enzyme consisting of two α and two γ subunits that is essential in the cone phototransduction cascade. It converts the second messenger cGMP to 5'-GMP during light exposure. This results in closure of the cGMP-gated ion channel in the cone outer segment membrane, leading to hyperpolarization of the cell.[18]

Because *PDE6C* appeared to be an excellent candidate for cone photoreceptor disorders, we performed direct sequencing of all 22 exons (Figure 1b).We detected homozygous missense mutations in exon 1 in both sibling pairs of family A (Figures 1b–1d). The first proband (AII-1) and his brother (AII-2) carried a homozygous missense mutation (p.R29W) affecting a conserved residue just upstream of the first GAF (GAF-A) domain (acronym derived from proteins in which these domains were initially identified) (Figure 1b). The arginine residue at position 29 is fully conserved in all depicted orthologs of the cone and rod a subunits (PDE6C and PDE6A), except for in bovine and canine PDE6C (Figure 1e). The second proband (BII-1) and her brother (BII-2) carried the homozygous missense mutation p.Y323N (Figures 1c and 1d). This mutation affects a fully conserved residue located in the second GAF (GAF-B) domain (Figures 1b and 1e, mutation M4), a region of the protein that binds cGMP and regulates the activity of the enzyme.[19] Protein homology modeling of the GAF-B domain on the basis of a recent GAF-A crystal structure[19] shows that the p.Y323N mutation is located near the cGMP binding site. Although not directly interacting with cGMP, Y323 neighbors D322, which is in direct contact with bound cGMP, as shown in Figure 2. D322 tightly interacts with cGMP by means of two hydrogen bonds, one originating from the peptide main chain and one originating from the aspartic acid side chain. Mutation of Y323 to N is likely to alter the local backbone conformation and mobility and is also likely to affect D322 and its interaction with cGMP. Both the orientation and the mobility of the amino acids equivalent to D322 in other GAF domains have been suggested to be of crucial importance in determining affinity and selectivity of these domains for cGMP.[19] We hypothesize that the p.Y323N mutation will probably alter the affinity of cGMP for the regulatory GAF-B domain.
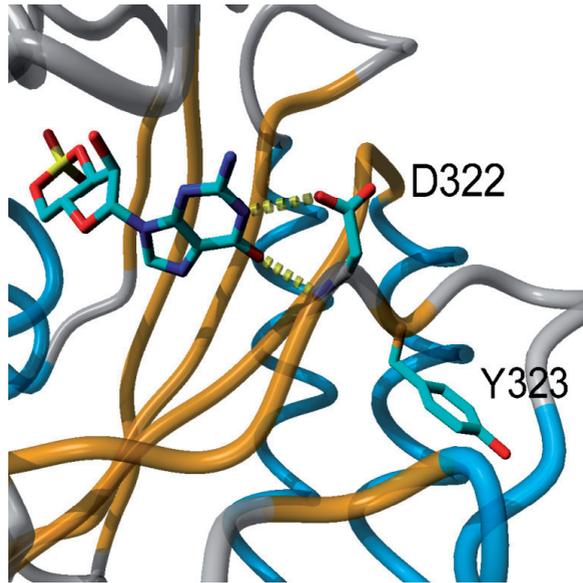
Figure 2. Molecular modeling of Y323 in the GAF-B domain of PDE6C.
The individual side-chain orientations of D322 and Y323 are shown in magenta. A peptide backbone trace of the remainder of the model is shown, with b sheets colored orange and a helices colored blue. The mutation site Y323 is located adjacent to D322. The latter aminoacid is shown interacting with bound cGMP via two hydrogen bonds, one originating from the peptide main chain and one originating from the aspartic acid side chain. Hydrogen bonds are indicated by yellow dashed lines.

Subsequently, we analyzed the remaining patients (N=114) for additional mutations in the *PDE6C* gene by direct sequencing of the coding region. Compound heterozygous mutations were detected in two additional probands. Patient CII-1 was compound heterozygous for a frameshift mutation (c.257_258 dupAG; p.L87GfsX57) in exon 1 and a 5 bp deletion (c.2367+1delGTAAG), which removes the first five nucleotides of intron 20, including the splice donor site (Figures 1c and 1d). An alternative splice donor site is predicted at position 2366 (splice prediction score 0.80, BGDP Splice Site Prediction by Neural Network).[20] Use of this splice site would lead to a shift in the open reading frame and premature termination of the phosphodiesterase 6C protein (p.E790SfsX12). Patient DII-1 and her affected sister (DII-2) revealed two missense variants (c.633G>C [p.E211D] and c.1363A>G [p.M455V]) (Figure 1c). The glutamic acid at position 211 is changed to the functionally conserved aspartic acid in five of six homologous rod PDE β subunits, and in frog PDE6C, strongly suggesting that the predicted amino acid change is a functionally neutral variant. The c.633G>C variant does, however, affect the last nucleotide of exon 2 and is predicted to completely abolish the splice donor site (BGDP Splice Site Prediction by Neural Network).[20] Because no alternative splice donor sites are predicted, the mutation may result either in removal of exon 2 from the mRNAor in nonsplicing of intron 2 (106 bp). In both options, this would result in a disruption of

the open reading frame. The p.M455V mutation affects a conserved residue located just downstream of the GAF-B domain (Figures 1b and 1e). In those families in which DNA was available from parents (families B and D), mutations M3, M4, and M5 segregated as expected for pathologic variants (Figure 1d). None of the six *PDE6C* mutations were found in 180 ethnically matched controls.

In four other unrelated patients with arCD, we found four different heterozygous amino acid changes (c.413T>C [p.L138S], c.696G>A [p.M232I], c.2096A>G [p.E699G], and c.2477T>C [p.I826T]). In these patients, we did not find a second mutation on the other allele in the coding region of this gene, despite complete *PDE6C* sequencing. We considered the possibility of a digenic disease model, with mutations in both *PDE6C* and an interacting gene, and performed sequence analysis of the gene encoding the cone γ subunit of cGMP phosphodiesterase (*PDE6H*). We did not detect mutations in this gene. The four heterozygous variants in *PDE6C* were not detected in 180 ethnically matched control individuals. The missense variants p.M232I, p.E699A, and p.I826T were predicted by SIFT software to be tolerated; only variant p.L138S was predicted not to be tolerated. Moreover, the isoleucine at position 826 is substituted by a threonine in the mouse and rat orthologs, rendering this a very likely benign amino acid change. The patients carrying the p.L138S, p.E699A, and p.I826T variants were part of the 5.0 Affymetrix SNP screening. A copy-number variant analysis of the SNP data with Partek GS software did not reveal a deletion or duplication of twenty intragenic SNPs and five copynumber variant probes evenly spaced across the *PDE6C* gene (Supplemental Figure 1). Though very small deletions encompassing single exons or part of the promoter cannot be excluded, these data strongly suggest that the heterozygous *PDE6C* missense variants represent rare benign sequence variants.

Table 1 shows a summary of the clinical findings of all patients with *PDE6C* mutations on both alleles. Patients AII-1 and AII-2 carried a homozygous missense mutation, located just upstream of the GAF-A domain (Figure 1a). They showed an early-onset CD; their visual acuity and cone ERG progressively declined in their early teens. Patients BII-1 and BII-2 had a homozygous missense mutation in the GAF-B domain, which presumably affects the interaction with cGMP. This sibling pair presented with an incomplete ACHM; the cone ERG responses were significantly reduced but measurable both in childhood and on recent examination, whereas the rod ERG parameters were normal. Patient CII-1, carrying a protein-truncating mutation and a splice defect, had the most severe cone phenotype. At four years of age, the visual acuity was 0.10, the cone ERG was nonrecordable, and the rod function was completely normal (Figure 3). Patients DII-1 and DII-2, each carrying a splice defect and a p.M455V missense mutation, were clinically diagnosed as complete ACHM because they exhibited a low visual acuity of 0.16 with nystagmus since early childhood and absent cone responses on ERG.

Table 1. Clinical findings in probands and affected relatives, stratified according to genotype

Patient	PDE6C mutations	Diagnosis	Age		Best corrected visual acuity best eye		Visual complaints		Refractive error	Color vision defects		Macular appearance		Periphery	Cone ERG	
			Age first exam	Age last exam	First exam	Last exam	Photo-phobia	Nystag-mus	Spherical equivalent	First exam	Last exam	First exam	Last exam	Last exam	First exam	Last exam
AII-1	p.R29W / p.R29W	Early onset CD	6	51	0.40	0.16	Yes	Yes	-11	Severe	Severe	No foveal reflex	Mild pigmentary changes	Normal	Reduced	No responses
AII-2	p.R29W / p.R29W	Early onset CD	7	47	0.30	0.20	Yes	Yes	-3.5	Severe	Severe	Pigmentary changes	Pigmentary changes	Normal	Reduced	No responses
BII-1	p.Y323N / p.Y323N	Incomplete ACHM	7	23	0.16	0.10	No	Yes	-10	Severe	Severe	Mild pigmentary changes	Mild pigmentary changes	Normal	ND	ND
BII-2	p.Y323N / p.Y323N	Incomplete ACHM	10	20	0.16	0.10	No	Yes	-2	Severe	Severe	No foveal reflex	No foveal reflex	Normal	Reduced	Reduced
CII-1	p.L87GfsX57 / c.2367+1delGTAAG	Complete ACHM	2	4	0.10	0.10	Severe	Yes	+10.5	Severe	Severe	No foveal reflex	No foveal reflex	Normal	No responses	No responses
DII-1	c.633G>C / p.M455V	Complete ACHM	12	37	0.16	0.10	Severe	Yes	-5	Severe	Severe	No foveal reflex	Mild pigmentary changes	Normal	No responses	No responses
DII-2	c.633G>C / p.M455V	Complete ACHM	11	36	0.16	0.10	Severe	Yes	-1.5	Severe	Severe	No foveal reflex	No foveal reflex	Normal	No responses	No responses

Abbreviations are as follows: BVCA, best corrected visual acuity; CD, cone dystrophy; ACHM, achromatopsia; ND, not determined.

Rod and mixed rod/cone responses

30 Hz cone flicker response
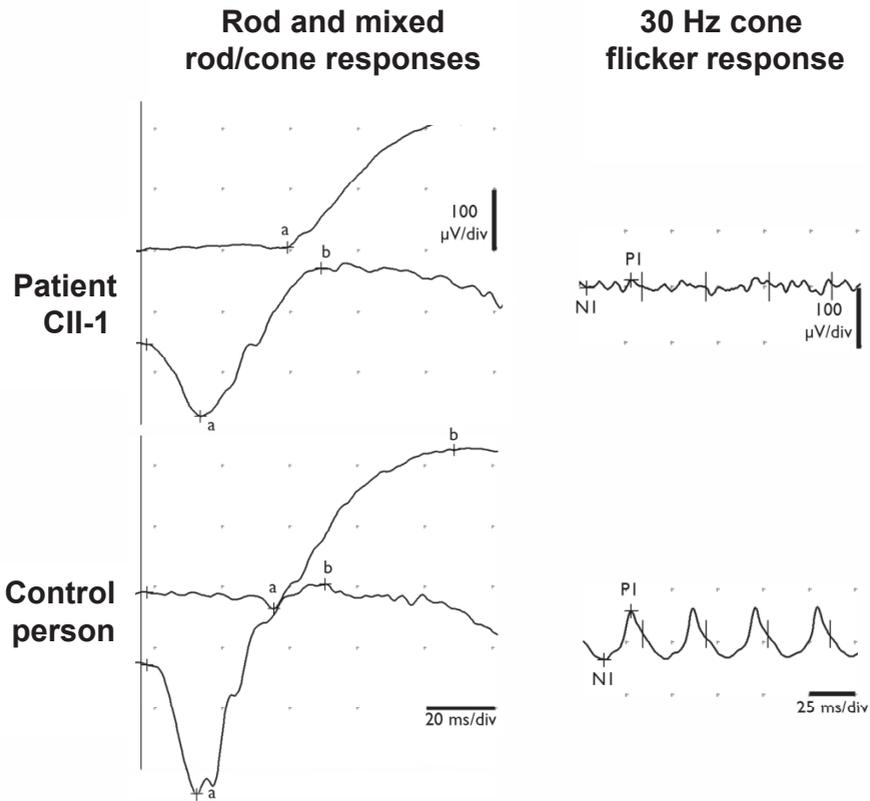
Figure 3. Electroretinogram of patient CII-1.

An electroretinogram performed with an abbreviated standard International Society for Clinical Electrophysiology of Vision protocol at the age of 4 years without sedation is shown at top, with normal control traces at bottom for purposes of comparison. Note normal rod-specific response (top trace at left), with no significant contribution of cones to combined rod-cone response (bottom trace at left for patient CII-1); dark-adapted oscillatory responses as seen on ascending limb of the b-wave are residual at most. The absence of cone specific function was demonstrated by the absence of cone specific response to 30 Hz flicker stimulation (at right).

In the adult patients, we performed Spectral Domain-OCT (Heidelberg) at the most recent ophthalmologic examination. The absence of the photoreceptor cell layer in the fovea, a site with predominantly cone photoreceptor cells, was apparent in all patients. A typical OCT picture for patients from family A (patient AII-2) is shown in Figure 4b; a characteristic OCT image for patients from families B and D (patient DII-1) is shown in Figure 4d. The area of absent cone photoreceptors in patient DII-1, which spans almost the entire fovea, is significantly larger than the lesion in patient AII-2 (Figures 4b and 4d). We hypothesize that the missense variant in family A, which is located outside function-ally important domains, may have a less severe effect on the function of PDE6C than the mutations observed in the other families.
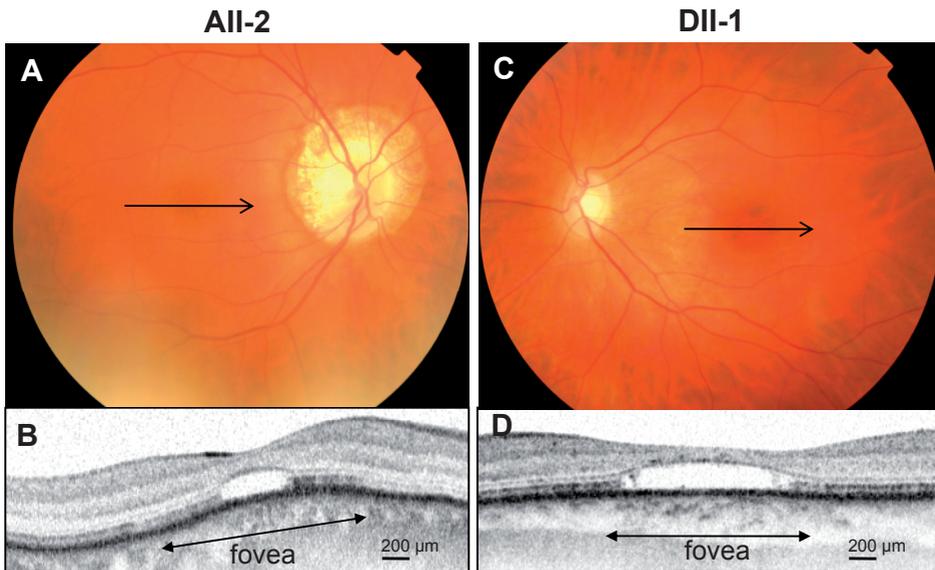
Figure 4. Retinal phenotypes of early-onset cone dystrophy and complete achromatopsia in families A and D.
(a) Fundus photography of the right eye of patient AII-2, performed at age 51 years, showing myopic changes in the peripapillary region. In the macular region, mild pigmentary changes are present. The arrow denotes the position of the optical coherence tomography (OCT) image in (b).
(b) The Spectral Domain-OCT of this patient reveals a serous detachment of the photoreceptor layer in the central fovea. The retinal pigment epithelium is intact, but the outer and inner segments of the photoreceptors are absent. The length of the lesion is ~500 mm. The OCT cross-section is not fully perpendicular.
(c) Fundus photography of the left eye of patient DII-1, performed at age 37 years, showing mild pigmentary changes in the macula. The arrow denotes the position of the OCT image in (d).
(d) The Spectral Domain-OCT of this patient displays a large area of ~1300 mm with absent cone photoreceptors, which involves almost the entire fovea.

In zebrafish, mutations in the ortholog of PDE6C are responsible for progressive cone photoreceptor degeneration.[21,22] An intron 11 splice acceptor site mutation[21] and a p.M175R missense mutation in the GAF-A domain[22] lead to rapid degeneration of cone photoreceptors soon after their formation. Unlike in humans, zebrafish photoreceptors are continuously generated at the retinal margin by a population of mitotic progenitor cells, so cone photoreceptors can be found at the periphery throughout the life of these mutant fish. The splice site mutation in zebrafish also results in the degeneration of rod photoreceptors in the central part of the retina.[21] In zebrafish with the p.M175R missense mutation, rods show an abnormal morphology and rhodopsin mislocalization but otherwise function normally.[22] These findings suggest that the effect of the zebrafish Pde6c p.M175R mutation is more cone specific than that of the Pde6c splice defect.

To test the involvement of rod photoreceptors in human patients, we repeated the ERG on the two oldest patients with *PDE6C* mutations (AII-1 and AII-2; 47 and 51 years old,

respectively), and we did not find abnormal rod responses. Normal rod responses were also observed in patients CII-1, DII-1, and DII-2. We concluded that rod involvement does not appear to be a major consequence of *PDE6C* mutations in humans, although some dysfunction of rods may still occur later in life.

In conclusion, through homozygosity mapping of patients with cone photoreceptor disorders from nonconsanguineous and consanguineous families, we identified another causative gene, *PDE6C*. PDE6C has a crucial role in the cone phototransduction cascade. Similar to the other disease genes in this cascade (*CNGA3*, *CNGB3*, and *GNAT2*),[4–6] *PDE6C* mutations result in a severe early-onset cone disorder. We show that early-onset CD, incomplete ACHM, and complete ACHM form a continuous spectrum of a similar etiology. The observed variability in phenotypes may be a result of differences in the functional effects of *PDE6C* mutations. Our findings will improve diagnosis and counseling of patients and their families and represent another step toward solving the etiology of cone photoreceptor disorders.

SUPPLEMENTAL TABLE & FIGURE

Supplemental Table 1. Homozygous regions for families A and B.

| Chr.	Start	End	Sample ID(s)	Length region (Mb)	# SNPs
10	80.888.184	107.352.036	A ll-1	26,5	4.399
11	48.125.240	56.227.770	A ll-1	8,1	434
12	33.234.603	37.599.402	A ll-1	4,4	271
14	89.229.236	93.489.863	A ll-1	4,3	677
6	34.180.193	36.208.710	A ll-1	2,0	214
2	188.650.371	190.654.845	A ll-1	2,0	236
5	155.393.372	157.303.002	A ll-1	1,9	359
6	102.266.106	103.917.101	A ll-1	1,7	211
11	37.664.444	39.256.145	A ll-1	1,6	217
14	39.393.635	40.642.718	A ll-1	1,2	231
5	65.087.560	66.311.040	A ll-1	1,2	258
8	126.936.549	127.965.642	A ll-1	1,0	216
1	159.531.547	160.529.894	A ll-1	1,0	215
13	42.822.997	43.692.360	A ll-1	0,9	202
16	25.380.356	49.895.689	B ll-1 and -2	24,5	1.394
10	84.963.195	95.977.303	B ll-1 and -2	11,0	1.975
4	7.188.532	16.863.548	B ll-1 and -2	9,7	2.164
18	19.088.173	25.421.520	B ll-1 and -2	6,3	1.010
19	48.854.873	54.922.139	B ll-1 and -2	6,1	534
9	2.293.782	5.834.807	B ll-1 and -2	3,5	870
12	127.192.344	129.994.218	B ll-1 and -2	2,8	674
17	40.825.939	42.234.514	B ll-1 and -2	1,4	219
11	82.983.190	84.287.750	B ll-1 and -2	1,3	210
6	26.233.321	26.715.651	B ll-1 and -2	0,5	274
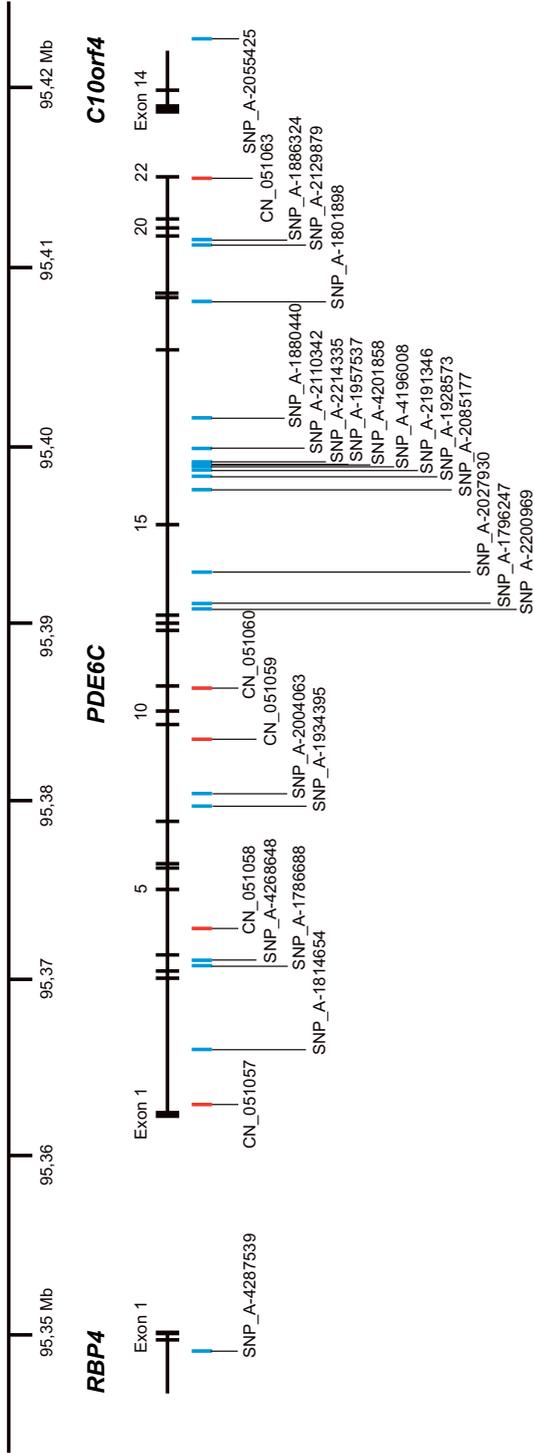
Supplemental Figure 1. Exon-intron structure and copy number probes of *PDE6C*.

Exon-intron structure of *PDE6C* and copy number probes in this genomic region based on the March 2006 UCSC genome build (hg18). The genomic structure of *PDE6C* is depicted on scale. In blue, 20 intragenic and two flanking single nucleotide polymorphisms (SNPs), and in red, the five intragenic copy number (CN) probes are shown that are present on the Affymetrix GeneChip Genome-Wide Human Array 5.0. Using Partek Genomics Suite software we analyzed the raw signal intensities for all probes shown above. For patients 25456 (heterozygous carrier of p.L138S), 36419 (heterozygous carrier of p.E699G), and 43627 (heterozygous carrier of p.I826T), the raw signal intensities were within the normal variation of the average signal intensities of 400 tested individuals, and never lower than 75%. We have not performed a genome-wide SNP array analysis for patient 50488, heterozygous carrier of the *PDE6C* variant p.M321I.

REFERENCES

1. Michaelides M., Hunt DM, Moore AT. The cone dysfunction syndromes. Br J Ophthalmol. 2004;88:291-297.

2. Hamel CP Cone rod dystrophies. Orphanet J Rare Dis. 2007;2:1-7.

3. Michaelides M., Hardcastle AJ, Hunt DM, Moore AT. Progressive cone and cone-rod dystrophies: phenotypes and underlying molecular genetic basis. Surv Ophthalmol. 2006;51:232-258.

4. Kohl S, Baumann B, Rosenberg T, et al. Mutations in the cone photoreceptor G-protein alpha-subunit gene GNAT2 in patients with achromatopsia. Am J Hum Genet. 2002;71:422-425.

5. Kohl S, Varsanyi B, Antunes GA, et al. CNGB3 mutations account for 50% of all cases with autosomal recessive achromatopsia. Eur J Hum Genet. 2005;13:302-308.

6. Wissinger B, Gamer D, Jagle H, et al. CNGA3 mutations in hereditary cone photoreceptor disorders. Am J Hum Genet. 2001;69:722-737.

7. Thiadens AA, Slingerland NWR, Roosing S, et al. Genetic etiology and clinical consequences of complete and incomplete achromatopsia. Ophthalmology. 2009;116:1984-9.

8. Jiang L, Katz BJ, Yang Z, et al. Autosomal dominant cone dystrophy caused by a novel mutation in the GCAP1 gene (GUCA1A). Mol Vis. 2005;11:143-151.

9. Nishiguchi KM, Sokal I, Yang L, et al. A novel mutation (I143NT) in guanylate cyclase-activating protein 1 (GCAP1) associated with autosomal dominant cone degeneration. Invest Ophthalmol Vis Sci. 2004;45:3863-3870.

10. Vervoort R, Lennon A, Bird AC, et al. Mutational hot spot within a new RPGR exon in X-linked retinitis pigmentosa. Nat Genet. 2000;25:462-466.

11. Demirci FY, Rigatti BW, Wen G, et al. X-linked cone-rod dystrophy (locus COD1): identification of mutations in RPGR exon ORF15. Am J Hum Genet. 2002;70:1049-1053.

12. Kitiratschky VB, Grau T, Bernd A, et al. ABCA4 gene analysis in patients with autosomal recessive cone and cone rod dystrophies. Eur J Hum Genet. 2008;16:812-819.

13. Wycisk KA, Zeitz C, Feil S, et al. Mutation in the auxiliary calcium-channel subunit CACNA2D4 causes autosomal recessive cone dystrophy. Am J Hum Genet. 2006;79:973-977.

14. Michaelides M, Aligianis IA, Ainsworth JR, et al. Progressive cone dystrophy associated with mutation in CNGB3. Invest Ophthalmol Vis Sci. 2004;45:1975-1982.

15. Thiagalingam S, McGee TL, Weleber RG, et al. Novel mutations in the KCNV2 gene in patients with cone dystrophy and a supernormal rod electroretinogram. Ophthalmic Genet. 2007;28:135-142.

16. Wissinger B, Dangel S, Jagle H, et al. Cone dystrophy with supernormal rod response is strictly associated with mutations in KCNV2. Invest Ophthalmol Vis Sci. 2008;49:751-757.

17. Marmor MF, Fulton AB, Holder GE, et al. ISCEV Standard for full-field clinical electroretinography (2008 update). Doc Ophthalmol. 2009;118:69-77.

18. Burns ME, Baylor DA. Activation, deactivation, and adaptation in vertebrate photoreceptor cells. Annu Rev Neurosci. 2001;24:779-805.

19. Martinez SE, Heikaus CC, Klevit RE, Beavo JA. The structure of the GAF A domain from phosphodiesterase 6C reveals determinants of cGMP binding, a conserved binding surface, and a large cGMP-dependent conformational change. J Biol Chem. 2008;283:25913-25919.

20. Reese MG, Eeckman FH, Kulp D, Haussler D. Improved splice site detection in Genie. J Comput Biol. 1997;4:311-323.

21. Stearns G, Evangelista M, Fadool JM, Brockerhoff SE. A mutation in the cone-specific pde6 gene causes rapid cone photoreceptor degeneration in zebrafish. J Neurosci. 2007;27:13866-13874.

22. Nishiwaki Y, Komori A, Sagara H, et al. Mutation of cGMP phosphodiesterase 6alpha'-subunit gene causes progressive degeneration of cone photoreceptors in zebrafish. Mech Dev. 2008;125:932-946.
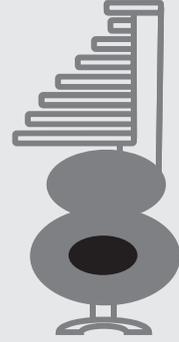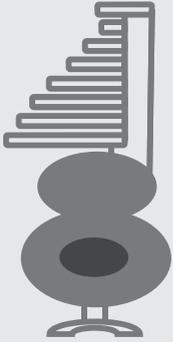
Chapter 3c

Clinical course of cone dystrophy caused by mutations in the *RPGR* gene

ABSTRACT

Background: Mutations in the *RPGR* gene predominantly cause rod photoreceptor disorders with a large variability in clinical course. In this report, we describe two families with mutations in this gene and cone involvement.

Methods: We investigated an X-linked cone dystrophy family (1) with 25 affected males, 25 female carriers and 21 non-carriers, as well as a small family (2) with 1 affected and 1 unaffected male. The *RPGR* gene was analyzed by direct sequencing. All medical records were evaluated, and all available data on visual acuity, color vision testing, ophthalmoscopy, fundus photography, Goldmann perimetry, and full-field electroretinography (ERG) were registered. Cumulative risks of visual loss were studied with Kaplan–Meier product-limit survival analysis.

Results: Both families had a frameshift mutation in ORF15 of the *RPGR* gene; family 1 had p.Ser1107ValfsX4, and family 2 had p.His1100GlnfsX10. Mean follow up was 13 years (SD 10). Virtually all affected males showed reduced photopic and normal scotopic responses on ERG. Fifty percent of the patients had a visual acuity of <0.5 at age 35 years (SE 2.2), and 75% of the patients was legally blind at age 60 years (SE 2.3). Female carriers showed no signs of ocular involvement.

Conclusions: This report describes the clinical course and visual prognosis in two families with cone dystrophy due to *RPGR* mutations in the 3′ terminal region of ORF15. Remarkable features were the consistent, late onset phenotype, the severe visual outcome, and the non-expression in female carriers. Expression of *RPGR* mutations in this particular region appears to be relatively homogeneous and predisposed to cones.

INTRODUCTION

Cone dystrophy (CD) is a progressive disease in which the cone photoreceptors are primarily affected. Patients experience increasing photophobia, and develop loss of visual acuity, color vision disturbances, and central visual field defects. An important clinical hallmark for diagnosis is reduction of cone responses with preservation of rod responses on full-field electroretinogram (ERG).[1,2] All three inheritance patterns occur in CD; 15% is autosomal dominant, 80% autosomal recessive, and 5% X-linked. Revelation of the genetic background and genotype-phenotype correlation in CD is currently ongoing, improving clinical counseling and prediction of visual decline.

A common cause of X-linked retinitis pigmentosa (RP) are mutations in the retinitis pigmentosa GTPase regulator gene (*RPGR;* Xp21.1)[3-8] The gene has also been reported in X-linked cone-rod dystrophy (CRD)[9-13] or even in pure CD.[3,14,15] Although the clinical course of patients with *RPGR* mutations and RP has been evaluated,[16] how the disease progresses in CD patients is currently unknown.

In this report, we present two families with CD due to mutations at the 3' terminal end of ORF15. We carefully studied the course of disease in 26 affected males and 25 female carriers during a long period of follow up, and established a model for visual outcome that can be used for clinical counseling.

PATIENTS AND METHODS

Study Population
We studied a pedigree of 71 relatives (25 affected males; 25 female carriers; 21 non-carriers) of one Dutch family (family 1), as well as one affected male and one unaffected sibling of the second family (family 2) (Figure 1). All affected males of family 1 had been diagnosed with CD. We were not able to contact five patients and 11 female carriers. All other patients were ascertained at three medical centers in the Netherlands: the Netherlands Institute for Neuroscience (NIN), Erasmus Medical Center Rotterdam, and the St. Oosterschelde Hospital in Goes. The study was approved by the Medical Ethics Committee of Erasmus Medical Center and adhered to the tenets of the Declaration of Helsinki. All participants provided signed, informed consent for participation in the study, retrieval of medical records, and use of blood and DNA for research.

Clinical Examination

Medical charts were retrieved from the patients' ophthalmologists, and all available data on Snellen visual acuity, color vision (Hardy-Rand-Rittler colorvision test, Ishihara pseudoisochromatic plates, or Farnsworth Panel D15/D28 test), Goldmann perimetry, slitlamp and fundus examination, and ERGs were recorded. Patients with incomplete or no available data from the last five years were invited for a work-up examination at one of the clinics. Patients underwent a full-field ERG with contact lens electrodes, following the recommendations of the International Society for Clinical Electrophysiology of Vision (ISCEV).[17]

Molecular Genetic Analysis

Blood samples were obtained from all participating family members of family 1 (N=87), and family 2 (N=3). DNA was isolated from peripheral blood lymphocytes by standard procedures. Molecular analyses were carried out as described.[18] In short, the coding region and intron/exon boundaries of the *RPGR* ORF15 region were amplified by polymerase chain reaction (PCR) using M13 tail sequences at the 5' ends of the target specific primers. Sanger sequencing reactions were performed using these M13 tail sequences. Primer sequences and reaction conditions are available upon request.

Statistical Analysis

Proportions of categorical variables between two groups were compared using the chi-square test. Cumulative risks of visual loss were studied with Kaplan–Meier product-limit survival analysis, with low vision (visual acuity<0.5) or legal blindness (visual acuity ≤0.1) as outcomes. Participants older than 60 years were pooled to maintain unbiased estimates.

RESULTS

Mutation Analysis

Pedigrees of both families are provided in Figure 1. In 25 affected males and in 25 female carriers of family 1, the 1bp insertion c.3317dup (p.Ser1107ValfsX4) in *RPGR* ORF15 (NM_001034853.1) was detected as the causative mutation (Figure 2a). This earlier described frameshift mutation[11] is located at the C-terminus of the ORF15 protein and results in premature truncation of the protein. Full co-segregation of the mutation and the disease was observed in the pedigree; no mutation was detected in 10 unaffected males and 11 unaffected females.
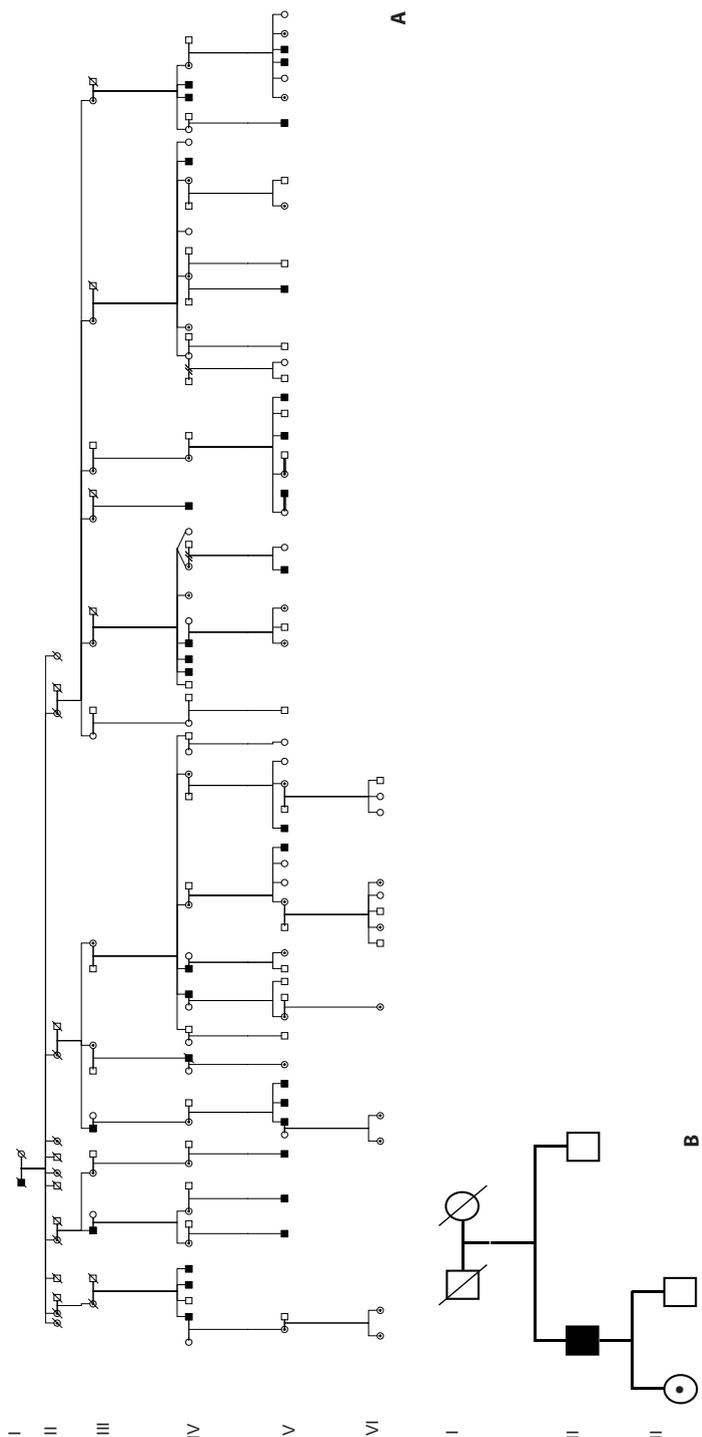
Figure 1. Pedigree of the two families with cone dystrophy and mutations in the *RPGR* ORF15 gene.

(a) Pedigree of family 1 with X-linked cone dystrophy (CD) showing segregation of the c.3317dup (p.Ser1107ValfsX4) mutation in ORF15 of the *RPGR* gene.

(b) Pedigree of family 2 with CD showing segregation of the c.3300_3301del (p.His1100GlnfsX10) mutation in ORF15 of the *RPGR* gene.

Open square and circle, unaffected males and females; black square, affected males; open circle with a dot, an obligate female carrier; dashed symbols denote deceased individuals.
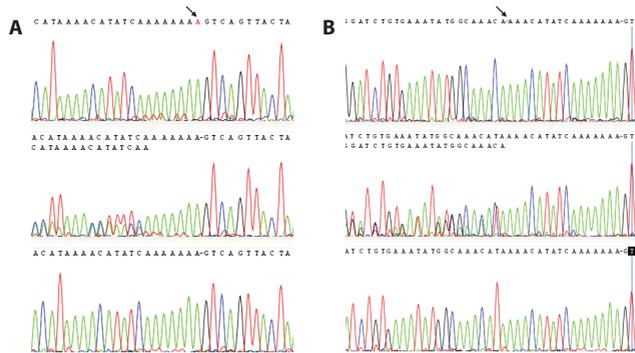
Figure 2. Sequence chromatograms of the *RPGR* ORF15 gene for family 1 and 2.
(a) Sequence chromatograms of the *RPGR* ORF15 gene for family 1 with c.3317dup (p.Ser1107ValfsX4) mutation. The top chromatogram shows a hemizygous mutated allele (duplication of an adenine nucleotide in the A base stretch); the middle chromatogram a heterozygous mutated sequence in a female carrier; the bottom chromatogram shows the normal allele.
(b) Sequence chromatograms of the *RPGR* ORF15 gene for family 2 with c.3300_3301del (p.His1100GlnfsX10) mutation. The top chromatogram shows the hemizygous deleted allele; the middle chromatogram shows the heterozygous mutated allele in a female carrier; the bottom chromatogram the normal allele. The displayed chromatograms in figure A and B are reverse sequences causing the typical disturbed sequence patterns in such a heterozygous carrier chromatogram to the left.

In the proband of family 2, a novel 2bp deletion c.3300_3301del (p.His1100GlnfsX10) in *RPGR* ORF15 was identified (Figure 2b). This mutation also resulted in a frameshift mutation, leading to a premature truncation of the protein at aminoacid 1110 of the C-terminus. This mutation was also present in his unaffected daughter, and was not identified in his unaffected brother.

Clinical findings and risk of visual decline

For family 1, the clinical findings of all affected males (N=25), female carriers (N=25) and non-carriers (N=21) are summarized in Table 1. Data on multiple visits were available with a mean follow-up of 13 years (SD 10). The mean age at onset was 36.2 (SD 3.1) years, and all patients showed progression of the disease. Hemeralopia was a first symptom in 8/25 (32%), preceding visual loss. Nystagmus was not observed in any patient. High myopia, refractive error of -6 D or worse, was common (19/25, 76%) in patients, significantly more common than in female carriers (2/25, 8%; *P*< 0.001). High myopia was not present in non-carriers. All three color axes were severely disturbed in all patients, except in one. This patient was relatively young (21 years), had normal visual acuity, only mild color vision disturbances, and a normal macula.

Table 1. Clinical findings at onset and last exam of all males with *RPGR* gene defect and cone dystrophy, the female carriers and the non-carriers of family 1.

Family (N=71)	Mean age (years)		Legal blindness (N)		Refractive error (%)			Color vision (%)		Electroretinogram (%)	
	Onset	Last exam	<40 years	> 40 years	-2D to+2D	<-2D to -6D	<-6D	Mild	Severe	Reduced cones only	Reduced cones > rods
Cone dystrophy (N=25)	36	49	1	9	3/25 (12%)	4/25 (16%)	18/25 (72%)	1/25 (4%)	24/25 (96%)	24/25 (96%)	1/25 (4%)
Carriers (N=25)	NA	41			21/25 (84%)	2/25 (8%)	2/25 (8%)	4/25 (16%)	2/25 (8%)	NA	NA
Non carriers (N=21)	NA	37			19/21 (90%)	2/21 (10%)	0	3/21 (14%)	1/21 (5%)	NA	NA

Family (N=71)	Macular appearance: Onset (%)				Macular appearance: Last exam (%)			
	Normal	Pigmentary changes	Bulls eye maculopathy	RPE atrophy	Normal	Pigmentary changes	Bulls eye maculopathy	RPE atrophy
Cone dystrophy (N=25)	7/25 (28%)	13/25 (52%)	4/25 (16%)	1/25 (4%)	1/25 (4%)	11/25 (44%)	10/25 (40%)	3/25 (12%)
Carriers (N=25)	25/25 (100%)	0	0	0	25/25 (100%)	0	0	0
Non carriers (N=21)	24/25 (96%)	1/25 (4%)	0	0	24/25 (96%)	1/25 (4%)	0	0

Macular appearance deteriorated progressively in most patients, and ranged from no abnormalities to a bull's eye maculopathy or atrophy (Figure 3). Goldmann perimetry was abnormal in all patients, and showed a reduced central sensitivity (N=3) or a (relative) central scotoma (N=22). ERG demonstrated reduced or absent photopic responses with normal scotopic responses in 24/25 patients. In these patients, the latter remained normal during follow-up. In the remaining patient (age 72 years), the ERG did show slightly reduced rod responses, however, this occurred only after 22 years of disease duration. All carriers and non-carriers had a normal visual acuity, normal macular appearance, and normal ERG.

Figure 3. Fundus photographs.

(a) Composite fundus photograph of the left eye of patient V-4, of family 1 with a c.3317dup (p.Ser1107ValfsX4) mutation in the *RPGR* ORF15 gene, performed at age 27 years. No macular abnormalities are apparent yet.

(b) Composite fundus photographs of the left eye of patient IV-19 of family 1 with the c.3317dup (p.Ser1107ValfsX4) mutation in *RPGR* ORF15, performed at age 71 years. The retina shows retinal pigment epithelium atrophy in the macular region and peripapillary atrophy. The patient has high myopia.

Figure 4 shows the cumulative risk of visual decline as a function of age in all affected males of family 1. Low vision was present in 50% of patients at age 35 years (SE 2.2); and in 75% of patients at 40 years (SE 1.1). Legal blindness was present in 50% at 47 years (SE 3.4), and in 75% at 60 years (SE 2.3).
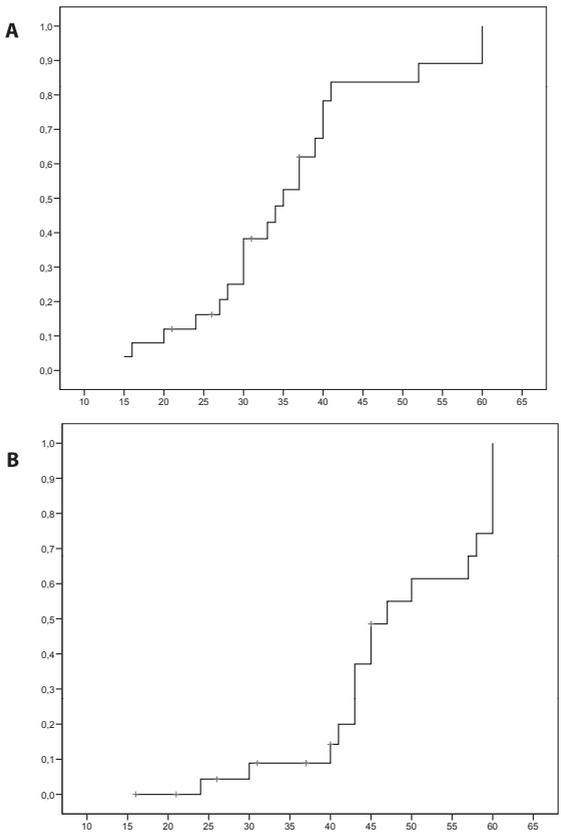
Figure 4. Kaplan-Meier survival curves as a function of age.
(a) Kaplan-Meier survival curves showing the cumulative incidence of poor vision (visual acuity <0.50) as a function of age.
(b) Kaplan-Meier survival curves showing the cumulative incidence of legal blindness (visual acuity ≤0.10) as a function of age.

With respect to family 2, the proband developed color vision disturbances at age 16 years, and a progressively deteriorating visual acuity since age 43 years to counting fingers at age 75 years. He had high myopia, severely disturbed color vision in all three axes, and atrophic lesions in the macula. Goldmann perimetry showed a central scotoma with a normal periphery, and ERG revealed absent photopic responses with normal rod responses. His brother had a normal visual acuity with no color vision disturbances and a normal macular appearance.

DISCUSSION

In this report, we describe two families with *RPGR* mutations in the 3' terminal end of ORF15 and cone pathology. The onset in these families was relatively late, i.e., 3rd and 4th decade, and visual acuity declined to legal blindness within two decades thereafter. The onset and clinical course were rather homogeneous in all affected individuals. It was remarkable that rod function remained unaffected in almost all patients. Only in one patient with a long duration of disease, rod responses were slightly diminished. This coincided with a normal peripheral visual field and no nyctalopia, indicating that the rod decay in this person was not clinically significant.

The *RPGR* gene is known to express different isoforms caused by alternative splicing.[3] Two of these protein isoforms are localized in the connecting cilium of cone and rod photoreceptors. The first is encoded by the most commonly expressed transcript, RPGR-ORF15, containing exons 1 through ORF15 (a large exon consisting of exon 15 extending into a part of intron 15). The other, RPGR-ex1-19, contains exons 1 through19 but lacks exons 14 and 15.[3] Exons 1-14 contain six RCC1-like domains; their main function is to facilitate interaction with other proteins.[19-22] Mutations within these domains lead to reduced or abolished protein interactions.[19] The ORF15 region encodes for a repetitive glycine and glutamic acid rich protein domain of unknown function.[3,4] It has been demonstrated in the mouse that reduction of this repetitive region can preserve a normal protein function.[21] Most reported mutations in the first 14 exons are nonsense or frameshift mutations which can lead to nonsense-mediated decay of the mRNA (NMD), and low or absent levels of the transcript. In contrast, nonsense or frameshift mutations in ORF15 are less likely to lead to NMD since this is the last exon of the transcript,[23] and a series of truncated proteins of varying length can be found.[7]

Until now, 300 pathogenic mutations have been discovered in the *RPGR* gene. Most lead to RP (N=287), only seven mutations have been associated with CRD (Figure 5).[24] Systemic involvement like respiratory tract infections or hearing loss has been described in only a few patients.[25] One paper described atrophic macular degeneration[26] and three earlier publications reported a phenotype of pure CD.[3,14,15] More than half (164/287; 57%) of the mutations leading to RP occur in the ORF15 region; and all mutations that cause CRD and CD have been found at this site. No mutations have been detected in exon 16-19 (Figure 5).
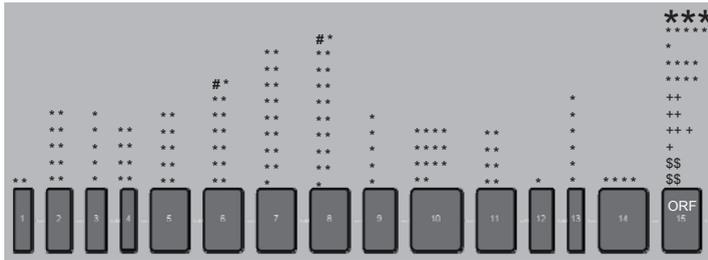
Figure 5. Localization of all known mutations in the *RPGR* ORF15 isoform (N=300) stratified per phenotype and per exon.
*, Retinitis pigmentosa (N=287, large asterix symbolizes 50 different mutations); +, Cone-rod dystrophy(N=7); $, Cone dystrophy (N=4); #, Retinitis pigmentosa with systemic ciliary dysfunction (N=2).

Literature on the clinical course in CD patients with mutations in *RPGR* is lacking. In this report, we describe the onset and course of visual acuity in 25 patients of a family with a known duplication (c.3317dup), and in a proband with a newly identified deletion (c.3300_3301del) in ORF15. Both are frameshift mutations located in the terminal 3' region of this exon, causing premature termination of the protein. Both mutations resulted in a loss of only ~40-50 amino acids at the C-terminus. We propose that this could explain the late onset of the disease with legal blindness occurring after a mean age of 60 years. In comparison, the mean age of legal blindness for mutations in the first 14 exons and in the 5' region of ORF15 was 45 years in RP patients.[16]

Why do some ORF15 mutations affect rods, and others cause predominantly cone involvement?[27] Several speculations can be made. Mutant mice with different mutations exhibit mis-localization of rod and/or cone (rhod)opsins. Which opsin is mis-localized most depends on the type of mutation.[28] In humans, there is also a genotype-phenotype relation: certain mutations predispose to rod cell loss and others affect mostly cones. The RPGR protein is expressed in the basal body of the connecting cilium of both rod and cone photoreceptors. The connecting cilium serves as a conduit for bidirectional transport of protein complexes, and is important for the outer segment disc morphogenesis and renewal.[29] For execution of its transport function, the RPGR protein interacts with other ciliary proteins like RPGRIP1, CEP290, NPHP5, and NPHP6.[30] These protein interactions are known to differ among rods and cones, and certain mutations may have more effect on cone interactions than those of rods and vice versa.

The duplication of family 1 (c.3317dup) had been reported earlier by Demirci et al,[11] who observed this mutation in an individual with CRD. In our family, the rods were spared in virtually all patients. Variation in phenotype in patients with identical mutations may be due to post-translational effects by modifying genes or environmental factors.[31]

However, the homogeneity of the phenotype in family 1 signifies that these effects are probably small.

The female carriers in both our families did not have any ocular involvement. In many reports of RP families with ORF15 mutations, carriers have mild or even severe ophthalmologic abnormalities, ranging from pigmentary changes in the periphery to severe visual loss.[32,33,5] Mutations causing a widespread photoreceptor decay may be more difficult to compensate for the non mutated X-allele than mutations causing a more restricted dysfunction of the photoreceptors.[5]

A large proportion of the CD patients in our families had high myopia of more than 6 D (17/25;73%). Photoreceptor disorders commonly have high myopia, independent of genetic etiology or inheritance mode.[34-36] The reasons for this phenomenon remain unclear. One explanation may be that scleral growth is stimulated by signals from dysfunctional photoreceptors; another is that high myopia and primary photoreceptor disorders are part of the same syndrome.

In conclusion, this is a comprehensive clinical report of two families with pure cone involvement due to *RPGR* ORF15 mutations. Our survival analyses can be useful to counsel such patients. This report adds to the growing evidence that *RPGR*, an established gene for rod cell loss, can be restricted to cone cell loss.

REFERENCES

1. Michaelides M, Hardcastle AJ, Hunt DM, Moore AT. Progressive cone and cone-rod dystrophies: phenotypes and underlying molecular genetic basis. Surv Ophthalmol. 2006;51:232–258.

2. Michaelides M, Hunt DM, Moore AT. The cone dysfunction syndromes. Br J Ophthalmol. 2006;88:291–7.

3. Vervoort R, Lennon A, Bird AC, et al. Mutational hot spot within a new RPGR exon in X-linked retinitis pigmentosa. Nat Genet. 2000;25:462-6.

4. Vervoort R, Wright AF. Mutations of RPGR in X-linked retinitis pigmentosa (RP3). Hum Mutat. 2002;19:486-500.

5. Neidhardt J, Glaus E, Lorenz B, et al. Identification of novel mutations in X-linked retinitis pigmentosa families and implications for diagnostic testing. Mol Vis. 2008;14:1081-93.

6. Bader I, Brandau O, Achatz H, et al. X-linked retinitis pigmentosa: RPGR mutations in most families with definite X linkage and clustering of mutations in a short sequence stretch of exon ORF15. Invest Ophthalmol Vis Sci. 2003;44:1458-63.

7. Shu X, Black GC, Rice JM, et al. RPGR mutation analysis and disease: an update. Hum Mutat. 2007;28:322-8.

8. Jin ZB, Gu F, Ma X, Nao-i N. Identification of a novel RPGR exon ORF15 mutation in a family with X-linked retinitis pigmentosa. Arch Ophthalmol. 2007;125:1407-12.

9. Bergen AAB, Pinckers AJLG. Localization of a Novel X-Linked Progressive Cone Dystrophy Gene to Xq27: Evidence for Genetic Heterogeneity. Am J Hum Genet. 1997;60:1468-1473.

10. Mears AJ, Hiriyanna S, Vervoort R, et al. Remapping of the RP15 locus for X-linked cone-rod degeneration to Xp11.4-p21.1, and identification of a de novo insertion in the RPGR exon ORF15. Am J Hum Genet. 2000;67:1000-3.

11. Demirci FY, Rigatti BW, Wen G, et al. X-linked cone-rod dystrophy (locus COD1): identification of mutations in RPGR exon ORF15. Am J Hum Genet. 2002;70:1049-53.

12. Jalkanen R, Demirci FY, Tyynismaa H, et al. A new genetic locus for X linked progressive cone-rod dystrophy. J Med Genet. 2003;40:418-23.

13. Ebenezer ND, Michaelides M, Jenkins SA, et al. Identification of novel RPGR ORF15 mutations in X-linked progressive cone-rod dystrophy (XLCORD) families. Invest Ophthalmol Vis Sci. 2005;46:1891-8.

14. Yang Z, Peachey NS, Moshfeghi DM, et al. Mutations in the RPGR gene cause X-linked cone dystrophy. Hum Mol Genet. 2002;11:605-11.

15. Robson AG, Michaelides M, Luong VA, et al. Functional correlates of fundus autofluorescence abnormalities in patients with RPGR or RIMS1 mutations causing cone or cone rod dystrophy. Br J Ophthalmol. 2008;92:95-102.

16. Sandberg MA, Rosner B, Weigel-DiFranco C, et al. Disease course of patients with X-linked retinitis pigmentosa due to RPGR gene mutations. Invest Ophthalmol Vis Sci. 2007;48:1298-304.

17. Marmor MF, Fulton AB, Holder GE, et al. ISCEV Standard for full-field clinical electroretinography (2008 update). Doc Ophthalmol. 2009;118:69-77.

18. Booij JC, Bakker A, Kulumbetova J, et al. Simultaneous Mutation Detection in 90 Retinal Disease Genes in Multiple Patients Using a Custom-designed 300-kb Retinal Resequencing Chip. Ophthalmology. 2011;118:160-167.

19. Roepman R, van Duijnhoven G, Rosenberg T, et al. Positional cloning of the gene for X-linked retinitis pigmentosa 3: homology with the guanine-nucleotide-exchange factor RCC1. Hum Mol Genet. 1996;5:1035-41.

20. Roepman R, Bernoud-Hubac N, Schick DE, et al. The retinitis pigmentosa GTPase regulator (RPGR) interacts with novel transport-like proteins in the outer segments of rod photoreceptors. Hum Mol Genet. 2000;9:2095-2105.

21. Hong DH, Pawlyk BS, Adamian M, Li T. Dominant, gain-of-function mutant produced by truncation of RPGR. Invest Ophthalmol Vis Sci. 2004;45:36-41.

22. He S, Parapuram SK, Hurd TW, et al. Retinitis Pigmentosa GTPase Regulator (RPGR) protein isoforms in mammalian retina: insights into X-linked Retinitis Pigmentosa and associated ciliopathies. Vision Res. 2008;48:366-76.

23. Nagy E, Maquat LE. A rule for termination-codon position within intron-containing genes: when nonsense affects RNA abundance. Trends Biochem Sci. 1998;23:198-9.

24. Fokkema IFAC, Den Dunnen JT and Taschner PEM. LOVD: easy creation of a locus-specific sequence variation database using an "LSDB-in-a-Box" approach. Hum Mutat. 2005;26:63-8.

25. Zito I, Downes SM, Patel RJ, et al. RPGR mutation associated with retinitis pigmentosa, impaired hearing, and sinorespiratory infections. J Med Genet. 2003;40:609-15.

26. Ayyagari R, Demirci FY, Liu J, et al. X-linked recessive atrophic macular degeneration from RPGR mutation. Genomics. 2002;80:166-71.

27. Demirci FY, Gupta N, Radak AL, et al. Histopathologic study of X-linked cone-rod dystrophy (CORDX1) caused by a mutation in the RPGR exon ORF15. Am J Ophthalmol. 2005;139:386-8.

28. Hong DH, Pawlyk BS, Shang J, et al. A retinitis pigmentosa GTPase regulator (RPGR)-deficient mouse model for X-linked retinitis pigmentosa (RP3). Proc Natl Acad Sci U S A. 2000;97:3649-54.

29. Zhao Y, Hong DH, Pawlyk B, et al. The retinitis pigmentosa GTPase regulator (RPGR)- interacting protein: subserving RPGR function and participating in disk morphogenesis. Proc Natl Acad Sci U S A. 2003;100:3965-70.

30. Roepman R, Wolfrum U. Protein networks and complexes in photoreceptor cilia. Subcell Biochem. 2007;43:209-35.

31. Walia S, Fishman GA, Swaroop A, et al. Discordant phenotypes in fraternal twins having an identical mutation in exon ORF15 of the RPGR gene. Arch Ophthalmol. 2008;126:379-84.

32. Adamian M, Pawlyk BS, Hong DH, Berson EL. Rod and cone opsin mislocalization in an autopsy eye from a carrier of X-linked retinitis pigmentosa with a Gly436Asp mutation in the RPGR gene. Am J Ophthalmol. 2006;142:515-8.

33. Amzallag T, Puech B, Hache JC, François P. Progressive cone dystrophy: electrophysiological changes in female carriers. J Fr Ophtalmol. 1990;13:421-8.

34. Sharon D, Sandberg MA, Rabe VW, et al. RP2 and RPGR mutations and clinical correlations in patients with X-linked retinitis pigmentosa. Am J Hum Genet. 2003;73:1131-46.

35. Pras E, Abu A, Rotenstreich Y, et al. Cone-rod dystrophy and a frameshift mutation in the PROM1 gene. Mol Vis. 2009;15:1709-16.

36. Smith M, Whittock N, Searle A, et al. Phenotype of autosomal dominant cone-rod dystrophy due to the R838C mutation of the GUCY2D gene encoding retinal guanylate cyclase-1. Eye (Lond). 2007;21:1220-5.
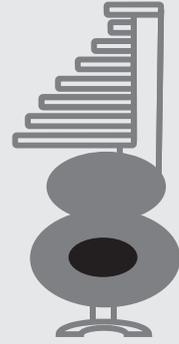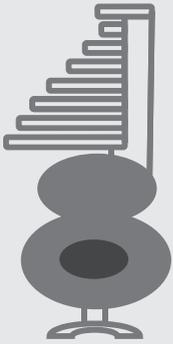
Chapter 3d

**Clinical course, etiology, and visual outcome
in cone and cone-rod dystrophy**

ABSTRACT

Objective: To evaluate the clinical course, genetic etiology, and visual prognosis in patients with cone dystrophy (CD) and cone-rod dystrophy (CRD).

Design: Retrospective multicenter study.

Participants: Consecutive probands with CD (N=98), CRD (N=83), and affected relatives (N=41 and N=17, respectively) from various ophthalmogenetic clinics in the Netherlands, Belgium, and United Kingdom.

Methods: Data on best-corrected Snellen visual acuity, color vision, ophthalmoscopy, fundus photography, Goldmann perimetry, standard ISCEV electroretinogram (ERG) from all patients were registered from medical charts during a mean follow up of 19 years (SD 15). The *ABCA4, CNGB3, KCNV2, PDE6C,* and *RPGR* genes were analyzed by direct sequencing.

Main outcome measures: 10-year progression of all clinical parameters; cumulative risk of low vision and legal blindness.

Results: Mean onset of CD was 16 years (SD 11), of CRD 12 years (SD 11, $P = 0.02$); 92% of CD and 90% of CRD had an autosomal recessive (AR) inheritance. Ten years after diagnosis, 91% of CD and 98% of CRD had severe color vision defects; 35% of CD and 51% of CRD had atrophy of the RPE in the macula; .and 67% of CD, and 91% of CRD ($P = 0.06$) showed enlargement of central visual field defects. Legal blindness was present in 50% of CD at age 48 (SE 3.1) and in 50% of CRD at age 23 (SE 1.1; $P <0.001$). Mutations were found in *ABCA4* in 9/90 (10%) of AR-CD, and in 17/65 (26%) of AR-CRD. In AR-CD probands, mutations in *CNGB3* (3/90; 3%), *KCNV2* (4/90; 4%), and in *PDE6C* (1/90; 1%) were found. Three *KCNV2* mutations were novel. *RPGR* was affected in all X-linked (XL)-CD and in 4/5 (80%) of XL-CRD probands. *ABCA4* mutations as well as age of onset <20 years were significantly associated with a higher risk of legal blindness in both AR-CD and AR-CRD ($P <0.001$).

Conclusions: CRD had a more unfavorable clinical course and visual outcome than CD; however, the majority of both disorders reached legal blindness before 50 years. Mutations in the *ABCA4* gene and early onset of disease were independent prognostic parameters. Our data may serve as an aid in counseling patients with progressive cone disorders.

INTRODUCTION

Cone dystrophy (CD) and cone-rod dystrophy (CRD) are the most common hereditary cone disorders with a frequency of 1:30,000-40,000 worldwide.[1-3] Both are characterized by a loss of cone photoreceptors, a progressive visual decline, and a heterogeneous etiology. However, CD and CRD are also distinct disease entities with considerable variability in genetic causes and clinical consequences.

Patients with CD present with poor visual acuity and severe color vision disturbances. The macular appearance ranges from normal to a bull's eye maculopathy, and the optic disc may show a variable degree of temporal pallor. Visual fields generally show a central scotoma. Cone amplitude responses, as registered by full-field electroretinogram (ERG), deteriorate progressively, whereas rod responses are initially normal. All modes of Mendelian inheritance have been reported, but the autosomal recessive (AR) form is by far the most common. The genetic causes of the autosomal dominant (AD)[4-6] and X-linked (XL)[7,8] forms have been elucidated to a large extent, but in contrast, the genetic causes of the AR form are mostly unknown.[9-13]

CRD can be distinguished from CD by the early involvement of rod photoreceptors. Symptoms resemble those of CD, but patients may also experience nyctalopia due to rod involvement. The macular appearance resembles that of CD, but some patients may also develop retinal vascular attenuation and peripheral pigment deposits. Visual fields show a central scotoma with a variable degree of peripheral involvement. The ERG shows reduced cone and rod responses, with cone responses more severely affected. As in CD, all modes of inheritance are present, and currently, 17 genes and some additional loci have been reported to be involved.[3,14] *ABCA4* appears to be the most prominent causal gene, however, the etiologic fraction for this gene varies widely between studies (24-65%).[15-21] Hence, a large proportion of AR-CRD patients still has an unknown etiology.

Patient management and counseling is currently challenging for clinicians who encounter CD and CRD patients. Age of onset, decline of visual acuity and visual fields, progression to legal blindness, genetic etiology, and genotype-phenotype correlations have not been studied in large patient groups with these diagnoses. How CD and CRD progress, at what age patients will not be able to drive or read anymore, and at what age legal blindness occurs are questions which remain largely unanswered.

The purpose of this study was to evaluate clinical parameters as a function of age in a large series of CD and CRD patients, and to study the relative contribution of known causal genes. Probands and relatives were ascertained from multiple ophthalmogenetic

clinics, were included consecutively without knowledge of genetic defect or visual out-come, and were diagnosed according to standardized protocols. Disease parameters were systematically evaluated from medical charts, and complemented by a clinical and genetic work-up. This enabled us to study the causes and consequences of both CD and CRD, as well as their potential differences.

PATIENTS AND METHODS

Study Population

All patients were ascertained from eight ophthalmogenetic centers located in the Neth-erlands, Belgium and the United Kingdom. Most patients (~70%) were selected from ERG databases using the terms 'reduced' or 'absent' cone amplitude responses. The remain-ing patients (~30%) were ascertained as consecutive patients who visited one of the clinics during the study period (2006-2009). In total, we included 98 CD patients with 41 affected relatives, and 83 CRD patients with 17 affected relatives. We retrieved all clinical data from medical charts, and two independent clinical graders (A.T. and C.K.) made a final diagnosis based on a standard protocol. Discrepancies were discussed and solved by consensus. Inclusion criteria for CD were: progressive decline of visual acuity, color vision disturbances, and reduced cone amplitude responses on ERG, with preserved rod responses for at least five years. Inclusion criteria for CRD were: a progressive decline of visual acuity, color vision disturbances, and reduction of both cone and rod responses on ERG, with cones equally, or more severely reduced than rods. Exclusion criteria were congenital nystagmus and syndromic disorders. Patients suspected to have Stargardt disease (STGD) with a typical fundus flavimaculatus and only mild cone involvement on ERG were also excluded from the study. Visual field testing was executed with Goldmann perimetry; depth of scotomata was scored as relative or absolute; location of scotomata as central or peripheral.

The study was approved by the Medical Ethics Committee of Erasmus Medical Center and adhered to the tenets of the Declaration of Helsinki. All participants provided signed, informed consent for participation in the study, retrieval of medical records, and use of blood and DNA for research.

Clinical Examination

We registered the existing ophthalmologic data in a database, including all data from ophthalmologists who had been visited in the past. These data included Snellen visual acuity, color vision (Hardy-Rand-Rittler color vision test or Lanthony Panel D-15 tests), slitlamp and fundus examination, perimetry and ERGs. Patients with incomplete or

unavailable data from the past five years were invited for an additional ophthalmologic examination, Goldmann perimetry, and ERG. Color vision defects were classified as 'mild' or 'severe' in accordance with the criteria provided in the manuals. ERGs were performed with contact lens electrodes and followed the recommendations of the International Society for Clinical Electrophysiology of Vision (ISCEV).[22] We used standard criteria from the United States to define low vision (best corrected visual acuity <0.5 in the better eye), and legal blindness (best corrected visual acuity ≤ 0.1 in the better eye).

Molecular Genetic Analysis

Blood samples were obtained from probands, affected relatives, and parents. DNA was isolated from peripheral blood lymphocytes by standard procedures. For all patients with AR-CD, the coding region and intron/exon boundaries of the *CNGB3, KCNV2* and *PDE6C* genes were amplified by polymerase chain reaction (PCR), followed by direct sequencing. These analyses were executed at the Department of Human Genetics, Radboud University Nijmegen Medical Center. XL-C(R)D probands were screened for mutations in the *RPGR* gene at the Netherlands Institute for Neuroscience (NIN) in Amsterdam. If possible, segregation analysis was performed when mutations were detected in autosomal genes or one mutation was found in an X-linked gene. *ABCA4* gene mutations were analyzed in AR-C(R)D patients with microarray screening performed by Asper Biotech (Tartu, Estonia) according to previously described methods.[23] If only one *ABCA4* allele was affected, the pathogenicity of mutations was calculated with various online prediction programs including SIFT, Polyphen, Grantham score, SMART and BLOSUM62.[24] If only one pathologic affected allele was found, denaturing gradient gel electrophoresis (DGGE) was performed to detect a second disease allele. Novel variants were screened in 100 ethnically matched control subjects.

Statistical Analysis

Frequency differences between CD and CRD patients were compared by Student's *t*-test for continuous variables, and Pearson Chi-square test for categorical data. Cumulative risks of visual loss were studied with Kaplan-Meier product-limit survival analysis, with low vision or legal blindness as outcomes. Analyses were stratified for the diagnosis CD or CRD, and for mode of inheritance (XL, AR, or AD). Cumulative risks were compared between groups using the logrank test. Cox regression survival analyses were performed for early onset (<20 years) and presence of *ABCA4* mutations with low vision and legal blindness as outcomes. Participants beyond 60 years were pooled to maintain unbiased estimates.

RESULTS

Clinical characteristics and visual outcomes

The most common mode of inheritance was AR in both disease groups (92% and 90%). The first symptom was visual loss in 88% (123/139) of CD, and in 85% (85/100) of CRD. Other symptoms at onset were: dyschromatopsia (CD:7/139; CRD: 8/100), nyctalopia (CRD: 2/100), photophobia (CD: 7/139; CRD: 5/100) or hemeralopia (CD:2/139). Baseline characteristics of all probands are summarized in Table 1. The mean age of disease onset was significantly earlier in CRD (12 years vs 16 years; *P* =0.02). High myopia (more than -6 D) was observed in 17% (17/98) of CD, and in 17% (14/83) of CRD patients (*P* =0.53); all XL patients had high myopia. High refractive errors were very unusual in AR-CD/CRD patients with *ABCA4* mutations (3/26;12%).

Table 1. Baseline characteristics of cone dystrophy (CD) and cone-rod dystrophy (CRD) probands.

	CD, N total=98	CRD, N total=83
Mean age at onset, N (SD*)	16 (11)	12 (11)
Inheritance		
Autosomal recessive or sporadic, N (%)	90 (92)	75 (90)
Autosomal dominant, N (%)	6 (6)	3 (4)
X-linked, N (%)	2 (2)	5 (6)
Gender		
Male, N (%)	60 (61)	63 (76)
Refractive error		
Emmetropia -2/+2 D, N (%)	40 (41)	43 (52)
Mild myopia -2/-6 D, N (%)	29 (30)	16 (18)
High myopia < -6 D, N (%)	17 (17)	14 (17)
Mild hypermetropia +2/+6 D, N (%)	11 (11)	10 (12)
High hypermetropia > +6 D, N (%)	1 (1)	2 (1)

*SD: standard deviation

Clinical findings at first ophthalmologic exam and at 10 years follow-up are presented in Table 2. At diagnosis, peripheral visual fields were intact in all CD patients, and in 31% (31/100) of CRD. We classified the latter group as CRDs with only central visual field involvement (cfCRD), as opposed to CRDs who showed central and peripheral visual field defects at diagnosis (cpfCRD). The mean age of onset in cfCRD was 17 years (SD 13) as opposed to 12 years in cpfCRD.

Table 2. Clinical findings at first ophthalmologic exam and at 10 years follow-up stratified for cone dystrophy (CD) and cone-rod dystrophy (CRD).

	CD, N total=139		CRD, N total=100			
	Ntot=139*	N=90*	cfCRD† Ntot=31*	cfCRD† N=24*	cpfCRD‡ Ntot=69*	cpfCRD‡ N=57*
	@ diagnosis	*@ 10 years*	*@ diagnosis*	*@ 10 years*	*@ diagnosis*	*@ 10 years*
Color vision						
….*Mild, n/N (%)*	28/139 (20)	16/90 (9)	13/31 (42)	3/24 (12)	10/69 (14)	1/57 (2)
….*Severe, n/N (%)*	111/139 (80)	74/90 (91)	18/31 (58)	21/24 (88)	59/69 (86)	56/57 (98)
Macular appearance						
….*Normal, n/N (%)*	25/137 (18)	15/90 (17)	10/31 (32)	3/24 (13)	16/69 (23)	3/57 (5)
….*Pigmentary changes, n/N (%)*	72/137 (53)	43/90 (48)	12/31 (39)	7/24 (29)	32/69 (46)	25/57 (44)
….*Bull's eye/atrophy, n/N (%)*	40/137 (29)	32/90 (35)	9/31 (29)	14/24 (58)	21/69 (31)	29/57 (51)
Goldmann Perimetry						
….*Normal, n/N (%)*	6/137 (4)					
….*Central scotoma, n/N (%)*	131/137 (96)	33/90 (35)	31/31 (100)	2/24 (9)	69/69 (100)	5/57 (9)
….*Enlarged central scotoma, n/N (%)*		57/90 (67)		12/24 (50)		52/57 (91)
….*Peripheral scotoma, n/N (%)*				10/24 (41)	69/69 (100)	
….*Enlarged peripheral scotoma, n/N (%)*						57/57 (100)
Electroretinogram						
….*Reduced cones, n/N (%)*	139/139 (100)	54/90 (63)				
….*Reduced cones>rods, n/N (%)*		36/90 (37)	31/31 (100)	24/24 (100)	69/69 (100)	57/57 (100)

*: Probands and affected relatives combined
†: cfCRD: Cone-rod dystrophy with central visual field loss at diagnosis.
‡: cpfCRD: Cone-rod dystrophy with central and peripheral visual field loss at diagnosis.

Mean follow-up was 19 years (SD 15). Ten years after diagnosis, 91% of CD, 88% of cfCRD, and 98% of cpfCRD had severe color vision defects; 35% of CD, 58% of cfCRD, and 51% of cpfCRD had a bull's eye maculopathy or atrophy; 37% of CD developed reduced rod responses on ERG; 67% of CD showed enlargement of the central scotoma on visual fields, and none developed peripheral visual field defects. Also at 10 years, 41% of cfCRD developed peripheral visual field defects, and all cpfCRD showed progression of the already existing peripheral scotomas.

Risk of visual loss showed no significant differences for mode of inheritance (AR, XL, or AD) in either group (P =0.30), although visual loss appeared to be slightly more detrimental in XL before middle age. Visual outcomes after middle age appeared similar,

but statistical power to detect differences was low for these ages. Figure 1 shows the cumulative risk of visual decline in CD, cfCRD, and cpfCRD as a function of age. In CD, low vision was present in 50% at age 19 years (SE 1.8), and in 75% at age 32 (SE 1.7). Legal blindness was present in 50% at 48 years (SE 3.1), and in 75% at age 58 (SE 3.5). In cfCRD, low vision was present in 50% at age 27 (SE 6.8), and in 75% at age 36 (SE 2.8); legal blindness in 50% at age 40 (SE 3.1), in 75% at age 59 (SE 2.8). In cpfCRD, low vision was present in 50% at age 9 years (SE 0.9), and in 75% at age 24 (SE 1.0); legal blindness in 50% at age 23 (SE 1.1), and in 75% at age 53 years (SE 8.6).The cumulative risks of CD differed significantly from the risks of cpfCRD ($P<0.001$), but not from those of cfCRD (low vision: $P = 0.53$; legal blindness: $P = 0.76$).
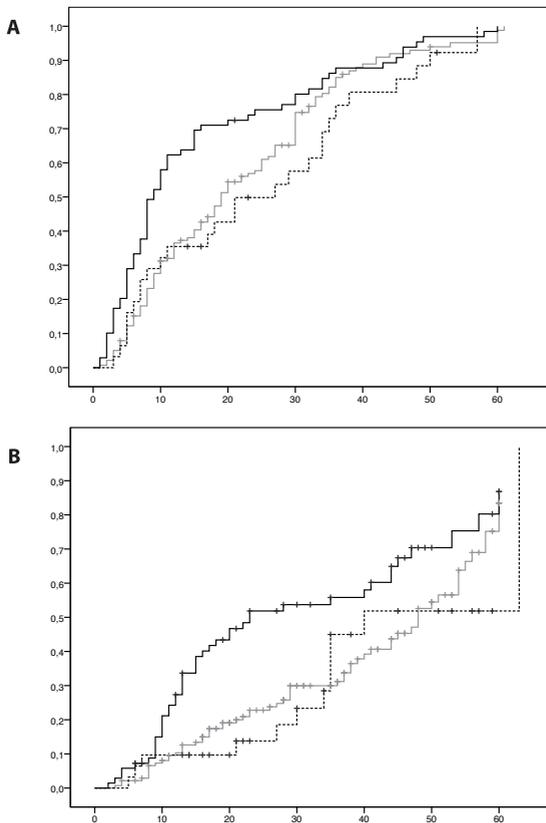

Figure 1. Kaplan-Meier survival curves as a function of age for cone disorders.
(a) Kaplan-Meier survival curves showing the cumulative incidence of poor vision (visual acuity <0.50) as a function of age stratified for cone dystrophy (CD), cone-rod dystrophy with only central visual field involvement (cfCRD), and CRD with central and peripheral visual field involvement (cpfCRD). Grey line: CD; dashed line: cfCRD; black line: cpfCRD.
(b) Kaplan-Meier survival curves showing the cumulative incidence of legal blindness (visual acuity ≤0.10) as a function of age for CD, cfCRD and cpfCRD.

Mutation Analysis

Results of mutation analysis are provided in Table 3. For AR-CD (Table 3a), two allelic *ABCA4* mutations were detected in 10% (9/90) of probands while only one allelic *ABCA4* variant was found in 17% (15/90). Of these latter patients, five different variants were predicted with SIFT, Polyphen, Grantham score and BLOSUM62 to be pathogenic; two as non-pathogenic. *CNGB3* mutations were found in 3/90 (~3%) probands,[25] a single *CNGB3* mutation was found in only one proband. Two *KCNV2* mutations were detected in 4/90 (~4%) probands; of these, one proband carried a novel homozygous stop mutation (c.563G>A, p.W188X) leading to a premature truncation of the protein. Another proband had a novel homozygous missense mutation (c.782C>A, p.A261D), which resided in a voltage dependent potassium channel. This region was conserved in almost all species. Segregation analysis showed that affected siblings shared the same mutant alleles as the proband, while unaffected relatives did not have these allele combinations. In six additional probands, only one mutation was identified on a single *KCNV2* allele, while the other allele did not show non-synonymous sequence changes. Two of these showed supra-normal rod responses on ERG (proband with the novel variant: c.6_9delCAAA, and proband with c.339C>A). *PDE6C* mutations were detected in only one proband.[26] *RPGR* gene mutations were found in all XL-CDs. To the best of our knowledge, the four newly described mutations have not been reported before.

For AR-CRD (Table 3b), two allelic *ABCA4* mutations were detected in 26% (17/65) of pro-bands, five of these CRD probands did not show peripheral visual field loss (cfCRD). Only one allelic *ABCA4* mutation was present in 23% (15/65) of probands. Of these patients, three different variants were predicted to be possibly pathogenic with SIFT, Polyphen, Grantham score and BLOSUM62, and six non-pathogenic. An additional DGGE screening did not reveal the second affected allele in all AR-CD and AR-CRD probands with only one possibly pathogenic *ABCA4* allele. *RPGR* gene mutations were found in 4/5 (80%) of XL-CRD probands.

Table 3a. Cone dystrophy (CD) patients and distribution of mutations in the *ABCA4*, *CNGB3*, *KCNV2*, *PDE6C* and *RPGR* genes.

Disease	Gene	Allele 1		Allele 2		Allele 3	N
		Alteration nucleotide	Alteration polypeptide	Alteration nucleotide	Alteration polypeptide		
AR[†]-CD[#]	*ABCA4*	c.214G>A	p.G72R	c.5461-10T>C	splice defect		1
		c.768G>T	p.V256V / splice defect	c.2588G>C	p.G863A	*CNGB3*: c.1148delC (p.T383IfsX13)	1
		c.768G>T	p.V256V / splice defect	c.5313-10T>C	splice defect		1
		c.768G>T	p.V256V / splice defect	c.768G>T	p.V256V / splice defect		2
		c.1822T>A	p.F608I	c.5882G>A	p.G1961E		1
		c.2588G>C	p.G863A	c.2828G>A	p.R943Q		1
		c.4539+1G>T	splice defect	c.5762_5763dup	p.A1922WfsX18		1
		c.6229C>G	p.R2077G	c.6449G>A	p.C2150Y		1
		c.5882G>A	p.G1961E	+	+	*CNGB3*: c.1148delC (p.T383IfsX13)	1
		c.768G>T	p.V256V / splice defect	+	+		3
		c.2690C>T	p.T897I	+	+		3
		c.5461-10T>C	splice defect	+	+		5
		c.5908C>T	p.L1970F	+	+		1
		Non-pathogenic *ABCA4* variants					
		c.2701A>G	p.T901A	+	+		1
		c.3813G>C	p.E1271D	+	+		1
AR-CD	*CNGB3*	c.819_826del8	p.R274VfsX12	c.886-896del11insT	p.R296YfsX9		1
		c.886-896del11insT	p.R296YfsX9	c.991-3T>G	splice defect		1
		c.1208G>A	p.R403Q	c.1208G>A	p.R403Q		1
		c.1208G>A	p.R403Q	+	+		1
AR-CD	*KCNV2*	**c.563G>A**	p.W188X	**c.563G>A**	p.W188X	*CNGB3* : **c.2383G>A**	1
		c.782C>A	p.A261D	**c.782C>A**	p.A261D		1
		c.323_329del7	p.Y108WfsX14	g.2570596_2807413del	*KCNV2* completely deleted		1
		c.556_571del16	p.G186GfsX20	c.1381G>A	p.G461R		1
		c.6_9delCAAA	p.K3RfsX96	+	+		1
		c.263G>A	p.G88D	+	+		1
		c.339C>A	p.C113X	+	+		1
		c.647T>C	p.I216T	+	+		1
		c.1123G>A	p.V375M	+	+		1

Table 3a. Continued

Disease	Gene	Allele 1		Allele 2		Allele 3	N
		Alteration nucleotide	Alteration polypeptide	Alteration nucleotide	Alteration polypeptide		
		c.1132G>A	p.V378I	+	+		1
AR-CD	*PDE6C*	c.85C>T	p.R29W	c.85C>T	p.R29W		1
XL‡ -CD	*RPGR*	g.ORF15+1564-1565insA					1
		g.ORF15+1580delTA					1

† AR; autosomal recessive
# CD; cone dystrophy
‡ XL; X-linked
The variants in bold are newly identified.

Table 3b. Cone-rod dystrophy (CRD) patients and distribution of mutations in the *ABCA4* and *RPGR* genes.

Disease	Gene	Allele 1		Allele 2		Allele 3	N
		Alteration nucleotide	Alteration polypeptide	Alteration nucleotide	Alteration polypeptide		
AR†-CRD+	*ABCA4*	c.768G>T	p.V256V / splice defect	c.5461-10T>C	splice defect		4+1#
		c.1714C>T	p.R572X	c.1822T>A	p.F608I		1#
		c.2588G>C	p.G863A / ΔG863	c.1853G>A / c.4297G>A	p.G618E / p.V1433I		1#
		c.3259G>A	p.E1087K	c.4128+1G>A	splice defect		1
		c.3602T>G	p.L1201R	c.6320G>A	p.R2107H		1
		c.4297G>A	p.V1433I	c.164A>G	p.H55R		1
		c.4539+1G>T	splice defect	c.3085C>T	p.Q1029X		1
		c.4773+1G>A	splice defect	c.5461-10T>C	splice defect		1#
		c.5461-10T>C	splice defect	c.5461-10T>C	splice defect		3+1#
		c.6729+5_19del	splice defect	c.6729+5_19del	splice defect		1
		c.634C>T	p.R212C	+	+		1
		c.768G>T	p.V256V / splice defect	+	+	*CNGB3*: c.1148delC (p.T383IfsX13)	3
		c.1648G>A	p.G550R	+	+		1
	Non-pathogenic *ABCA4* variants						
		c.455G>A	p.R152Q	+	+		1
		c.514G>A	p.G172S	+	+		1
		c.2791G>A	p.V931M	+	+		2
		c.2546T>C	p.V849A	+	+		3
		c.4909G>A	p.A1637T	+	+		1

Table 3b. Continued

Disease	Gene	Allele 1		Allele 2		Allele 3	N
		Alteration nucleotide	**Alteration polypeptide**	**Alteration nucleotide**	**Alteration polypeptide**		
		c.6416G->A	p.R2139Q	+	+		2
XL‡ -CRD	*RPGR*	g.ORF15+652-653delAG					1
		g.ORF15+822G>T					1
		g.ORF15+1444-1445delAG					1
		g.ORF15+1635-1636delTT					1

† AR; autosomal recessive
+ CRD; cone-rod dystrophy
‡ XL; X-linked
# Cone-rod dystrophy probands with only central visual field defects at diagnosis (cfCRD)

Genotype-phenotype relationships

To investigate potential genotype-phenotype relations, we estimated cumulative risk of visual decline as a function of age in AR-CD/CRD carrying pathogenic *ABCA4* mutations versus those with other genetic causes (Figure 2). For *ABCA4* probands with AR-CD, low vision was present in 50% at age 8 years and in 75% at age 10 (SE 1.0); legal blindness in 50% at age 12 and in 75% at age 21 (SE 3.8). The ages of these percentiles were significantly younger for *ABCA4* than those for other genetic causes. For *ABCA4* and CRD, low vision was present in 50% at age 7 years, in 75% at age 9 (SE 1.2); legal blindness was present in 50% at age 13, and in 75% at age 17 (SE 1.7). Again, *ABCA4* was significantly more detrimental than other genetic causes (P <0.001). When patients with only one possibly pathogenic mutation were included in the analysis, ages shifted a few years upward for CRD: 7 to 8 years for low vision, 13 to 15 years for legal blindness. For CD, this shift was from 12 to 13 years regarding the risk of legal blindness.
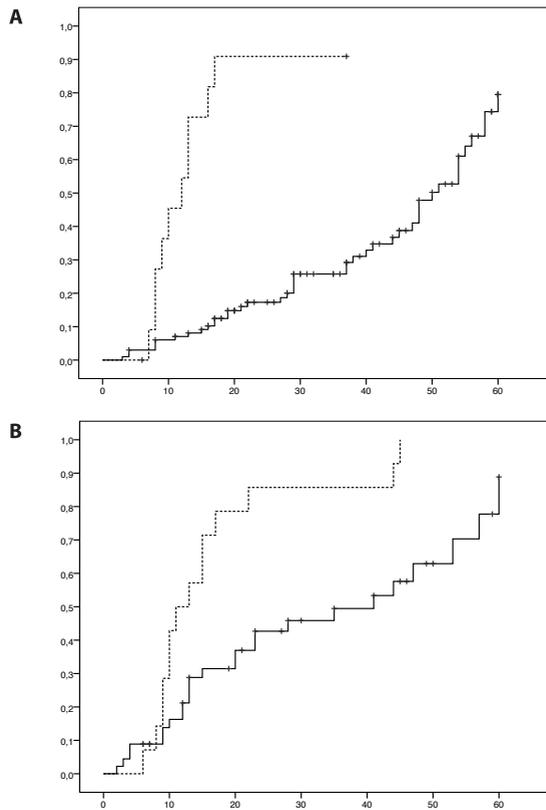
Figure 2. Kaplan-Meier survival curves as a function of age for cone and cone-rod dystrophy probands with or without pathogenic *ABCA4* mutations.
(a) Kaplan-Meier survival curves showing the cumulative incidence of legal blindness (visual acuity ≤0.10) as a function of age in autosomal recessive (AR) cone dystrophy (CD) probands with pathogenic *ABCA4* mutations and AR-CD probands with no pathogenic *ABCA4* variants. Dashed line: *ABCA4* probands; black line: probands without pathogenic *ABCA4* mutations.
(b) Kaplan-Meier survival curves showing the cumulative incidence of legal blindness as a function of age in AR-CRD probands with pathogenic *ABCA4* mutations, and AR-CRD probands with no pathogenic *ABCA4* variants.

We investigated whether early onset of disease (<20 years) predisposed to early development of low vision and legal blindness. In early onset CD, low vision was present in 50% of patients at age 12 (SE 2.5), and legal blindness was present in 50% at age 40. For early onset CRD, these ages were 8 and 22 years (SE 4.2), respectively. With Cox regression analysis, *ABCA4* carriership and an early age at onset independently increased the risk of low vision and legal blindness (*P* <0.001 and *P* <0.001, respectively), and these outcomes occurred at earlier ages.

DISCUSSION

We investigated a large series of CD and CRD patients, and carefully evaluated clinical and genetic characteristics. Both disorders had an onset within the first two decades, followed by a gradual visual decline, ending in legal blindness in the majority of cases. For both CD and CRD, *ABCA4* was an important genetic cause associated with a remarkably poor visual outcome. Despite these similarities, differences between the two diseases were also noticed. CRD appeared to be a more severe disease: mean age of onset was 4 years earlier (12 vs 16 yrs; *P* = 0.02), all clinical parameters showed a higher proportion of progression, and mean age of legal blindness was considerably lower (23 vs 48 years; *P* <0.001).

In this study, ERG was the gold standard for diagnosis, and diminished cone amplitudes were obligatory for all patients. Intact rod responses for at least five years allowed for a diagnosis of CD, faster rod decline was considered CRD. Despite these diagnostic criteria, a considerable proportion of CRD patients (31%) did not show peripheral visual field defects at onset. These CRD patients had a milder course of disease, more comparable to CD (Figure 1). The functionally delayed rod impairment in these patients may imply a diagnosis of CD rather than CRD. On the other hand, a proportion of CD patients (37%; 36/90) had diminished rod responses on ERG at 10 years follow up (Table 2), and these patients may be more appropriate for a diagnosis of CRD. Despite these diagnostic considerations, our classification allowed for detection of considerable differences in clinical course.

ABCA4 was already known to be an important cause of AR retinal disorders. Previous reports estimated that *ABCA4* causes the vast majority of AR-STGD, ~18% of AR-CD, and 24-65% of AR-CRD cases.[9,15-21] We determined *ABCA4* mutations with the Asper Biotech array, and found somewhat lower proportional contributions (10% for AR-CD; 26% for AR-CRD). This array contains all disease-associated genetic variants, many polymorphisms of the *ABCA4* gene, and has a mutation detection rate of 55-65% for patients with STGD.[23,29] The detection rate for STGD was reported to increase to ~70% with subsequent DGGE screening.[30] In the AR-CD/CRD probands with only one possibly pathogenic variant in *ABCA4*, we did not succeed in finding the second allele. These probands showed a similar clinical course as those with two *ABCA4* mutations. It is therefore likely that the majority of these patients has a currently unknown, second allele in intergenic or intronic sequences, and that *ABCA4* explains the genetic cause. In the probands with only one non-pathogenic allele, it is possible that *ABCA4* is not the causative gene. Carriership of an *ABCA4* variant occurs in ~1/15 healthy persons.[20]

All AR-CD and AR-CRD probands with two pathogenic *ABCA4* mutations had a significantly worse visual outcome than patients without these mutations. These probands had a lower mean age of onset and developed legal blindness at a younger age (Figure 2). *ABCA4* encodes a transmembrane protein located at the rim of the discs of rod and cone outer segments. It functions as a flippase for N-retinylidene-PE, thereby facilitating the transport of all-trans-retinal from the luminal to the cytosolic side of the photoreceptor discs. *ABCA4* genetic variability can lead to a diversity of retinal disorders, and an association with severity of the mutation has been proposed.[30-33] Although we found combinations of *ABCA4* mutations in both CD and CRD, truncating mutations appeared to occur more often in CRD (CRD 76%;26/34 vs CD 55%;10/18) (Table 3). On the other hand, we also found similar combinations in both disorders, which is in accordance with former studies reporting that the same mutations can lead to very different phenotypes.[34] It has been proposed that in these cases modifier genes and environmental factors may explain the differences in expression of *ABCA4* gene defects.[35] Summarizing, our study shows that the *ABCA4* gene is important for primary cone function, and the most prominent causative gene for AR-CD and AR-CRD known to date.

In AR-CD, mutations in genes other than *ABCA4* were found in 9% of the consecutive probands (Table 3a). The *CNGB3* gene revealed mutations in a small proportion of AR-CD patients (3/90; 3%).[25] This gene encodes the β subunit of the cGMP (CNG) channel type 3, located on the outer membrane segment of cones, and plays an important role in the cone phototransduction cascade.[37] *KCNV2* gene mutations were identified in 10/90 AR-CD probands, but only four had two allelic *KCNV2* mutations (4%). These patients all had supra-normal rod responses on ERG as described for this gene defect.[10,11] The *KCNV2* gene encodes a voltage-gated potassium channel subunit in cone and rod photoreceptors. How mutations in this gene causes repolarization disturbances of rods is unclear.[10,11] A homozygous missense mutation in the *PDE6C* gene was found in one CD patient.[26] This gene encodes the cone α-subunit of cGMP phosphodiesterase, which converts cGMP to 5'-GMP, and thereby plays an essential role in cone phototransduction. In XL-CD, *RPGR* gene mutations were present in all probands with CD and 4/5 (80%) probands with CRD. These mutations were located in the mutational hot spot ORF15. The *RPGR* gene encodes a transport protein located in the connecting cilium of cone and rod photoreceptors, and is associated with mis-localization of rhodopsins and/or cone opsins.[7,8,36]

Taking all probands with two mutations together, we were able to identify the causal genetic defect in ~20% (17/90) of AR-CD, ~26% (17/65) of AR-CRD, as well as in almost all XL-CD/CRD probands (Table 3).

A large proportion of the causal genes in CD and CRD could not be identified using these conventional genetic screening techniques. It is likely that new methods such as next generation sequencing, retinal gene chips (300-kb Retinal Resequencing Chip), and whole genome sequencing will facilitate identification of a large proportion of additional causal mutations.[38-40] The knowledge of the genetic etiology of retinal disorders is of great importance, since new gene-based intervention methods are arising. In addition, complete genetic data will enable studies of genotype-phenotype correlations, and will help improve prognostic models.

In conclusion, we found that CD and CRD are distinct cone disorders with each specific characteristics and clinical course. However, both had a relatively early onset and an ominous visual prognosis. *ABCA4* is an important genetic cause of both disorders, and serves as a prognostic factor for severe visual decline. Early onset independently affected the course and visual outcome. We believe our results may aid in the clinical and genetic counseling of CD and CRD patients.

REFERENCES

1. Michaelides M, Hunt DM, Moore AT. The cone dysfunction syndromes. Br J Ophthalmol. 2004;88:291-297.

2. Michaelides M, Hardcastle AJ, Hunt DM, Moore AT. Progressive cone and cone-rod dystrophies: phenotypes and underlying molecular genetic basis. Surv Ophthalmol. 2006;51:232-258.

3. Berger W, Kloeckener-Gruissem B, Neidhardt J. The molecular basis of human retinal and vitreo-retinal diseases. Prog Retin Eye Res. 2010;29:335-75.

4. Kohn L, Kadzhaev K, Burstedt MS, et al. Mutation in the PYK2-binding domain of PITPNM3 causes autosomal dominant cone dystrophy (CORD5) in two Swedish families. Eur J Hum Genet. 2007;15:664-671.

5. Payne AM, Downes SM, Bessant DA, et al. A mutation in guanylate cyclase activator 1A (GUCA1A) in an autosomal dominant cone dystrophy pedigree mapping to a new locus on chromosome 6p21.1. Hum Mol Genet. 1998;7:273-277.

6. Michaelides M, Wilkie SE, Jenkins S, et al. Mutation in the gene GUCA1A, encoding guanylate cyclase-activating protein 1, causes cone, cone-rod, and macular dystrophy. Ophthalmology. 2005;112:1442-1447.

7. Demirci FY, Rigatti BW, Wen G, et al. X-linked cone-rod dystrophy (locus COD1): identification of mutations in RPGR exon ORF15. Am J Hum Genet. 2002;70:1049-1053.

8. Yang Z, Peachey NS, Moshfeghi DM, et al. Mutations in the RPGR gene cause X-linked cone dys-trophy. Hum Mol Genet. 2002;11:605-611.

9. Kitiratschky VB, Grau T, Bernd A, et al. ABCA4 gene analysis in patients with autosomal recessive cone and cone-rod dystrophies. Eur J Hum Genet. 2008;16:812-819.

10. Wu H, Cowing JA, Michaelides M, et al. Mutations in the gene KCNV2 encoding a voltage-gated potassium channel subunit cause "cone dystrophy with supernormal rod electroretinogram" in humans. Am J Hum Genet. 2006;79:574-579.

11. Wissinger B, Dangel S, Jagle H, et al. Cone dystrophy with supernormal rod response is strictly associated with mutations in KCNV2. Invest Ophthalmol Vis Sci. 2008;49:751-757.

12. Michaelides M, Aligianis IA, Ainsworth JR, et al. Progressive cone dystrophy associated with muta-tion in CNGB3. Invest Ophthalmol Vis Sci. 2004;45:1975-1982.

13. Wycisk KA, Zeitz C, Feil S, et al. Mutation in the auxiliary calcium-channel subunit CACNA2D4 causes autosomal recessive cone dystrophy. Am J Hum Genet. 2006;79:973-7.

14. den Hollander AI, Black A, Bennett J, Cremers FPM. Lighting a candle in the dark: advances in genetics and gene therapy of recessive retinal dystrophies. J Clin Invest. 2010;120:3042-53.

15. Cremers FPM, van de Pol DJ, van Driel M, et al. Autosomal recessive retinitis pigmentosa and cone-rod dystrophy caused by splice site mutations in the Stargardt's disease gene ABCR. Hum Mol Genet. 1998;7:355-62.

16. Ducroq D, Rozet JM, Gerber S, et al. The ABCA4 gene in autosomal recessive cone-rod dystrophies. Am J Hum Genet. 2002;71:1480-1482.

17. Fishman GA, Stone EM, Eliason DA, et al. ABCA4 gene sequence variations in patients with auto-somal recessive cone-rod dystrophy. Arch Ophthalmol. 2003;121:851-855.

18. Klevering BJ, Blankenagel A, Maugeri A, et al. Phenotypic spectrum of autosomal recessive cone-rod dystrophies caused by mutations in the ABCA4 (ABCR) gene. Invest Ophthalmol Vis Sci. 2002;43:1980-1985.

19. Klevering BJ, Yzer S, Rohrschneider K, et al. Microarray-based mutation analysis of the ABCA4 (ABCR) gene in autosomal recessive cone-rod dystrophy and retinitis pigmentosa. Eur J Hum Genet. 2004;12:1024-1032.

20. Maugeri A, Klevering BJ, Rohrschneider K, et al. Mutations in the ABCA4 (ABCR) gene are the major cause of autosomal recessive cone-rod dystrophy. Am J Hum Genet. 2000;67:960-966.

21. Webster AR, Heon E, Lotery AJ, et al. An analysis of allelic variation in the ABCA4 gene. Invest Ophthalmol Vis Sci. 2001;42:1179-1189.

22. Marmor MF, Fulton AB, Holder GE, et al. International Society for Clinical Electrophysiology of Vision. ISCEV Standard for full-field clinical electroretinography (2008 update). Doc Ophthalmol. 2009;118:69-77.

23. Jaakson K, Zernant J, Külm M, et al. Genotyping microarray (gene chip) for the ABCR (ABCA4) gene. Hum Mutat. 2003;22:395-403.

24. Cotton RG, Scriver CR. Proof of "disease causing" mutation. Hum Mutat. 1998;12:1-3.

25. Thiadens AA, Roosing S, Collin RWJ, et al. Comprehensive analysis of the achromatopsia genes CNGA3 and CNGB3 in progressive cone dystrophy. Ophthalmology. 2010;117:825-30.

26. Thiadens AA, den Hollander AI, Roosing S, et al. Homozygosity mapping reveals PDE6C mutations in patients with early-onset cone photoreceptor disorders. Am J Hum Genet. 2009;85:240-7.

27. Ernest PJ, Boon CJ, Klevering BJ, et al. Outcome of ABCA4 microarray screening in routine clinical practice. Mol Vis. 2009;15:2841-7.

28. Wu Y, Hayes VM, Osinga J, et al. Improvement of fragment and primer selection for mutation detection by denaturing gradient gel electrophoresis. Nucleic Acids Res. 1998;26:5432-40.

29. Rivera A, White K, Stöhr H, et al. A comprehensive survey of sequence variation in the ABCA4 (ABCR) gene in Stargardt disease and age-related macular degeneration. Am J Hum Genet. 2000;67:800-13.

30. Allikmets R, Singh N, Sun H, et al. A photoreceptor cell-specific ATP-binding transporter gene(ABCR) is mutated in recessive Stargardt macular dystrophy. Nat Genet. 1997;15:236-246.

31. Weng J, Mata NL, Azarian SM, et al. Insights into the function of Rim protein in photoreceptors and etiology of Stargardt's disease from the phenotype in abcr knockout mice. Cell. 1999;98:13-23.

32. Sun H, Smallwood PM, Nathans J: Biochemical defects in ABCR protein variants associated with human retinopathies. Nat Genet. 2000;26:242-6.

33. Molday LL, Rabin AR, Molday RS. ABCR expression in foveal cone photoreceptors and its role in Stargardt macular dystrophy. Nat Genet. 2000;25:257-8.

34. van Driel MA, Maugeri A, Klevering BJ, et al. ABCR unites what ophthalmologists divide(s). Ophthalmic Genet. 1998;19:117-22.

35. Lois N, Holder GE, Fitzke FW, et al. Intrafamilial variation of phenotype in Stargardt macular dystrophy-Fundus flavimaculatus. Invest Ophthalmol Vis Sci. 1999;40:2668-75.

36. Vervoort R, Lennon A, Bird AC, et al. Mutational hot spot within a new RPGR exon in X-linked retinitis pigmentosa. Nat Genet. 2000;25:462-6.

37. Kaupp UB, Seifert R. Cyclic nucleotide-gated ion channels. Physiol Rev. 2002;82:769-824.

38. Booij JC, Bakker A, Kulumbetova J, et al. Simultaneous mutation detection in 90 retinal disease genes in multiple patients using a custom-designed 300-kb retinal resequencing chip. Ophthalmology. 2011;118:160-167.

39. Ng SB, Turner EH, Robertson PD, et al. Targeted capture and massively parallel sequencing of 12 human exomes. Nature. 2009;461:272-6.

40. Choi M, Scholl UI, Ji W, et al. Genetic diagnosis by whole exome capture and massively parallel DNA sequencing. Proc Natl Acad Sci U S A. 2009;106:19096-101.
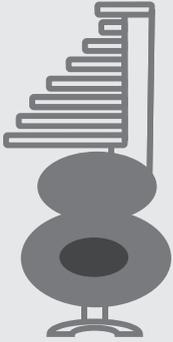
Chapter 4

Cone disorders as part of a syndrome
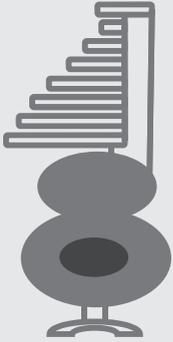
Chapter 4a

Cone-rod dystrophy can be a manifestation of Danon disease

ABSTRACT

Background: Danon disease is a neuromuscular disorder with variable expression in the eye. We describe a family with Danon disease and cone-rod dystrophy (CRD).

Methods: Affected males of one family with Danon were invited for an extensive ophthalmologic examination, including color vision testing, fundus photography, Goldmann perimetry, full-field electroretinogram (ERG), and OCT. Previous ophthalmologic data were retrieved from medical charts. The *LAMP2* and *RPGR* gene were analyzed by direct sequencing.

Results: Two siblings had no ocular phenotype. The third sibling and a cousin developed CRD leading to legal blindness. ERG showed more reduced photopic responses than scotopic, and color vision was severely disturbed. OCT revealed thinning of photoreceptor and RPE layer. Visual fields demonstrated central scotoma. The causal mutation was p.Gly384Arg in *LAMP2;* no mutations were found in *RPGR*.

Conclusions: This is the first description of a CRD in Danon disease. The retinal phenotype was a late onset but severe dystrophy characterized by loss of photoreceptors and RPE cells. With this report, we highlight the importance of a comprehensive ophthalmologic examination in the clinical work-up of Danon disease.

INTRODUCTION

Danon disease is a rare genetic condition caused by mutations in the X-linked lysosome-associated membrane protein gene (*LAMP2*). Danon consists of the triad muscle weakness, cardiomyopathy, and mental impairment. The mortality rate in males is high; the most frequent cause of death is a heart arrhythmia. Female carriers can show a mild phenotype, often restricted to cardiomyopathy.[1,2]

To date, ophthalmologic involvement has been described in only a few cases.[1,3,4,5] Retinal abnormalities were reported, however, detailed work up including psychophysical testing was missing. It was therefore unclear which retinal cell types were affected, whether it included rods and cones, and whether the disease progressed to legal blindness. Here we present the results of a comprehensive ophthalmologic examination in a small Danon family with cone-rod dystrophy (CRD) due to an uncommon missense mutation in *LAMP2*.

METHODS

Clinical Examination

A proband with Danon disease presented at our clinic with visual complaints. After his visit, we invited his three cousins with Danon for an eye examination. They all underwent an extensive examination, including best corrected Snellen visual acuity (BCVA), refractive error, color vision testing (American Optical Hardy-Rand-Rittler Test), full-field electroretinogram (ERG), fundus photography centered on the macula (TRC 50IX; Topcon, Tokyo, Japan), and SD-Optical Coherence Tomography (OCT). ERGs incorporated the recommendations of the ISCEV.[6] Direct sequencing of the entire coding regions and flanking sequences of the genes *LAMP2* and *RPGR* gene was performed at the Netherlands Institute of Neurosciences, Amsterdam, The Netherlands. The study was approved by the Medical Ethics Committee of Erasmus Medical Center and adhered to the tenets of the Declaration of Helsinki. The participants provided signed, informed consent for participation in the study, retrieval of medical records, and use of blood and DNA for research.

A
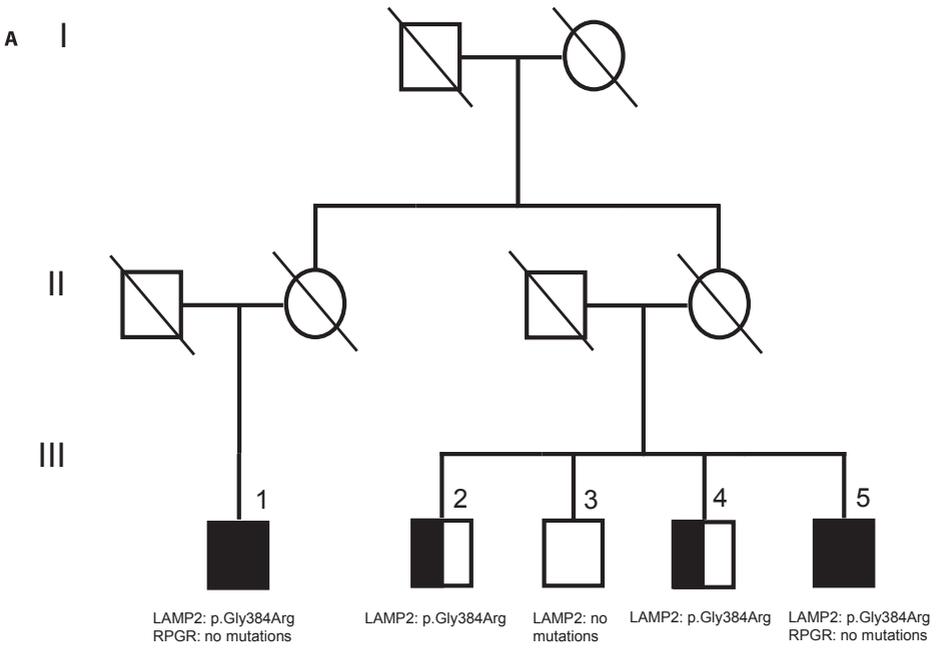
Figure 1a. Pedigree of the family with Danon disease and cone-rod dystrophy.
It shows two affected siblings with cone-rod dystrophy (CRD), the mutation p.Gly384Arg in the *LAMP2*
gene and no mutations in the *RPGR* gene. Open square: unaffected male; black square: affected males
with Danon disease and CRD; half-open square: affected males with Danon disease but without CRD;
dashed symbols denote deceased individuals.

Table 1. Clinical characteristics of the four relatives with Danon disease and a mutation in the *LAMP2* gene.

Family member	*LAMP2* mutation	Danon triad			CRD#	Ophthalmologic examination					
		Mental Retardation	Muscle weakness	Cardio-myopathy		VA*	Color vision	Macula	Periphery	Goldmann Perimetry	ERG†
III-1	+	-	+	-	+	HM‡	All axes disturbed	Bull's eye maculopathy	Normal	Central scotoma	Cones > rods reduced
III-2	+	-	+	-	-	1.0	Normal	Normal	Normal	Not tested	Normal
III-4	+	-	+	-	-	1.0	Normal	Normal	Normal	Not tested	Normal
III-5	+	-	+	+	+	0.05	All axes disturbed	Bull's eye maculopathy	Pigmentary changes	Central scotoma	Cones > rods reduced

\# CRD: Cone-rod dystrophy
* VA: visual acuity
† ERG: electroretinogram
‡ HM: hand movements

RESULTS

The proband (III-1) and three of the four cousins (III-2, III-4, III-5) had Danon disease caused by a missense mutation, c.1150G>C, leading to an aminoacid change (p.Gly384Arg) in splice variant B (exon 9B) of the *LAMP2* gene (reference sequence NM_013995.1; nomenclature according to http://www.hgvs.org/Mutnomen/). One cousin was unaffected (III-3) and had no *LAMP2* mutation. No *RPGR* mutations were found (Figure 1a). Table 1 shows the clinical findings of this family.

Case 1
Proband III-1 developed visual problems long before other symptoms were apparent. Visual decline and photophobia started at age 49 years. At age 70, BCVA deteriorated to hand movements at 1 meter. Fundus examination revealed a bull's eye maculopathy with a normal peripheral retina (Figure 1b). Photopic responses were more severely reduced than scotopic on ERG (Figure 1f). OCT showed thinning of the outer segments and RPE in the macula (Figure 1b). Muscle weakness started at age 64 and progressed rapidly to wheelchair dependency.[7]

Case 2
Cousin III-2 was 63 years old at the time of last examination, and had no visual complaints. BCVA was 1.0 and ophthalmoscopy showed no retinal abnormalities (Figure 1d). Other physical signs of Danon were weakness of the shoulder, upper arm, and distal legs.[7]

Case 3
Cousin III-4 was 69 years old at time of the last examination and had no ocular abnormalities (Figure 1e). He suffered from a generalized proximal muscle weakness in arms and legs since the age of 45, which led to wheelchair dependency. His two daughters appeared to be not affected.

Case 4
Cousin III-5 had a gradually deteriorating visual acuity to 0.05 at age 64 years. Fundus examination revealed a bull's eye maculopathy and a peripheral salt-and-pepper retinopathy (Figure 1c). The SD-OCT showed a thinner but intact photoreceptor layer and thinning of the RPE layer (Figure 1c). He suffered from muscle weakness since childhood, and became wheelchair depended at age 40. This patient developed a hypertrophic cardiomyopathy.[7] The daughter of this patient suddenly died at the age of 29 due to cardiomyopathy.
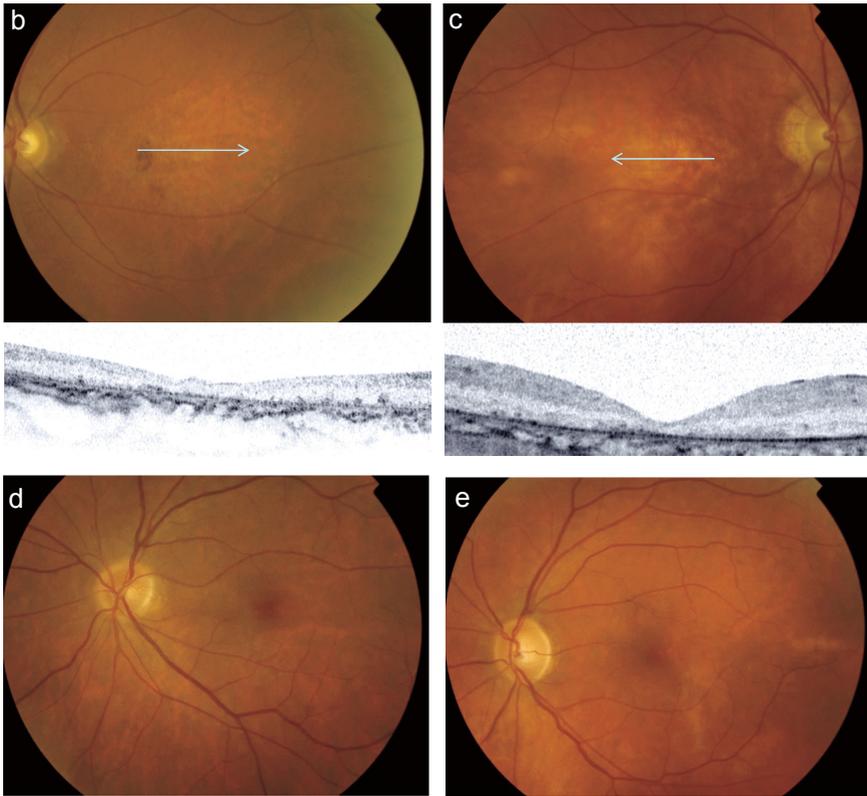
Figure 1 b-e. Fundus photographs and Spectral Domain- optical coherence tomography (OCT) of the family with Danon disease and cone-rod dystrophy (CRD).

(b) Fundus photograph of the left eye of the proband III-1, performed at age 70, showing RPE clumping and atrophy in the macula. The arrow denotes the position of the OCT image, showing thinning of the outer segments and RPE, pigment deposits at the RPE layer and in the photoreceptor cell layer, and window defects due to RPE atrophy.

(c) Fundus photograph of the right eye of the affected cousin III-5, performed at age 64, showing RPE atrophy in the macula. The arrow denotes the position of the OCT image, showing a thinner but intact photoreceptor layer and thinning of the RPE cell layer.

(d) Fundus photograph of the left eye of the unaffected cousin III-2, performed at age 68, showing a normal macular appearance.

(e) Fundus photograph of the left eye of the unaffected cousin III-4, performed at age 66, showing a normal macular appearance.
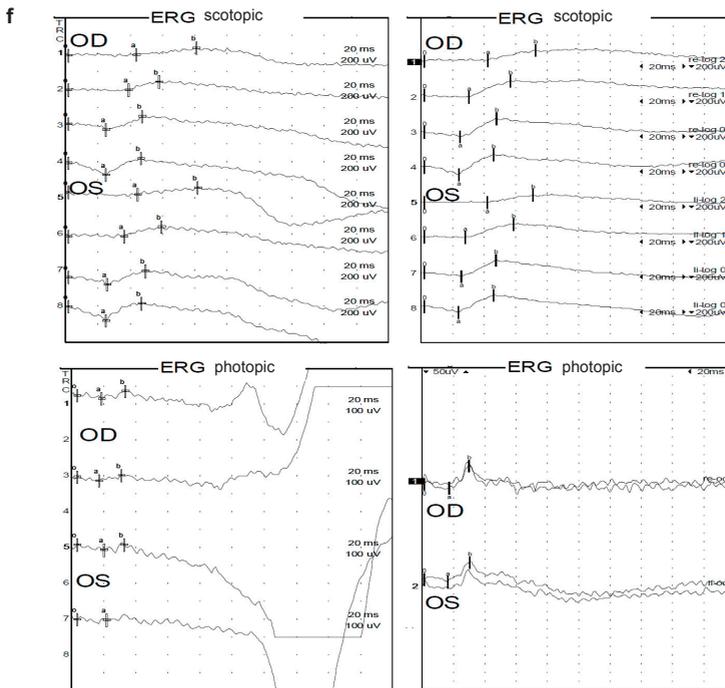
Figure 1f. Electroretinogram of the family with Danon disease and cone-rod dystrophy.
On the left, an electroretinogram (ERG) performed with the protocol of standard ISCEV of the proband
(III-1) showing severely reduced photopic responses and mildly diminished scotopic responses. A normal
ERG is shown on the right.

DISCUSSION

In our family with Danon disease, two of the four affected males presented with all
features of CRD: more severely reduced photopic than scotopic responses on ERG, color
vision disturbances, central visual field defect, and progressive visual decline. The onset
in this family was relatively late, i.e., middle-age, and visual acuity declined to legal
blindness within two decades thereafter.

In the retina, strong expression of *LAMP2* has been demonstrated in the lysosomes of
RPE cells.[5] These lysosomes play a crucial role in the constant renewal of cone and rod
outer segments. Daily, at least 2000-4000 packets of shedded discs are phagocytosed
by the RPE, and subsequently imported and degraded into the lysosome. Mutations in
the *LAMP2* gene lead to RPE lysosome dysfunction, leading to accumulation of deposits
and ultimately cell death. Eventually this will lead to loss of cone and rod photoreceptor
cells (Figure 1g).

g
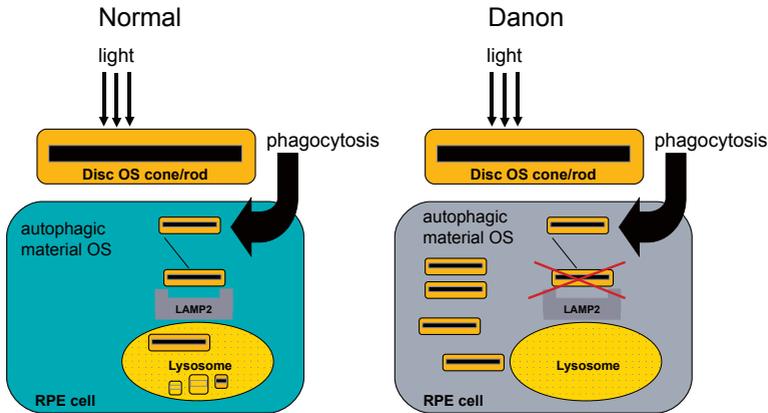
Figure 1g. Schematic drawing showing the presumed localization of the LAMP2 protein in the RPE lysosome, and the accumulation of outer segment remnants in the RPE cell in Danon disease.

Previously described cases with ophthalmologic involvement in Danon disease had frameshift or nonsense mutations in the *LAMP2* gene, leading to absence of the protein. The family of this report carried a recently identified missense mutation (p.Gly384Arg) in exon 9 of the *LAMP2* gene, allowing formation of the protein.[7] An important function of exon 9 is the creation of two different splice products, LAMP2a and LAMP2b, both shown to be expressed in RPE cells.[5] Gly384Arg is located in the coding sequence for splice variant LAMP2b, jeopardizing function of only this specific isoform. The late onset of the two affected cousins in our family could be explained by the presence of this residual LAMP2 protein.

It remains intriguing why not all family members with a pathogenic mutation in the *LAMP2* gene developed CRD. The non-expression in the two carriers of the p.Gly384Arg mutation (III-2, III-4) suggests that a normal function of lysosomes in the RPE can be maintained, despite a mutation in *LAMP2*. Other lysosomal proteins such as LAMP1 are also capable of phagocytosis of autophagic material in the RPE and may compensate for a defective LAMP2 protein.[8] Other explanations could be the presence of protective environmental factors in the non-affected siblings which prohibit lysosomal degradation, or a still unidentified gene that explains CRD in the two affected relatives.

Summarizing, this is the first description of a family with CRD and a rare missense mutation in the *LAMP2* gene. CRD belongs to the clinical spectrum of Danon disease, and we therefore recommend incorporation of a comprehensive ophthalmologic examination into the regular clinical work-up of Danon patients.

REFERENCES

1. Prall R, Drack A, Taylor M, et al. Ophthalmic Manifestations of Danon Disease. Ophthalmology. 2006;113:1010-3.

2. Maron BJ, Roberts WC, Arad M, et al. Clinical outcome and phenotypic expression in LAMP2 cardiomyopathy. JAMA. 2009;301:1253-9.

3. Lacoste-Collin L, Garcia V, Uro-Coste E, et al. Danon's disease (X-linked vacuolar cardiomyopathy and myopathy): a case with a novel Lamp-2 gene mutation. Neuromuscul Disord. 2002;12:882-5.

4. Laforêt P, Charron P, Maisonobe T, et al. Charcot-Marie-Tooth features and maculopathy in a patient with Danon disease. Neurology. 2004;63:1535.

5. Schorderet DF, Cottet S, Lobrinus JA, et al. Retinopathy in Danon disease. Arch Ophthalmol. 2007;125:231-6.

6. Marmor MF, Fulton AB, Holder GE, et al. ISCEV Standard for full-field clinical electroretinography (2008 update). Doc Ophthalmol. 2009;118:69-77.

7. van der Kooi AJ, van Langen IM, Aronica E, et al. Extension of the clinical spectrum of Danon disease. Neurology. 2008;70:1358-9.

8. Sawada R, Jardine KA, Fukuda M. The genes of major lysosomal membrane glycoproteins, lamp-1 and lamp-2. 5'-flanking sequence of lamp-2 gene and comparison of exon organization in two genes. J Biol Chem. 1993;268:9014-22.
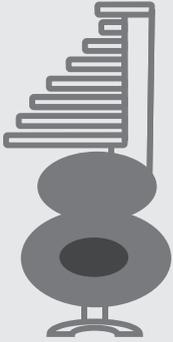
General Discussion

GENERAL DISCUSSION

In this thesis, we aimed to characterize cone disorders at a phenotypic and at a molecular genetic level. We investigated the clinical course and prognosis in these patients, and identified the genetic defects underlying these diseases. Our findings have led to new insights into their etiology, pathogenesis, and clinical course, and may support in the development of future therapeutic options. In this chapter, the main findings of this thesis are recapitulated, and placed in a broader perspective.

Diagnostic challenges in the identification of cone disorders

Cone disorders form a large heterogeneous group of retinal disorders with a severe visual outcome. To identify cone disorders in a clinical setting, a comprehensive clinical characterization is mandatory. In our study group, we investigated age of disease onset, visual complaints, medical history and family pedigree. We examined Snellen visual acuity, performed slit-lamp examination, ophthalmoscopy, and fundus photography. These standard ophthalmologic examinations often revealed macular changes such as RPE alterations or a bull's eye maculopathy, however, sometimes no retinal abnormalities were observed. This potentially hampers a proper diagnosis of cone disorders. To make a definite diagnosis, additional testing such as full-field ERG (ffERG), examination of visual fields, and testing of color vision is essential. Regarding the latter, many different tests are available. In **Chapter 1a,** we examined the discriminative accuracy of the four most commonly used color vision tests, and found that the HRR and desaturated Panel D-15 test are most appropriate to identify cone disorders. Both these tests enabled screening of all three color axes, as well as quantification of the color defect.

What other diagnostic tests could be considered to improve early detection of patients with retinal disorders, and cone disorders in particular?

mfERG - Another specialized type of ERG is the multifocal ERG (mfERG), which tests cone generated responses that subtend 25 degree radially from fixation. In patients with stable and accurate fixation, this test can determine whether macular dysfunction is present.[50,51] It can be very useful to evaluate or compare treatment responses in various macular conditions, but we question its usefulness in the diagnosis of generalized photoreceptor disorders. Although the density of cones is very high in the fovea, these cones contribute only 10-15% of the total photopic response.[16] Contrary to mfERG, ffERG tests a mass response of cone photoreceptors, thereby better reflecting overall cone function. The mass response is necessary for the diagnosis of most cone disorders. An exception is oligocone trichromacy, a very rare disease which is characterized by a low visual acuity, virtually absent cone responses on mfERG, but a nearly normal color vision

and a still recordable ffERG. This condition appears to have a reduced number of only foveal cones, and additional testing of mfERG is needed for diagnosis.

Color ERG - Other types of ERGs are red/green and blue cone driven tests. The three different cone cell types can each create a distinct electrical response. In one report, the specific contributions per cell type were studied by color ERG in six patients with cone disorders. It showed that blue cone driven ERGs had a totally different waveform than those driven by red and green cones.[52-55] The waveforms of both red and green cones resembled each other, and were equally affected in these patients. Large investigations of color ERGs in cone disorder patients are lacking, but it would be interesting to know whether these patients have specific loss of red, green, and blue signals, and whether this is distinct from other retinal dystrophies. Color ERG in particular may be suitable to identify blue cone monochromacy (BCM).

Dark adaptation test – The dark adaptation test measures the thresholds of cone and rod sensitivity to light. The patient is first light adapted, then the light is extinguished, and the threshold of perceiving a test light is plotted against time. The normal adaptation plot starts with a cone sensitivity decline, followed by a cone-rod break, and a rod decline reaching a plateau phase thereafter. These measurements can help in evaluating cone disorders by demonstrating the degree of cone adaptation.

SD-OCT - Imaging of cones has recently become possible by spectral domain optical coherence tomography (SD-OCT). This device is an in vivo representation of retinal histopathology, and well visualizes cone cell loss. In **Chapter 2b,** we used this device in a large series of ACHM patients, and observed that cone cell loss occurred much earlier than was expected by evaluation of fundus photographs. We recommend to implement SD-OCT imaging as part of a regular clinical work-up of cone disorders.

Autofluorescence (AF) – AF is the intrinsic fluorescence emitted by a substance after being stimulated by excitation energy. When the RPE phagocytoses photoreceptor outer segments, which consist of retinoids, fatty acids and proteins, lipofuscin accumulates as an oxidative by-product within the RPE cells, and the pigment within lipofuscin causes AF. RPE cell dysfunction may be accompanied by an increase in AF, while RPE cell death is associated with nonfluorescence.[56] Since accumulation of lipofuscin is not a clinical hallmark of cone disorders, the benefit of AF in its diagnosis is probably not significant.

Adaptive Optics (AO) - A device offering the opportunity to visualize individual cones and other retinal cells would provide information on morphological features, number, and

distribution of cones, and physical interaction of cones with other cells. Recently, Adaptive Optics (AO) SD-OCT was developed for this purpose.[57] AO technology reduces optical aberrations in the visual system by wavefront analysis. It has a high 3D-resolution and speed, increases quality of the image, and makes visualization of individual retinal cells feasible. Although these qualities make AO a promising new tool in the understanding of retinal disorders, the device is not yet practical for clinical use. Reduction of exposure duration and motion artefacts are needed to enhance clinical implementation.[58,59]

Summarizing, a thorough clinical examination is essential in the diagnostic process and follow-up of hereditary cone disorders. Several newly developed or relatively unknown devices may aid in this process, and can be incorporated in the clinical work-up. Nevertheless, it remains important to combine information from all tests before one establishes the diagnosis 'cone disorder'.

The genetic etiology of cone disorders

During the last decennia, considerable progress has been made to improve our understanding of the pathogenesis of retinal disorders, and many causative genes and chromosomal loci have now been identified. Nevertheless, a large proportion of these patients still has an unknown etiology. The detection of new genes is very important to improve knowledge of the disease mechanisms, patient counseling, and to aid in the development of future therapies. Candidate gene studies, linkage studies, and homozygosity mapping using high-resolution SNP analysis can be applied to find causal genes. We used all three methods for the studies described in this thesis.

ACHM - In **Chapter 2a,** we investigated the genetic etiology in ACHM probands, and found mutations in the *CNGB3* gene in 91% of probands, and mutations in the *CNGA3* gene in 4%. The *CNGA3* and *CNGB3* genes are cone-specific, and encode for the α- and β-subunits of the CNG-channels. In two ACHM and in one CD family, we identified a new causative gene: the *PDE6C* gene (2%) (**Chapter 3b**). The *PDE6C* gene encodes the cone α-subunit of cGMP phosphodiesterase, which converts cGMP to 5'-GMP, and thereby plays an essential role in cone phototransduction. In conclusion, almost all ACHM genes have been identified (Figure 1a). All four causal genes encode essential proteins in the cone phototransduction cascade. In the remaining 3% which is still unexplained, misclassification of the diagnosis 'ACHM' may have occurred.
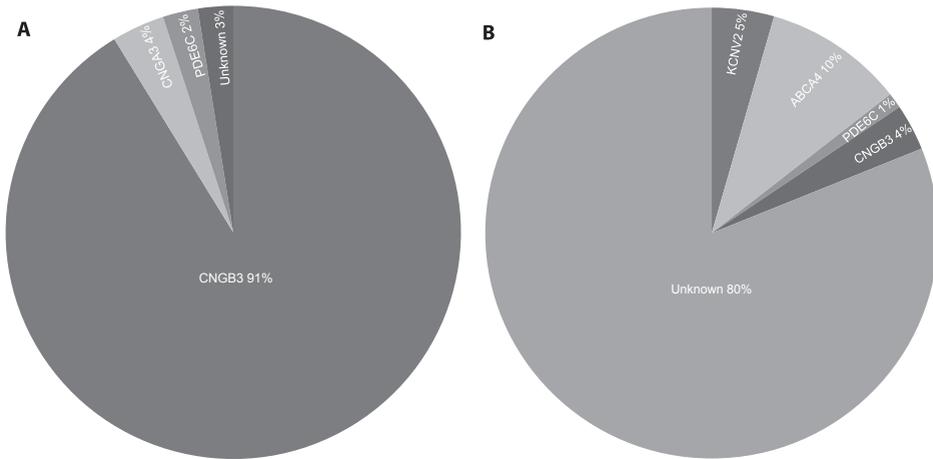
Figure 1. Causal genes and their relative contribution to achromatopsia and autosomal recessive cone dystrophy in the present study.
(a) Achromatopsia
(b) Cone dystrophy

CD and CRD - The current knowledge on genes that cause CD and CRD is scarce, and only a few genes have been identified for all Mendelian inheritance forms. The mechanisms for the known genes include the following: disruption of the photoreceptor disc morphogenesis (*PROM1, PRPH2*), defects in the development of cones and rods (*CRX*), interruption of protein transport across the connecting cilium (*RPGR, RPGRIP1*) and transport of phospholipids (*PITPNM3*), disturbances in terminal synaptic neurotransmitter release or transmission (*CACNA2D4, CACNA1F, RIM1*), defects in the visual cycle (*ABCA4, RLBP1, RDH5*), defects in the structure of RPE cells (*ADAM9*), defective cone phototransduction (*GUCA1A, GUCY2D, CNGB3, CNGA3, GNAT2*), voltage-gated potassium channel disruption (*KCNV2*), disturbed synthesis of phototransduction enzymes (*AIPL1*), and defects in the synthesis of RPE membrane proteins (*SEMA4A*).[38,60]

In our studies, we observed *ABCA4* gene mutations in 10% of AR-CD probands and in 26% of AR-CRD probands. *KCNV2* mutations were detected in only four AR-CD probands (5%), and *RPGR* mutations in the majority of CD and CRD probands with XL inheritance. CD patients with *KCNV2* mutations showed supra-normal rod responses on ERG (**Chapter 3d**). The *RPGR* mutations were all located in the ORF15 region (**Chapters 3c, 3d**). In **Chapter 3a** we described mutations in the ACHM-gene *CNGB3* in three AR-CD probands. In these probands, we hypothesized that the *CNGA3* gene had an additive causative effect on the disease. The CNG-channels are tetrameric proteins composed of two α- and two β-subunits in the cone cell membrane, and we suspect that these *CNGA3* mutations further deteriorated the already compromised CNG-channel (Figure 1b).

To summarize the findings of our studies: 20% of the genetic etiology of AR-CD and 26% of AR-CRD was explained. A limitation of our study was that the genetic screening in CRD was not comprehensive, as we only screened for mutations in the *ABCA4* gene. In addition, we did not investigate families with AD inheritance. Follow-up studies will focus on the remaining CD and CRD probands with an unsolved genetic etiology. The techniques which will be employed are next generation sequencing (NGS) of all exons in the genome (exome sequencing), combined with homozygosity mapping in patients with a clear AR inheritance. This latter technique is a powerful tool to identify novel genes in homozygous patients, and subsequently, findings may be used to screen for mutations in all AR patients.

Future prospects - Recently, a retinal resequencing chip was developed which allows for direct sequencing of all coding regions of 90 retinal disease genes.[61] It can detect both known and new sequence changes, contrary to the currently used APEX-based mutation chips. The disadvantages are that small deletions and duplications, which constitute ~15% of all genetic variants, cannot be detected. The NGS technology, preferably with a coverage of >40 times, does offer these possibilities. NGS can provide robust sequence data for up to 25 million base pairs per single sequencing run, and makes it possible to screen very large genetic regions, or, for instance, all exons of the whole genome.[62,63] Exome sequencing has already been successfully used in the identification of new ocular disease genes.[64] In the future, these techniques will complement or may even replace the current methods to find genes for cone disorders.

Clinical course of cone disorders

In the studies described in this thesis, we observed that cone disorders form a genetically complex disease spectrum with a large phenotypic variability. In ACHM and CD (**Chapters 2a, 3d**), different mutations resulted in similar phenotypes. In *RPGR* as well as in *LAMP2* and *CNGB3* (**Chapters 3c, 4a, and 3a**), mutations in the same gene led to different phenotypes. There is still a large gap between knowledge of gene mutations on the one hand, and events on cellular levels leading to cell death on the other hand. In CD, we found that patients with gene defects in *CNGA3* and *CNGB3* had functional cones early in life, but developed cone dysfunction thereafter. In ACHM, however, we observed that patients with the same gene defects can have a congenital cone dysfunction. What determines this variability in phenotype, or more specifically, why can cones which bear gene mutations survive for some time despite a death-promoting stimulus? Which pathogenic factors eventually trigger the 'decision' for cones to die? These questions remain largely unsolved, however, we will make some hypotheses about the underlying reasons.

Apoptosis - All retinal dystrophies share an important feature: photoreceptor cell death by apoptosis. This final common pathway arises in a diseased photoreceptor or RPE cell due to a defective mechanism in the cell cycle. A large number of pathways and pro-apoptotic stimuli in the retina have already been identified. For specific factors like Ca^{2+}, the role in triggering cell death is well known.[65,66] Gene mutations in knock-out mice can induce an increase in intracellular calcium levels leading to neuronal apoptosis in rod and cone photoreceptor cells. *CNGA3* and *CNGB3* genes code for subunits of the cGMP dependent channels which are essential for the phototransduction cascade.[67,68] Mutations in these genes result in a continuous influx of Ca^{2+} ions, and trigger cone cell apoptosis (**Chapters 2a, 3a**). Apoptosis is not only induced by genetic defects, an important environmental factor is light exposure. Light can induce cell damage and death through phototoxic mechanisms. In rods, it has been demonstrated that the regeneration rate of rhodopsin is crucial for the initiation of light-induced apoptosis. When rhodopsin is not capable of normal regeneration after light exposure, the increasing intracellular Ca^{2+}, nitric oxide (NO), and reactive oxygen species (ROS) levels will initiate cell death.[69,70] It is likely that this will also happen when cone regeneration is disturbed. Another cause of light-induced apoptosis in retinal degeneration is increased oxygen levels in the outer retina due to a decreased utilization. These high levels can also cause increased ROS and enhancement of apoptosis.[71] Summarizing, many factors can determine photoreceptor apoptosis. The sum of these factors as well as the interaction between them will determine when apoptosis is initiated.

Genetic modifiers - Genetic factors which can determine phenotypic variability are functional consequences of the causative mutation in combination with genetic modifiers.[72,73] An example of the phenotypic variability caused by variable functional consequences is the *ABCA4* gene, which expresses a broad phenotypic spectrum of retinal diseases. This can vary from Stargardt disease, to CRD, or even retinitis pigmentosa (RP), and is also mentioned as a risk factor for age related macular degeneration.[41-48] Our CD patients mostly had compound heterozygous missense mutations causing a gradual visual decline. In contrast, our CRD patients often had truncating mutations resulting in a more severe effect on the protein, and a more detrimental visual decline (**Chapter 3d**). Genetic modifiers can affect the phenotypic outcome of a given genotype by interacting in the same biological pathway as the causative gene. The effect can be enhancing, leading to a more severe phenotype, or suppressive, reducing the phenotype, or even completely restoring the normal condition. For Joubert and Bardet-Biedl syndrome specific modifier genes have been identified.[74,75] We found hints for genetic modifiers in our patients with Danon disease caused by a *LAMP2* mutation. One carrier did not develop a retinal phenotype, while two other carriers in the family developed CRD (**Chapter 4a**).

We think that a retinal modifier gene acting in the same pathway as LAMP2 may have compensated for the dysfunctional lysosomal phagocytosis. In mice, this phenomenon has been described in more detail. Mice which had the same genetic mutation on a different genetic background developed different phenotypes. A locus was found which modified expression of the causative mutation.[72,73] In conclusion, the above mentioned genetic and environmental factors may trigger the cone cell death pathway, and interaction between these factors will eventually determine the time-point of cone cell apoptosis.

Clinical and genetic counseling

Important issues to discuss with a cone disorder patient who seeks counseling include genetic testing, visual and systemic prognosis, heritability, life style recommendations, and future prospects.

Genetic testing - Currently, more than 150 retinal degeneration genes are known to cause retinal degeneration.[38, RETNET website] Until recently, it was not feasible to screen all these genes in a patient with retinal dystrophy. Therefore, it has always been extremely important to determine the exact functional defects, and to make a correct diagnosis in patients with retinal disorders to facilitate the search of the mutation. We recommend to perform a comprehensive clinical workup including ERG, color vision testing, Goldmann perimetry, SD-OCT, and fundus autofluorescence images complementing the standard ophthalmologic exam in patients suspect for hereditary retinal disorders.[76] Genetic testing can confirm the defect at the molecular level, but does not always provide full insight into diagnosis and prognosis of the disease. In this thesis, we observed that the functional consequences of missense mutations can be different (CD or CRD, both due to *ABCA4*), and that mutations in different genes can cause a similar phenotype (*CNGB3* and *PDE6C* in ACHM). These observations emphasize that genetic testing has its own sensitivity, specificity, and positive predictive value, just like any other test. Nevertheless, knowledge of the genetic defect can have significant advantages. For example, supplementation of vitamin A can have a detrimental effect in patients with *ABCA4* mutations,[77] while this is beneficial for retinal dystrophy patients carrying mutations in other genes.[78,79] Identification of the molecular defect can sometimes facilitate a proper clinical diagnosis. For instance, we encountered a patient with an initial diagnosis of CD in whom we identified a BBS5 mutation by homozygosity mapping using a SNP microarray. After this identification, we thoroughly examined the patient for systemic involvement, and indeed found subtle signs indicative of Bardet-Biedl syndrome. Another advantage of genetic testing is monitoring for functional defects in individuals who are still in a preclinical stage (eg. screening for cardiomyopathy in patients with *LAMP2* mutations, **Chapter 4a**).

Prognosis - Individual prognoses regarding visual function can be made by extrapolation of the clinical course in the past. Early onset often leads to a worse prognosis, as does rapid decline of visual acuity and visual fields. Currently, it is difficult to provide a general prognostic profile for each disease entity. Data on genotype-phenotype correlations and prognosis are scarce for rare disorders. However, our data provide a rule of thumb for the prognosis of CD and CRD. Half of CD patients reached legal blindness at age ~50 years, half of CRD at age ~25 years (**Chapter 3d)**. Larger genotype-phenotype correlation studies with a follow-up of several decades are warranted to improve prognostic models and clinical counseling.

Heritability - Patients may have considerable worries about passing on the mutation to their children. The distinction between AR and XL inheritance can be difficult, and nonpenetrance may occur in autosomal dominant pedigrees. Identification of the gene defect can be very helpful to determine the inheritance pattern, and it can point out carriers and aid in family planning. Apart from patients, non-affected spouses of patients carrying mutations that have a high population frequency should be offered screening. Prenatal and preimplementation screening for cone disorders is still very controversial, but requests are made more and more often.

Life style and management - What type of life should cone disorder patients strive for? Patients generally have an early disease onset, and virtually all become legally blind after their fifties (**Chapters 2a, 3d**). This has large implications for performance of daily tasks and possibilities for professional life. The clinician should discuss future plans with the patient. Professions which require discrimination of visual details, color vision, or a driving license should be discouraged. Nevertheless, quality of life studies in cone disorders are absent, and providing objective advice is difficult. We attended the yearly national ACHM-day several times, and noticed a well-developed coping mechanism in these legally blind patients. They appeared to experience few professional limitations. Other points to discuss with the patient are lifestyle and dietary habits. This includes the advice to stop smoking; it is known that smoking induces oxidative stress by depressing antioxidants in the retina, and causes hypoxia, the formation of free radicals, and alteration of the choroidal blood flow.[80] Specific gene therapies, treatment with drugs, or other agents to preserve cone function are on their way. For now, the clinician can consider the recommendations for RP, such as supplementation of vitamin A, lutein, and docosahexaenoic acid (DHA). DHA is an unsaturated fatty acid highly concentrated in the phospholipid membrane of the outer segments, which serves as a target for oxidative damage.[81-83] A randomized trial showed that vitamin A supplementation of 15.000 IU/d slowed down the progression of retinal degeneration.[78] A deceleration of cone cell loss was observed in a subgroup of RP using vitamin A, an omega-3 rich fish diet, and

extra DHA supplementation. Recently, the use of 12 mg/d of lutein tablets in addition to vitamin A was evaluated, showing less progression of cone cell loss in RP.[84-87]

Future prospects of therapy

The retinal gene discoveries have led to new insights into disease mechanisms, which in turn have led to cautious optimism regarding retinal cell rescue. The eye is ideally suited as target organ for different interventions as it is easy to access, and it enables monitoring the application of therapeutics.[38] Therapies with gene replacements, neuro-protection, stem cells, and optogenetics have been shown to rescue photoreceptors in animal models, and in some humans with retinal dystrophies. We will briefly discuss the current status of these future therapeutic options.

Gene augmentation therapies - The vectors used in gene therapy are typically modified viruses, which serve as transport vehicles to deliver a gene cargo into the nucleus of targeted cells. Adeno-associated virus (AAV) vectors are particularly suitable for gene transport. A single administration of an AAV-vector is expected to yield functional expressed product of the transgene for the duration of the patient's life. Patients with Leber congenital amaurosis (LCA) due to mutations in the *RPE65* gene were the first to be treated successfully by gene augmentation therapy. Currently, ~30 patients received a subretinal injection of AAV. In 7/12 published patients (aged 8-44 years) there was a significant improvement in visual acuity after two years. The greatest improvement was noted in children, probably due to the less profound impact of amblyopia and the more intact photoreceptor cell layer. Subretinal gene therapy seemed safe at all administered dosages.[88-91] Studies of gene replacement therapy for cone disorders are on their way; the first results have been published for *CNGA3, CNGB3*, and *GNAT2* knock-out mice and dogs. In the rescued animals, cone ERG amplitudes recovered to nearly normal levels.[92-95] After safety studies have been performed in large animal models, the next step will be clinical trials for gene therapy in humans with cone disorders. In **Chapter 2b** we described that the first signs of cone cell decay in ACHM were already visible in early childhood. Therefore, when gene therapy becomes available, treatment should be performed in the first decade.

Another promising therapeutic agent with a mutation-specific treatment regime is PTC-124. This molecule is able to recognize a premature termination codon (PTC) caused by a nonsense mutation, and is able to place an amino acid in the position where this mutation resides. Instead of ending the translation, the ribosome will continue to translate the mRNA. This allows formation of a full length protein instead of a premature truncation.[96,97] In a recent report, patients with cystic fibrosis due to mutations in the *CFTR* gene were treated for 28 days with a daily oral administration of PTC-124; in 13/23 patients

the defective chloride channels were restored.[98] PTC-124 has also been investigated for patients with Duchenne muscular dystrophy, which led to positive results.[99] These findings implicate that this type of therapy may be suitable for a broader spectrum of diseases,[100] and it can be an interesting option for patients with cone disorders due to nonsense mutations.

Neuroprotection therapies - The large genetic heterogeneity among cone and rod disorders hampers the development of gene specific therapies. If a treatment can be used to prolong retinal cell survival regardless of the genetic defect, this would have a great potential for patients with all sorts of retinal dystrophies. Neuroprotective agents for the retina have shown to have a beneficial effect on the survival of cones, rods, RPE cells, and retinal ganglion cells. There are many categories of these agents, and they include antioxidants, specific apoptosis inhibiting factors, and neurotrophic factors which are naturally produced by the human body. Although a long list of agents has shown some protection of photoreceptors in animal models, there has been a particular high interest in ciliary neurotrophic factor (CNTF). This factor is released as an intrinsic response to stress in the photoreceptor cells, and prolongs the survival of degenerating cells.[101] Recombinant CNTF injections in the vitreous of animals protected against light damage for 1-2 weeks.[102] In humans, an implantable device containing CNTF is currently under investigation. In a phase 1 trial, these capsules were implanted in the vitreous of patients with RP for 6 months; the first results showed no negative side effects and positive improvement of visual acuity in 3/10 patients.[103,104]

Stem cell therapies – Recent studies have demonstrated that photoreceptor transplantation is feasible in mice.[105] To establish this therapy in humans, a source of photoreceptor precursors is required. Stem cells with properties of self-renewal and with the potential to produce large numbers of neurons, would be an ideal donor source. Several potential stem cell populations have been investigated. Unfortunately, ciliary epithelial cells and amniotic fluid derived stem cells showed no evidence of differentiation into new photoreceptors.[106,107] More promising cell types like mouse and human bone marrow derived stem cells did have the potential to generate new photoreceptors, and these cells were effectively incorporated as rod photoreceptor precursor cells into the outer nuclear layer of the retina. Very recently, a rat model of RP showed a stabilization of photoreceptor loss after intravenous administration of such bone marrow derived stem cells.[108,109] Future options may be induced pluripotent stem cells (IPS) derived from skin fibroblasts or other cell types.[110] All these new techniques look promising, but have to be better understood and investigated before they can be extrapolated to clinical practice.

Optogenetics - The recently introduced term optogenetics describes a variety of techniques for expressing genes in nerve cells that render them responsive to light. This approach makes use of light-sensitive channel proteins, like rhodopsin, which can be used to manipulate neuronal function.[111] It may be very useful in patients with a generalized photoreceptor degeneration, and is independent of genetic etiology. In a recent study, rats with RP were injected with an AAV-vector which included a cloned rhodopsin gene: channelrhodopsin-2 (ChR2). The *ChR2* gene was mainly expressed in the retinal ganglion cells; 30% of these neuronal cells became light sensitive and increased VEP responses. A limitation of enlightening ganglion cells is that the sensitivity of these cells to light is less than that of normal cones. Moreover, normal cones have the ability to adapt to different light intensities, whereas ganglion cells have a fixed sensitivity range.[112,113] Overall, this technique looks promising for patients with an advanced photoreceptor cell loss, and demonstrated that retinal ganglion cells are able to be transformed into light sensitive cells.

In conclusion, at this point in time many promising therapeutic options are arising, but most of these still have a long way to go before they can be used for clinical care. AAV gene augmentation therapies look very promising for clinical application, but are hampered by the genetic heterogeneity of retinal dystrophies. The choice of therapy will depend on the time-point of intervention. When patients can be treated in an early phase, the focus should be on retinal cell rescue; gene augmentation or neuroprotection therapies are then most appropriate. When patients are treated later in the disease course, the focus should be on retinal cell replacement; stem cell, or optogenetic therapies will be more suitable in this situation.

Final remark

I hope our studies help to improve the insights into the causes and consequences of cone disorders, and stimulate further research. What will be the benefits? Knowledge of disease mechanisms, insight into gene function, development of precise prognostic models, better patient management and clinical counseling, and creation of new intervention strategies.
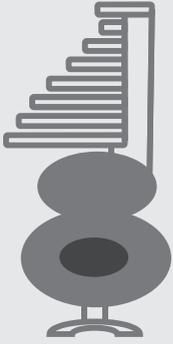
References

REFERENCES

1. Mustafi D, Engel AH, Palczewski K. Structure of cone photoreceptors. Prog Retin Eye Res. 2009;28:289-302.

2. Kawamura S, Tachibanaki S. Rod and cone photoreceptors: molecular basis of the difference in their physiology. Comp Biochem Physiol A Mol Integr Physiol. 2008;150:369-77.

3. Forrester JV, Dick AD, McMenamin PG, Lee, WR. The Eye, basic sciences in practice. Saunders. London. Second edition. 2002: 39-46.

4. Yau KW. Phototransduction mechanism in retinal rods and cones. The Friedenwald Lecture. Invest Ophthalmol Vis Sci. 1994;35:9-32.

5. Jindrová H. Vertebrate phototransduction: activation, recovery, and adaptation. Physiol Res. 1998;47:155-68.

6. Palczewski K, Polans AS, Baehr W, Ames JB. Ca(2+)-binding proteins in the retina: structure, function, and the etiology of human visual diseases. Bioessays. 2000;22:337-50.

7. Travis GH, Golczak M, Moise AR, Palczewski K. Diseases caused by defects in the visual cycle: retinoids as potential therapeutic agents. Annu Rev Pharmacol Toxicol. 2007;47:469-512.

8. Mata NL, Radu RA, Clemmons RC, Travis GH. Isomerization and oxidation of vitamin a in cone-dominant retinas: a novel pathway for visual-pigment regeneration in daylight. Neuron. 2002;36:69-80.

9. Muniz A, Villazana-Espinoza ET, Hatch AL, et al. A novel cone visual cycle in the cone-dominated retina. Exp Eye Res. 2007;85:175-84.

10. Wang JS, Kefalov VJ. The Cone-specific visual cycle. Prog Retin Eye Res. 2010;25:1-14.

11. Nathans J, Thomas D, Hogness DS. Molecular genetics of human color vision: the genes encoding blue, green, and red pigments. Science. 1986;232:193-202.

12. Nathans J, Davenport CM, Maumenee IH, et al. Molecular genetics of human blue cone monochromacy. Science. 1989;245:831-8.

13. Melamud A, Hagstrom S, Traboulsi EI. Color vision testing. Ophthalmic Genet. 2004;25:159-87.

14. Fishman GA, Birch DG, Holder GE, Brigell MG. Electrophysiologic testing in disorders of the retina, optic nerve, and visual pathway. Ophthalmology Monograph 2. Second edition. San Fransisco: American Academy of Ophthalmology;2001.

15. Grover S, Fishman GA, Birch DG, et al. Variability of full-field electroretinogram responses in subjects without diffuse photoreceptor cell disease. Ophthalmology. 2003;110:1159-63.

16. Marmor MF, Fulton AB, Holder GE, et al. International Society for Clinical Electrophysiology of Vision. ISCEV Standard for full-field clinical electroretinography (2008 update). Doc Ophthalmol. 2009;118:69-77.

17. Michaelides M, Hunt DM, Moore AT. The cone dysfunction syndromes. Br J Ophthalmol. 2004;88:291-7.

18. Kohl S, Varsanyi B, Antunes GA, et al. CNGB3 mutations account for 50% of all cases with autosomal recessive achromatopsia. Eur J Hum Genet. 2005;13:302-8.

19. Wissinger B, Gamer D, Jagle H, et al. CNGA3 mutations in hereditary cone photoreceptor disorders. Am J Hum Genet. 2001;69:722-37.

20. Kohl S, Baumann B, Rosenberg T, et al. Mutations in the cone photoreceptor G-protein alpha-subunit gene GNAT2 in patients with achromatopsia. Am J Hum Genet. 2002;71:422-5.

21. Michaelides M, Holder GE, Bradshaw K, et al. Oligocone trichromacy: a rare and unusual cone dysfunction syndrome. Br J Ophthalmol. 2004;88:497-500.

22. Andersen MK, Christoffersen NL, Sander B, et al. Oligocone trichromacy: clinical and molecular genetic investigations. Invest Ophthalmol Vis Sci. 2010;51:89-95.

23. Vincent A, Wright T, Billingsley G, et al. Oligocone trichromacy is part of the spectrum of CNGA3-related cone system disorders. Ophthalmic Genet. 2011;26:1-7.

24. Berson EL, Sandberg MA, Rosner B, Sullivan PL. Color plates to help identify patients with blue cone monochromatism. Am J Ophthalmol. 1983;95:741-7.

25. Gardner JC, Michaelides M, Holder GE, et al. Blue cone monochromacy: causative mutations and associated phenotypes. Mol Vis. 2009;15:876-84.

26. Schwartz M, Haim M, Skarsholm D. X-linked myopia: Bornholm eye disease. Linkage to DNA markers on the distal part of Xq. Clin Genet. 1990;38:281-6.

27. Michaelides M, Johnson S, Bradshaw K, et al. X-linked cone dysfunction syndrome with myopia and protanopia. Ophthalmology. 2005;112:1448-54.

28. Kohn L, Kadzhaev K, Burstedt MS, et al. Mutation in the PYK2-binding domain of PITPNM3 causes autosomal dominant cone dystrophy (CORD5) in two Swedish families. Eur J Hum Genet. 2007;15:664-671.

29. Payne AM, Downes SM, Bessant DA, et al. A mutation in guanylate cyclase activator 1A (GUCA1A) in an autosomal dominant cone dystrophy pedigree mapping to a new locus on chromosome 6p21.1. Hum Mol Genet. 1998;7:273-277.

30. Michaelides M, Wilkie SE, Jenkins S, et al. Mutation in the gene GUCA1A, encoding guanylate cyclase-activating protein 1, causes cone, cone-rod, and macular dystrophy. Ophthalmology. 2005;112:1442-1447.

31. Vervoort R, Lennon A, Bird AC, et al. Mutational hot spot within a new RPGR exon in X-linked retinitis pigmentosa. Nat Genet. 2000;25:462-6.

32. Yang Z, Peachey NS, Moshfeghi DM, et al. Mutations in the RPGR gene cause X-linked cone dystrophy. Hum Mol Genet. 2002;11:605-611.

33. Kitiratschky VB, Grau T, Bernd A, et al. ABCA4 gene analysis in patients with autosomal recessive cone and cone-rod dystrophies. Eur J Hum Genet. 2008;16:812-819.

34. Wu H, Cowing JA, Michaelides M, et al. Mutations in the gene KCNV2 encoding a voltage-gated potassium channel subunit cause "cone dystrophy with supernormal rod electroretinogram" in humans. Am J Hum Genet. 2006;79:574-579.

35. Wissinger B, Dangel S, Jagle H, et al. Cone dystrophy with supernormal rod response is strictly associated with mutations in KCNV2. Invest Ophthalmol Vis Sci. 2008;49:751-757.

36. Michaelides M, Aligianis IA, Ainsworth JR, et al. Progressive cone dystrophy associated with mutation in CNGB3. Invest Ophthalmol Vis Sci. 2004;45:1975-1982.

37. Wycisk KA, Zeitz C, Feil S, et al. Mutation in the auxiliary calcium-channel subunit CACNA2D4 causes autosomal recessive cone dystrophy. Am J Hum Genet. 2006;79:973-7.

38. Berger W, Kloeckener-Gruissem B, Neidhardt J. The molecular basis of human retinal and vitreo-retinal diseases. Prog Retin Eye Res. 2010;29:335-75.

39. Michaelides M, Hardcastle AJ, Hunt DM, Moore AT. Progressive cone and cone-rod dystrophies: phenotypes and underlying molecular genetic basis. Surv Ophthalmol. 2006;51:232-258.

40. Littink KW, Koenekoop RK, van den Born LI, et al. Homozygosity mapping in patients with cone-rod dystrophy: novel mutations and clinical characterizations. Invest Ophthalmol Vis Sci. 2010;51:5943-51.

41. Allikmets R, Singh N, Sun H, et al. A photoreceptor cell-specific ATP-binding transporter gene(ABCR) is mutated in recessive Stargardt macular dystrophy. Nat Genet. 1997;15:236-246.

42. Cremers FPM, van de Pol DJ, van Driel M, et al. Autosomal recessive retinitis pigmentosa and cone-rod dystrophy caused by splice site mutations in the Stargardt's disease gene ABCR. Hum Mol Genet. 1998;7:355-62.

43. Maugeri A, Klevering BJ, Rohrschneider K, et al. Mutations in the ABCA4 (ABCR) gene are the major cause of autosomal recessive cone-rod dystrophy. Am J Hum Genet. 2000;67:960-966.

44. Webster AR, Heon E, Lotery AJ, et al. An analysis of allelic variation in the ABCA4 gene. Invest Ophthalmol Vis Sci. 2001;42:1179-1189.

45. Ducroq D, Rozet JM, Gerber S, et al. The ABCA4 gene in autosomal recessive cone-rod dystrophies. Am J Hum Genet. 2002;71:1480-1482.

46. Klevering BJ, Blankenagel A, Maugeri A, et al. Phenotypic spectrum of autosomal recessive cone-rod dystrophies caused by mutations in the ABCA4 (ABCR) gene. Invest Ophthalmol Vis Sci. 2002;43:1980-1985.

47. Fishman GA, Stone EM, Eliason DA, et al. ABCA4 gene sequence variations in patients with auto-somal recessive cone-rod dystrophy. Arch Ophthalmol. 2003;121:851-855.

48. Klevering BJ, Yzer S, Rohrschneider K, et al. Microarray-based mutation analysis of the ABCA4 (ABCR) gene in autosomal recessive cone-rod dystrophy and retinitis pigmentosa. Eur J Hum Genet. 2004;12:1024-1032.

49. Koenekoop RK, Lopez I, den Hollander AI, et al. Genetic testing for retinal dystrophies and dys-functions: benefits, dilemmas and solutions. Clin Experiment Ophthalmol. 2007;35:473-85.

50. Hood DC, Bach M, Brigell M, et al. ISCEV guidelines for clinical multifocal electroretinography (2007 edition). Doc Ophthalmol. 2008;116:1-11.

51. Nagy D, Schönfisch B, Zrenner E, Jägle H. Long-term follow-up of retinitis pigmentosa patients with multifocal electroretinography. Invest Ophthalmol Vis Sci. 2008;49:4664-71.

52. Riemslag FC, Ringo JL, Spekreijse H, Verduyn Lunel HF. The luminance origin of the pattern elec-troretinogram in man. J Physiol. 1985;363:191-209.

53. Kremers J, Stepien MW, Scholl HP, Saito C. Cone selective adaptation influences L- and M-cone driven signals in electroretinography and psychophysics. J Vis. 2003;3:146-60.

54. Scholl HP, Kremers J. Alterations of L- and M-cone driven ERGs in cone and cone-rod dystrophies. Vision Res. 2003;43:2333-44.

55. Kremers J. The assessment of L- and M-cone specific electroretinographical signals in the normal and abnormal human retina. Prog Retin Eye Res. 2003;22:579-605.

56. Spaide RF. Fundus autofluorescence and age-related macular degeneration. Ophthalmology. 2003;110:392-399.

57. Duncan JL, Zhang Y, Gandhi J, et al. High-resolution imaging with adaptive optics in patients with inherited retinal degeneration. Invest Ophthalmol Vis Sci. 2007;48:3283-91.

58. Jonnal RS, Rha J, Zhang Y, et al. In vivo functional imaging of human cone photoreceptors. Opt Express. 2007;15:16141-60.

59. Jonnal RS, Besecker JR, Derby JC, et al. Imaging outer segment renewal in living human cone photoreceptors. Opt Express. 2010;18:5257-70.

60. den Hollander AI, Black A, Bennett J, Cremers FPM. Lighting a candle in the dark: advances in genetics and gene therapy of recessive retinal dystrophies. J Clin Invest. 2010;120:3042-53.

61. Booij JC, Bakker A, Kulumbetova J, et al. Simultaneous mutation detection in 90 retinal disease genes in multiple patients using a custom-designed 300-kb retinal resequencing chip. Ophthalmology. 2011;118:160-167.

62. Ng SB, Turner EH, Robertson PD, et al. Targeted capture and massively parallel sequencing of 12 human exomes. Nature. 2009;461:272-6.

63. Choi M, Scholl UI, Ji W, et al. Genetic diagnosis by whole exome capture and massively parallel DNA sequencing. Proc Natl Acad Sci U S A. 2009;106:19096-101.

64. Nikopoulos K, Gilissen C, Hoischen A, et al. Next-generation sequencing of a 40 Mb linkage interval reveals TSPAN12 mutations in patients with familial exudative vitreoretinopathy. Am J Hum Genet. 2010;86:240-7.

65. Portera-Cailliau C, Sung CH, Nathans J, Adler R. Apoptotic photoreceptor cell death in mouse models of retinitis pigmentosa. Proc Natl Acad Sci U S A. 1994;91:974-8.

66. Sancho-Pelluz J, Arango-Gonzalez B, Kustermann S, et al. Photoreceptor cell death mechanisms in inherited retinal degeneration. Mol Neurobiol. 2008;38:253-69.

67. Kaupp UB, Seifert R. Cyclic nucleotide-gated ion channels. Physiol Rev. 2002;82:769-824.

68. Biel M, Seeliger M, Pfeifer A, et al. Selective loss of cone function in mice lacking the cyclic nucleotide-gated channel CNG3. Proc Natl Acad Sci U S A. 1999;96:7553-7.

69. Wenzel A, Grimm C, Samardzija M, Remé CE. Molecular mechanisms of light-induced photoreceptor apoptosis and neuroprotection for retinal degeneration. Prog Retin Eye Res. 2005;24:275-306.

70. Vlachantoni D, Bramall AN, Murphy MP, et al. Evidence of severe mitochondrial oxidative stress and a protective effect of low oxygen in mouse models of inherited photoreceptor degeneration. Hum Mol Genet. 2011;20:322-35.

71. Organisciak DT, Vaughan DK. Retinal light damage: mechanisms and protection. Prog Retin Eye Res. 2010;29:113-34.

72. Haider NB, Ikeda A, Naggert JK, Nishina PM. Genetic modifiers of vision and hearing. Hum Mol Genet. 2002;11:1195-206.

73. Nadeau JH. Modifier genes in mice and humans. Nat Rev Genet. 2001;2:165-74.

74. Khanna H, Davis EE, Murga-Zamalloa CA, et al. A common allele in RPGRIP1L is a modifier of retinal degeneration in ciliopathies. Nat Genet. 2009;41:739-45.

75. Stoetzel C, Muller J, Laurier V, et al. Identification of a novel BBS gene (BBS12) highlights the major role of a vertebrate-specific branch of chaperonin-related proteins in Bardet-Biedl syndrome. Am J Hum Genet. 2007;80:1-11.

76. Thiadens AA, Klaver CCW. Genetic testing and clinical characterization of patients with cone-rod dystrophy. Invest Ophthalmol Vis Sci. 2010;51:6904-5.

77. Radu RA, Yuan Q, Hu J, et al. Accelerated accumulation of lipofuscin pigments in the RPE of a mouse model for ABCA4-mediated retinal dystrophies following Vitamin A supplementation. Invest Ophthalmol Vis Sci. 2008 ;49:3821-9.

78. Berson EL, Rosner B, Sandberg MA, et al. Vitamin A supplementation for retinitis pigmentosa. Arch Ophthalmol. 1993;111:1456-9.

79. Hartong DT, Berson EL, Dryja TP. Retinitis pigmentosa. Lancet. 2006;368:1795-809.

80. Tan JS, Mitchell P, Kifley A, et al. Smoking and the long-term incidence of age-related macular degeneration: the Blue Mountains Eye Study. Arch Ophthalmol. 2007;125:1089-95.

81. Komeima K, Rogers BS, Lu L, Campochiaro PA. Antioxidants reduce cone cell death in a model of retinitis pigmentosa. Proc Natl Acad Sci U S A. 2006;103:11300-5.

82. Komeima K, Rogers BS, Campochiaro PA. Antioxidants slow photoreceptor cell death in mouse models of retinitis pigmentosa. J Cell Physiol. 2007;213:809-15.

83. Sanz MM, Johnson LE, Ahuja S, et al. Significant photoreceptor rescue by treatment with a combination of antioxidants in an animal model for retinal degeneration. Neuroscience. 2007;145:1120-9.

84. Berson EL, Rosner B, Sandberg MA, et al. Clinical trial of docosahexaenoic acid in patients with retinitis pigmentosa receiving vitamin A treatment. Arch Ophthalmol. 2004;122:1297-305.

85. Berson EL, Rosner B, Sandberg MA, et al. Further evaluation of docosahexaenoic acid in patients with retinitis pigmentosa receiving vitamin A treatment: subgroup analyses. Arch Ophthalmol. 2004;122:1306-14.

86. Hoffman DR, Locke KG, Wheaton DH, et al. A randomized, placebo-controlled clinical trial of docosahexaenoic acid supplementation for X-linked retinitis pigmentosa. Am J Ophthalmol. 2004;137:704-18.

87. Berson EL, Rosner B, Sandberg MA, et al. Clinical trial of lutein in patients with retinitis pigmentosa receiving vitamin A. Arch Ophthalmol. 2010;128:403-11.

88. Bainbridge JW, Smith AJ, Barker SS, et al. Effect of gene therapy on visual function in Leber's congenital amaurosis. N Engl J Med. 2008;358:2231-9.

89. Maguire AM, Simonelli F, Pierce EA, et al. Safety and efficacy of gene transfer for Leber's congenital amaurosis. N Engl J Med. 2008;358:2240-8.

90. Maguire AM, High KA, Auricchio A, et al. Age-dependent effects of RPE65 gene therapy for Leber's congenital amaurosis: a phase 1 dose-escalation trial. Lancet. 2009;374:1597-605.

91. Simonelli F, Maguire AM, Testa F, et al. Gene therapy for Leber's congenital amaurosis is safe and effective through 1.5 years after vector administration. Mol Ther. 2010;18:643-50.

92. Alexander JJ, Umino Y, Everhart D, et al. Restoration of cone vision in a mouse model of achromatopsia. Nat Med. 2007;13:685–687.

93. Pang JJ, Alexander J, Lei B, et al. Achromatopsia as a potential candidate for gene therapy. Adv Exp Med Biol. 2010;664:639-46.

94. Komáromy AM, Alexander JJ, Rowlan JS, et al. Gene therapy rescues cone function in congenital achromatopsia. Hum Mol Genet. 2010;19:2581-93.

95. Michalakis S, Mühlfriedel R, Tanimoto N, et al. Restoration of cone vision in the CNGA3-/- mouse model of congenital complete lack of cone photoreceptor function. Mol Ther. 2010;18:2057-63.

96. Welch EM, Barton ER, Zhuo J, et al. PTC124 targets genetic disorders caused by nonsense mutations. Nature. 2007;447:87-91.

97. Du M, Liu X, Welch EM, et al. PTC124 is an orally bioavailable compound that promotes suppression of the human CFTR-G542X nonsense allele in a CF mouse model. Proc Natl Acad Sci U S A. 2008;105:2064-9.

98. Kerem E, Hirawat S, Armoni S, et al. Effectiveness of PTC124 treatment of cystic fibrosis caused by nonsense mutations: a prospective phase II trial. Lancet. 2008;372:719-27.

99. Linde L, Kerem B. Introducing sense into nonsense in treatments of human genetic diseases. Trends Genet. 2008;24:552-63.

100. Goldmann T, Overlack N, Wolfrum U, Nagel-Wolfrum K. PTC124 mediated translational read-through of a nonsense mutation causing Usher type 1C. Hum Gene Ther. 2011;14:1-33.

101. LaVail MM, Yasumura D, Matthes MT, et al. Protection of mouse photoreceptors by survival factors in retinal degenerations. Invest Ophthalmol Vis Sci. 1998;39:592-602.

102. Li Y, Tao W, Luo L, et al. CNTF induces regeneration of cone outer segments in a rat model of retinal degeneration. PLoS One. 2010;5:9495.

103. Emerich DF, Thanos CG. NT-501: an ophthalmic implant of polymer-encapsulated ciliary neurotrophic factor-producing cells. Curr Opin Mol Ther. 2008;10:506-15.

104. Kuno N, Fujii S. Biodegradable intraocular therapies for retinal disorders: progress to date. Drugs Aging. 2010;27:117-34.

105. MacLaren RE, Pearson RA, MacNeil A, et al. Retinal repair by transplantation of photoreceptor precursors. Nature. 2006;444:203-7.

106. Gualdoni S, Baron M, Lakowski J, et al. Adult ciliary epithelial cells, previously identified as retinal stem cells with potential for retinal repair, fail to differentiate into new rod photoreceptors. Stem Cells. 2010;28:1048-59.

107. Decembrini S, Cananzi M, Gualdoni S, et al. Comparative Analysis of the Retinal Potential of Embryonic Stem Cells and Amniotic Fluid-Derived Stem Cells. Stem Cells Dev. 2010;6:1-13.

108. Joe AW, Gregory-Evans K. Mesenchymal stem cells and potential applications in treating ocular disease. Curr Eye Res. 2010;35:941-52.

109. Wang S, Lu B, Girman S, et al. Non-invasive stem cell therapy in a rat model for retinal degeneration and vascular pathology. PLoS One. 2010;5:9200.

110. Jin ZB, Okamoto S, Osakada F, et al. Modeling retinal degeneration using patient-specific induced pluripotent stem cells. PLoS One. 2011;6:17084.

111. Fiala A, Suska A, Schlüter OM. Optogenetic approaches in neuroscience. Curr Biol. 2010;20:897-903.

112. Tomita H, Sugano E, Isago H, et al. Channelrhodopsin-2 gene transduced into retinal ganglion cells restores functional vision in genetically blind rats. Exp Eye Res. 2010;90:429-36.

113. Busskamp V, Duebel J, Balya D, et al. Genetic reactivation of cone photoreceptors restores visual responses in retinitis pigmentosa. Science. 2010;329:413-7.
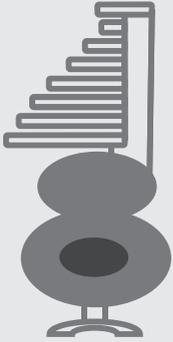
Summary

SUMMARY

Hereditary retinal disorders constitute a large heterogeneous group of diseases in which the photoreceptors are primarily affected. When cone cells are affected, one cannot see details or perceive color. In this thesis, we focused on the three most important diseases in which the cones are primarily affected: achromatopsia (ACHM), cone dystrophy (CD), and cone-rod dystrophy (CRD). Although cone disorders account for only a small portion of all retinal disorders, they have a great impact on daily life. This is mainly due to the early onset of disease, severe visual outcome, and lack of therapeutic options. Cone disorders can have an autosomal recessive, autosomal dominant or X-linked inheritance, but unfortunately the genetic etiology is still largely unknown. This hampers clinical and genetic counseling and the development of therapeutic options. This gap of knowledge encouraged us to initiate a multicenter study with the aim to investigate the clinical course of cone disorders and to unravel the genetic causes.

In the **General Introduction** an overview of the morphological and functional differences between cone and rod photoreceptors is presented. Subsequently, the process of light conversion into an electric neural signal in cones is systematically described. Finally, the different tests to diagnose cone disorders, and the clinical characteristics of all cone disorders are highlighted.

Chapter 1a describes the dilemma of proper color vision testing in clinical practice. Although these simple psychophysical tests are used by all ophthalmologists as a first step to identify cone disorders, their reliability in the diagnosis was still unclear. Therefore, we tested the discriminative accuracy of four commonly used color vision tests. The HRR and desaturated Panel D-15 test appeared to be the most reliable, even in the low vision strata.

Chapter 2a provides evidence that 90% of the genetic causes of ACHM can be attributed to the *CNGA3* and *CNGB3* genes. The *CNGB3* gene is by far the most important causal gene, and p.T383IfsX13 the most frequent mutation. A distinct genetic etiology does not predispose to an ACHM subtype (complete or incomplete), nor are any other genotype-phenotype correlations apparent. Thus, we propose that the distinction between complete and incomplete subtypes of ACHM does not have any clinical value.

In **Chapter 2b**, we reasoned that the rather homogeneous genetic etiology of ACHM renders this disease a suitable candidate for future gene-based therapies. Nevertheless, this requires the presence of viable cone cells in the retina. We therefore investigated the presence of cone cells in ACHM patients as a function of age using SD-OCT. The

first signs of cone cell loss were already evident in early childhood and progressed rapidly thereafter. Our results suggest that intervention with future gene-based therapies should be applied early in life, preferably in the first decade.

In **Chapter 3a**, we demonstrated that mutations in the ACHM genes, *CNGA3* and *CNGB3,* can also lead to CD. In three CD families, we discovered pathogenic compound heterozygous mutations in *CNGA3* and *CNGB3*. It remains unclear why similar mutations cause different phenotypes in these patients.

Chapter 3b reports the identification of a new disease gene for ACHM and early-onset CD. We detected mutations in *PDE6C,* a gene that is expressed specifically in cone photoreceptor cells, by homozygosity mapping using genome-wide SNP arrays. Pathogenic mutations in this gene were detected in several ACHM families and in one CD family. These findings provide more insight into the pathophysiology of cone disorders, and confirm that clinical and genetic overlap between ACHM and CD exists.

Chapter 3c describes two families with CD due to two different mutations at the 3' end of *RPGR*-ORF15. One family carried a novel mutation. The other family was very large, and included 26 affected males and 25 female carriers. Since we had access to clinical data with a long follow-up period in this family, we were able to study visual acuity as a function of age. The affected family members had a relatively late onset of CD, but a rapid decline thereafter. Our findings suggest that *RPGR* mutations at the 3' end of ORF15 can predispose to disease primarily affecting the cones, while mutations in other regions of the gene are known to cause rod-dominated disease.

Chapter 3d evaluates the clinical course and visual outcome in patients with CD and CRD. Half of CD patients reached legal blindness at age 48 years, while half of CRD patients did so at age 23 years. In 9/90 (10%) of CD and in 17/65 (26%) of CRD, two pathogenic *ABCA4* mutations were identified. The presence of mutations in the *ABCA4* gene and an early onset of disease were both independent prognostic factors for a worse clinical course and visual outcome. These results will help improve clinical counseling of CD and CRD patients.

Chapter 4a underscores the important role of the ophthalmologist in comprehensive screening of syndromic patients with eye involvement. We provided a detailed description of the clinical findings in a family with Danon and CRD due to *LAMP2* mutations. Two family members presented with a late-onset CRD leading to legal blindness within 20 years, while two other family members had no ophthalmologic involvement.

In the **General Discussion** the main findings of this thesis are recapitulated and placed in a broader perspective. First, we described differences and advantages of diagnostic testing to improve early detection of patients with retinal disorders. Then we summarized the genetic causes of cone disorders and commented on the emerging new techniques for the detection of (new) disease genes. We emphasized the differences in clinical course, and hypothesized which possible pathogenic factors can play a role in these different phenotypes. In the last paragraph, important issues for a cone disorder patient who seeks clinical and genetic counseling are discussed. Finally, we shined our lights on different future therapeutic interventions like gene augmentation therapies, stem cell therapies and optogenetics.
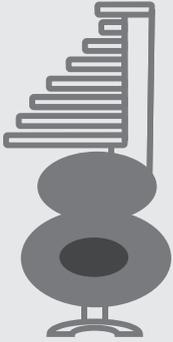
Samenvatting

SAMENVATTING

Erfelijke netvlies aandoeningen vormen een grote heterogene groep van ziekten waarbij primair de fotoreceptorcellen zijn aangedaan. Indien de kegelcellen zijn getroffen, resulteert dit in een slechte visus en in kleurenzienstoornissen. In dit proefschrift hebben wij ons gericht op de drie belangrijkste oogziekten waarbij primair de kegels zijn aangedaan: achromatopsie (ACHM), kegeldystrofie (CD) en kegel-staafdystrofie (CRD). Andere primaire kegelaandoeningen zijn de minder voorkomende ziekten: oligocone trichromacy, blauwe kegel monochromatisme en Bornholm eye disease. Alhoewel kegelaandoeningen slechts een klein onderdeel van alle netvliesaandoeningen vormen, hebben zij een grote impact op het dagelijkse leven. Dit wordt met name veroorzaakt doordat de ziekte vaak al voor de tweede decade optreedt; meestal leidt tot blindheid en er geen therapeutische mogelijkheden zijn. Kegelaandoeningen kunnen zowel via het X-chromosoom als via een van de andere chromosomen overerven. De betrokken genen zijn echter nog grotendeels onbekend. Dit beperkt de mogelijkheden voor klinische en genetische begeleiding en staat ontwikkeling van therapeutische mogelijkheden in de weg. Het gebrek aan kennis heeft ons aangemoedigd om een multicenter-studie te starten met als doel het ziektebeloop te onderzoeken en de genetische oorzaken van kegelaandoeningen te ontrafelen.

In de **General Introduction** geef ik een overzicht van de morfologische en functionele verschillen tussen kegel en staaf fotoreceptoren. Maar één op de 20 fotoreceptoren is een kegel. Echter door zijn unieke functionele eigenschappen zoals snelle signaaloverdracht en hoge dichtheid in het centrum van het netvlies, zijn wij in staat om scherp te kunnen zien en kleuren te kunnen onderscheiden.

Hoofdstuk 1a beschrijft het dilemma van het gebruik van kleurenzientesten in de kliniek. Alhoewel deze testen door alle oogartsen worden gebruikt, was het tot nu toe onduidelijk hoe betrouwbaar deze kleurenzientesten zijn voor het diagnosticeren van kegelaandoeningen. Daarom hebben wij het discriminerende vermogen van vier veelgebruikte kleurenzientesten getest. De HRR en de gedesatureerde Panel D-15 testen bleken de meest betrouwbare testen te zijn voor het detecteren van kegelaandoeningen, zelfs bij personen met een verlaagde visus.

In **Hoofdstuk 2a** wordt het bewijs geleverd dat ACHM voor 90% wordt veroorzaakt door mutaties in de *CNGA3* en *CNGB3* genen. Bij de overgrote meerderheid van deze ACHM patiënten is het *CNGB3* gen aangedaan en de meest voorkomende mutatie in dit gen is p.T383IfsX13. Bij een onderverdeling van patiënten in incomplete- of complete ACHM, hebben wij geen verschillen in klinisch beloop noch in prognose of genotype-fenotype

associaties gevonden. Wij denken daarom dat een onderscheid tussen deze subtypen geen klinische relevantie heeft.

In **Hoofdstuk 2b** hebben we voortgeborduurd op de bevinding dat slechts enkele genen ACHM veroorzaken. Deze eigenschap maakt ACHM tot een geschikte kandidaat voor toekomstige gentherapieën. Echter, voor deze therapieën zijn levensvatbare kegelcellen noodzakelijk. Daarom hebben wij de aanwezigheid van kegelcellen in ACHM onderzocht met behulp van een speciale beeldvormende techniek met een hoge resolutie, de zogenaamde SD-OCT. Met behulp van deze SD-OCT hebben wij waargenomen dat de eerste tekenen van kegelcelverlies al op jonge leeftijd optreden en dat dit beeld progressief verslechtert in de jaren die daarop volgen. Het is daarom wenselijk om toekomstige gentherapie al in de eerste decade te verrichten.

In **Hoofdstuk 3a** tonen we aan dat mutaties in de ACHM-genen**,** *CNGA3* en *CNGB3,* soms ook tot CD kunnen leiden. In drie families ontdekten we samengestelde heterozygote mutaties in het *CNGA3* en *CNGB3* gen die de CD konden verklaren. Het is nog onduidelijk waarom eenzelfde mutatie soms direct tot kegeldysfunctie leidt en in andere gevallen pas later in het leven de kegel aantast.

Hoofdstuk 3b rapporteert de ontdekking van een nieuw ziektegen voor ACHM en vroeg optredende CD. Met behulp van genoom-brede SNP arrays en homozygotie mapping tonen wij aan dat het kegel-specifieke gen *PDE6C* betrokken is bij deze aandoeningen. In verschillende families met ACHM en in één familie met CD vonden we mutaties die deze ziekten konden verklaren. Dit gen heeft ons meer inzicht gegeven in de pathofysiologie van kegelaandoeningen en het bewijs geleverd dat er klinische en genetische overlap bestaat tussen deze verschillende aandoeningen.

Hoofdstuk 3c beschrijft twee families met CD veroorzaakt door twee verschillende mutaties aan het einde van het *RPGR*-ORF15 gen. De eerste familie toonde een mutatie die nog niet eerder gevonden was. De tweede was een grote familie met 26 aangedane mannen en 25 vrouwelijke draagsters. Aangezien deze familie lange tijd is vervolgd, waren we in staat om het visuele beloop in kaart te brengen. De aangedane familieleden ontwikkelden pas laat ziekteverschijnselen, dat snel progressief verslechterde. Deze bevindingen tonen aan dat mutaties aan het einde van het *RPGR* gen kunnen leiden tot ziekten waarbij met name de kegels zijn aangedaan. Daarentegen leiden mutaties in de overige gebieden van het gen juist tot ziekten waarbij de staven van het netvlies zijn aangetast.

Hoofdstuk 3d bespreekt het klinische beloop en de visuele prognose bij patiënten met CD en CRD. De helft van de CD patiënten werd blind op 48-jarige leeftijd, de helft van de CRD patiënten op 23-jarige leeftijd. Bij 9/90 (10%) van de CD en bij 17/65 (26%) van de CRD patiënten zijn twee ziekte veroorzakende *ABCA4* mutaties gevonden. Voor beide groepen vormde *ABCA4* het meest voorkomende oorzakelijke gen. Wij hebben twee voorspellers voor een slechter klinisch beloop en visuele prognose van deze ziektebeelden gevonden: de aanwezigheid van deze *ABCA4* mutaties en een vroege presentatie van het ziektebeeld. Onze resultaten kunnen als handvat dienen bij de klinische en genetische begeleiding van patiënten met de kegelaandoeningen CD en CRD.

Hoofdstuk 4a benadrukt de belangrijke rol van de oogarts bij de screening van patiënten met oogafwijkingen in het kader van een syndroom. Wij hebben een gedetailleerde beschrijving gegeven van de klinische bevindingen in een familie met de ziekte van Danon en CRD veroorzaakt door mutaties in het *LAMP2* gen. Twee familieleden presenteerden zich met een laat optredende CRD leidend tot blindheid binnen 20 jaar na aanvang van de ziekte, terwijl twee andere familieleden ondanks deze mutatie geen oogheelkundige klachten ontwikkelden. Aangezien het al bekend was dat Danon tot netvliesafwijkingen kan leiden, concluderen wij hieruit dat mogelijk andere genen of omgevingsfactoren in staat zijn om de expressie van dit gen te modificeren

In de **General Discussion** zijn de belangrijkste bevindingen van dit proefschrift samengevoegd en in een breder perspectief geplaatst. In 97% van ACHM, in 20% van de CD en in 26% van de CRD patiënten hebben we de genetische oorzaken achterhaald. Wij hebben gezien dat er celdood optreedt bij de reeds slechtziende ACHM patiënten en dat CD en CRD vaak tot ernstige slechtziendheid leiden. Kegelgenen zijn hetzij heel specifiek voor de kegelfunctie zelf (*CNGA3*, *CNGB3*, *PDE6C*) of spelen juist een rol in alle fotoreceptoren (*ABCA4*, *RPGR*, *LAMP2*). Op dit moment zijn er geen therapeutische mogelijkheden voor patiënten met kegelaandoeningen. De toekomst ziet er echter hoopvol uit. Er zijn nieuwe interventies op komst zoals gen- en stamceltherapie, behandeling met neurotrofische factoren of het transformeren van andere retinale cellen in fotoreceptoren (optogenetica).

Dit proefschrift laat zien dat veel genetische oorzaken voor kegelaandoeningen nog niet opgehelderd zijn. De verwachting is dat de nieuwe DNA technieken die in ontwikkeling zijn hier soelaas zullen bieden. Het ontdekken van nieuwe genen zal de opheldering van de pathogenese faciliteren en een brug slaan naar nieuwe therapieën. Om de patiënt met kegeldysfunctie nu en in de toekomst optimale zorg te bieden, is een goede samenwerking tussen genetici, clinici en low vision specialisten onontbeerlijk. Wij hopen dat dit een 'kleurrijker' bestaan voor deze groep patiënten zal bevorderen.
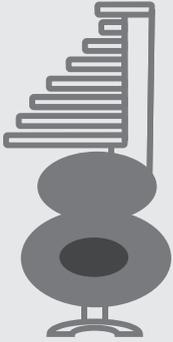
Dankwoord

DANKWOORD

"You cannot see a rainbow, when you have no tears in your eyes", zei Henk Thiadens eens tegen mij toen ik na een dag pipetteren zonder resultaat terugkwam uit het lab. En ik kon weer lachen. Dit staat symbool voor mijn promotie onderzoek, waarin mooie en verdrietige gebeurtenissen elkaar hebben afgewisseld. Ik heb dit citaat onthouden, want Henk had niet alleen een wijze uitspraak gedaan, het was dit keer ook oogheelkundig verantwoord.

Een aantal mensen wil ik persoonlijk bedanken die hebben bijgedragen aan de totstandkoming van dit proefschrift:

Caroline, mijn enthousiasme voor dit onderzoek ontstond toen ik meeliep met jouw oculogenetica spreekuur. Je enorme passie, enthousiasme en gedrevenheid voor het vak werken aanstekelijk. Ik weet nog goed dat ik halverwege het jaar 2006 aan jou vroeg of er een mogelijkheid bestond om promotie onderzoek te gaan doen. Jij zag die direct en samen zijn we *from scratch* gestart: geen geld, geen patiënten, geen samenwerkingspartners en geen METC goedkeuring. Onze inspanningen zijn beloond, dit boekje is het bewijs. Ik wil je heel erg bedanken voor je fantastische begeleiding. Dit boekje had niet tot stand kunnen komen zonder jouw enorme veelzijdigheid aan kennis op zowel oogheelkundig, epidemiologisch als genetisch gebied, je drang naar perfectie en heldere analytische wijze van werken. De vele (avond)uurtjes die je hebt gespendeerd om samen met mij te werken aan de artikelen en praatjes heb ik heel erg gewaardeerd. Jij bent als oogarts en wetenschapper een voorbeeld voor mij en ik ben dan ook trots dat ik je promovenda mocht zijn. Na deze beproeving kijk ik alweer uit naar de volgende: samen met jou de Kilimanjaro beklimmen!

Frans en Anneke, ik heb de 2 jaar in het lab bij jullie als zeer leerzaam en inspirerend beschouwd. Ik heb veel van jullie geleerd door jullie kritische blik en gedegen manier van werken. Door te mogen werken in het lab, heb ik de kans gekregen om de moleculaire kant van de patiënt te ontdekken. Ik wil jullie dan ook heel erg bedanken voor de zeer goede begeleiding en de hulp bij het schrijven van de artikelen. Erg fijn dat jullie mijn promotor en co-promotor zijn.

Professor van Rij, ik ben u erg erkentelijk voor uw steun en interesse in het kegelproject. Uw bereidheid om van mijn opleiding een AGIKO constructie te maken en uw financiële bijdrage, hebben het mogelijk gemaakt om dit onderzoek te verrichten. Ik ben vereerd dat u naast mijn opleider, ook mijn promotor bent.

Susanne, jij was een centraal persoon binnen het kegelproject. Heel veel dank voor alle hulp in het lab, het pipetteerwerk, je interesse en ook de gezelligheid. Dat jij op een gegeven moment 'besmet' bent geraakt met het *CNGB3* gen zegt eigenlijk al alles: je hebt echt veel werk verzet. Ik vind het ontzettend leuk dat jij nu het stokje overneemt en ik wens je dan ook veel succes in jouw promotietijd toe. Ik moest bij onderstaande regels van Cousteau meteen aan onze tijd in het lab denken: *What is a scientist after all? It is a curious man looking through a keyhole, the keyhole of nature, trying to know what's going on.*

Riet, ook jij was een spil in het kegelproject. Ontzettend bedankt voor al je inzet en enthousiasme de afgelopen jaren. We begonnen samen aan mijn bureau in de assistentenkamer met een praktisch leeg Excel-sheetje en nu staan de kasten vol met medische dossiers van deelnemende patiënten. Ik vond het altijd ontzettend gezellig met je.

Collega oogartsen, zonder jullie geen patiënten, zonder patiënten geen onderzoek. Dank voor de goede en vruchtbare samenwerking: Ingeborgh van den Born, Mary van Schooneveld, Arthur Bergen, Norka van Moll-Ramirez, Mies van Genderen, Janneke van Lith-Verhoeven, Jan Willem Pott, Andrew Lotery en Robert Koenekoop. Carel Hoyng, nog een extra woord van dank voor de vele patiënten die via jou zijn gekomen. Speciaal wil ik ook Bart Leroy hierin noemen; hartelijk dank voor de gastvrijheid om een aantal dagen in Gent te mogen verblijven.

Vijf oogartsen in spé hebben in het kader van hun afstudeeronderzoek meegeholpen aan onze studie en dit is van enorme waarde geweest voor het onderzoek. Gyan en Niki, veel dank voor jullie hulp bij het verzamelen van de klinische data en veel succes met de opleiding. Milan en Renate, jullie hebben enorm veel werk gehad aan het includeren van de C(R)D patiënten tijdens mijn zwangerschapsverlof en gedurende mijn labtijd. Zonder jullie hulp was het laatste artikel nooit afgekomen! Milan, veel succes met je opleiding in Nijmegen en Renate, met de voltooiing van je promotie onderzoek. Ville, thank you so much for all your work in collecting and interpreting the OCT data. We had a lot of fun together in Potsdam, during the ACHM-day and (what I have heard) at ARVO. I think you will become a great ophthalmologist in Helsinki.

Verder wil ik ook alle personen die (zijdelings) betrokken waren bij het kegelproject bedanken voor hun inzet en hulp: Rob Collin, Ralph Florijn, Elfride de Baere, Robert Kuijpers, Jacoline ten Brink, Gerhard Visser, Camiel Boon, Jan Roelof Polling, Karin Littink, Saskia vd Velde, Kristel Beumer, Gabriëlle Buitendijk, alle overige mensen uit het lab die mij hebben geholpen en alle stafartsen en assistenten oogheelkunde van het Erasmus MC. Als bezegeling van deze bijzondere onderzoekstijd hebben we bij Caroline thuis een heel geslaagd 'kegel-diner' gehad met alle personen die betrokken waren bij het project.

Zie onderstaande foto:

Een aantal andere personen wil ik ook bedanken:

Hans en Kim, zonder jullie als buurtjes had ik het maar saai gehad. Bedankt voor jullie onvoorwaardelijke steun en liefdevolle zorg voor Josephine en Reinier. Zij mogen zich rijk prijzen met zo'n lieve oom en tante.

Henk, tijdens het eerste lab jaar woonden wij even samen in Amerongen. Dank je voor deze inspirerende tijd waarin we veel bijzondere gesprekken hebben gevoerd, maar ook emotionele momenten beleefden in het huis waar de sfeer mijn ouders nog zo goed voelbaar was.

Ariane en Stef, tijdens het laatste lab jaar mocht ik bij jullie logeren. Josephine en ik waren echt helemaal thuis bij jullie en het voelde erg vertrouwd. Ik heb genoten van de fijne gesprekken en het lekkere eten. Veel dank voor deze onvergetelijke tijd.

Lieve familieleden, Reinette, Fridtjof en Madelyn, Klaske, Peter en Elisabeth, Albert en Christi, Marijke, alle overige familieleden en mijn dierbare vriendinnen, Willemijn, Peggy, Eefje, Karen, Babette, Su-San en Daphne, dank voor jullie vriendschap en betrokkenheid in mijn leven en dat van Josephientje en Reinier.

Lieve Zuni, dank voor je liefdevolle zorg voor de kinderen, ik had het niet gered zonder je. De kinderen zijn dol op je!

En mijn paranimfen, Charlotte en Tessa. Jullie staan naast mij op deze belangrijke dag en daar ben ik erg blij om. Charlotte, ik vind het bijzonder dat ik drie maanden geleden ook jouw paranimf mocht zijn; onze vriendschap is tijdloos en ik ben blij dat je er bent. Tessa, jouw vanzelfsprekende lieve steun voor mij en de kinderen op de 'vaste' dinsdagavond heb ik als erg bijzonder ervaren. Jij wordt nu bijna tropenarts en ik bewonder je avontuurlijkheid en ambities. Ik ben trots dat jij vandaag, als echte 'Thiadens', deze rol vervult.

En verder ik wil nog mijn inspiratiebronnen benoemen:

Toen ik mijn ouders vertelde over mijn plannen om promotie onderzoek te gaan doen, waren zij allebei erg enthousiast en steunden mij hierin. Het sprak mijn vader bovendien erg aan dat ik een genetisch onderwerp had gekozen. Mijn vader was moleculair bioloog en promoveerde (cum laude) in 1966 in Nijmegen. Zijn vader, mijn grootvader, was zenuwarts en promoveerde in 1936 in Leiden. Ik beloofde mijn ouders dat ik het onderzoek zou afmaken en als oudste uit ons gezin, de lijn van 'Dr.' zou voortzetten. Mijn moeder was al sinds ik klein was mijn steun en toeverlaat en een voorbeeld voor mij, mede omdat zij arts was. Ik hoop dat mijn beide ouders ergens meekijken vandaag en trots op me zullen zijn. Dit schreef mijn moeder aan mij toen ik 8 jaar oud was:

Per dag steeds meer weten in onze moedertaal;
rij-rekenen, schrijven, spontaan een verhaal…
van communie tot konijn
vertel jij allerhande groot en klein.
En mams schrijft hier twee letterstijlen.
Zij helpt jou dagelijks bij te vijlen,
Zodat jij even<u>wichtig</u> mag gaan worden.
Dan kom alles op z'n tijd in orde.
(Uit het poëziealbum van Alberta, door mamma Aafje, Huis ter Heide, oktober 1985)

Lieve Dirk-Jan, we hebben een zware periode achter de rug samen, waarin we veel gescheiden van elkaar zijn geweest door jouw werk in Brussel, Uruzgan en nu in Tanzania. Hierdoor ben ik veel alleen met de kindjes geweest en dat was moeilijk voor ons allebei. Ook al was je vaak op kilometers afstand, je was altijd mijn steun en toeverlaat en ik houd van je. Op het moment dat ik dit schrijf staan wij met 1 been in het vliegtuig naar Tanzania om eindelijk samen een gezin te vormen. Ik hoop dat we een heel gelukkige tijd met elkaar tegemoet gaan in Afrika: ik kijk er ontzettend naar uit.

En tot slot, lieve, lieve Fien en Reiniertje. Jullie zijn mijn mooiste geschenk, ik houd ontzettend veel van jullie en voel me erg gelukkig als ik 's ochtends opsta en jullie stralende gezichtjes zie. Voor altijd jullie mamma,

Alberta
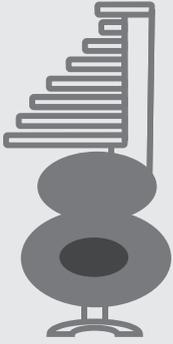
About the author

ABOUT THE AUTHOR

Alberta Thiadens was born on November 23rd 1976 in Utrecht. She graduated from the secondary school Montessori Lyceum Herman Jordan in Zeist. Subsequently she studied Medicine at the Erasmus University in Rotterdam and from her second year on, she worked as a medical student and team-leader at the psychiatric department of the Erasmus MC. During her studies she was an active member of several student committees, and participated in various research projects. In 1999 she travelled for two months to South-Africa to volunteer as a medical student in the Frere Hospital in East-London. In 2001 Alberta carried out primary health care in Tería, Panama, for the Panama Village Concept Project under supervision of Dr. M.S. Nazas. After obtaining her M.D. degree 'with distinction', she commenced in May 2003 her residency in Ophthalmology at the Erasmus MC in Rotterdam, headed by Prof.dr. G. van Rij. During three years she served as the ab-actis of the national association of residents in ophthalmology (LVAO). In 2006 the author assisted Dr. C.C.W. Klaver with her ophthalmogenetic consultations and this sparked her enthusiasm to start with her the PhD-project on cone disorders. During two years (2007-2009) Alberta worked in the laboratory with Prof.dr. F.P.M. Cremers and Dr. A.I. den Hollander at the Dept. of Human Genetics of the UMCN St Radboud in Nijmegen. She presented her work at several national and international meetings. In January 2011 the author completed her residency and moved, together with her husband Dirk-Jan and two little children, Josephine and Reinier, to Tanzania. Alberta will work as an ophthalmologist at the CCBRT Hospital in Dar es Salaam for at least the upcoming two years.
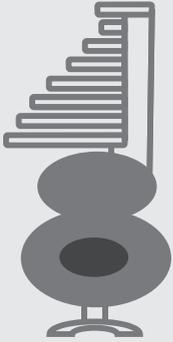
List of Publications

LIST OF PUBLICATIONS

1. **Thiadens AA**, Slingerland NWR, Roosing S, van Schooneveld MJ, van Lith-Verhoeven JJC, van Moll-Ramirez N, van den Born LI, Hoyng CB, Cremers FPM, Klaver CCW. Genetic etiology and clinical consequences of complete and incomplete achromatopsia. *Ophthalmology 2009;116:1984-9.*

2. **Thiadens AA**, den Hollander AI, Roosing S, Nabuurs SB, Zekveld-Vroon R, Collin RWJ, de Baere E, Koenekoop RK, van Schooneveld MJ, Strom TM, van Lith-Verhoeven JJC, Lotery AJ, van Moll-Ramirez N, Leroy BP, van den Born LI, Hoyng CB, Cremers FPM, Klaver CCW. Homozygosity mapping reveals *PDE6C* mutations in patients with early-onset cone photoreceptor disorders. *Am J Hum Genet. 2009;85:240-7.*

3. **Thiadens AA**, Roosing S, Collin RWJ, van Moll-Ramirez N, van Lith Verhoeven JJC, van Schooneveld MJ, den Hollander AI, van den Born LI, Hoyng CB, Cremers FPM, Klaver CCW. Comprehensive analysis of the achromatopsia genes *CNGA3* and *CNGB3* in progressive cone dystrophy. *Ophthalmology 2010;117:825-30.*

4. **Thiadens AA**, Somervuo V, van den Born LI, Roosing S, van Schooneveld MJ, Kuijpers RWAM, van Moll-Ramirez N, Cremers FPM, Hoyng CB, Klaver CCW. Progressive cone cell loss in achromatopsia. An imaging study using Spectral-Domain Optical Coherence Tomography. *Invest Ophthalmol Vis Sci. 2010;51:5952-7.*

5. **Thiadens AA**, Klaver CCW. Genetic testing and clinical characterization of patients with cone-rod dystrophy. *Invest Ophthalmol Vis Sci. 2010;51:6904-5.*

6. **Thiadens AA**, Slingerland NWR, Polling J, Visser GH, Klaver CCW. Cone-rod dystrophy can be a manifestation of Danon disease. (*Accepted*)

7. **Thiadens AA**, Soerjoesing GG, Florijn RJ, Tjiam AG, ten Brink JB, Buitendijk GHS, den Hollander AI, Bergen AAB, Klaver CCW. Clinical course of cone dystrophy caused by mutations in the *RPGR* gene. *(Under review)*

8. **Thiadens AA**, Phan TML, Zekveld-Vroon RC, Roosing S, Pott JR, van Schooneveld MJ, Lotery AJ, van Moll-Ramirez N, van Genderen MM, Boon CJF, den Hollander AI, Bergen AAB, de Baere E, Cremers FPM, van den Born LI, Leroy BP, Hoyng CB, Klaver CCW. Clinical course, etiology, and visual outcome in cone and cone-rod dystrophy. (*Under review*)

9. **Thiadens AA**, Hoyng CB, Simonsz HJ, Polling J, Bernaerts-Biskop R, van den Born LI, Klaver CCW. Accuracy of four commonly used color vision tests in individuals with cone disorders. (*Under review*)

10. Littink KW, van Genderen MM, Collin RW, Roosing S, de Brouwer AP, Riemslag FC, Venselaar H, **Thiadens AA**, Hoyng CB, Rohrschneider K, den Hollander AI, Cremers FP, van den Born LI. A novel homozygous nonsense mutation in *CABP4* causes congenital cone-rod synaptic disorder. *Invest Ophthalmol Vis Sci. 2009;50:2344-50.*

11. Azam M, Collin RW, Shah ST, Shah AA, Khan MI, Hussain A, Sadeque A, Strom TM, **Thiadens AA**, Roosing S, den Hollander AI, Cremers FPM, Qamar R. Novel *CNGA3* and *CNGB3* mutations in two Pakistani families with achromatopsia. *Mol Vis. 2010;16:774-81.*

12. Saelens IE, Bleyen I, Hillenaar T, **Thiadens AA**, Beekhuis WH, Remeijer L, Van Rij G. Long-term follow-up of hydrogel intracorneal lenses in 2 aphakic eyes. *J Cataract Refract Surg. 2010;36:2200-3.*

13. Said SAM, **Thiadens AA**, Fieren MJCH, Meijboom EJ, Van der Werf T, Bennink GBWE. Coronary artery fistulas. *Neth Heart J. 2002;10:65-78.*
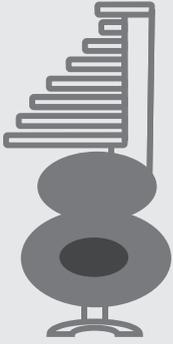
Abbreviations

ABBREVIATIONS

AAV	Adeno-associated virus
ACHM	Achromatopsia
AD	Autosomal dominant
AF	Autofluorescence
AR	Autosomal recessive
BCM	Blue cone monochromacy
BCVA	Best corrected Snellen visual acuity
CC	Connecting cilium
CD	Cone dystrophy
cGMP	Cyclic guanosine monophosphate
CNG-channel	Cyclic nucleotide gated channel
CNTF	Ciliary neurotrophic factor
CRD	Cone-rod dystrophy
Deutan	Green cone
DGGE	Denaturing gradient gel electrophoresis
DHA	Docosahexaenoic acid
DNA	Deoxyribonucleic acid
ERG	Electroretinogram
ETDRS	Early Treatment Diabetic Retinopathy Study
GCL	Ganglion cell layer
HRR	Hardy-Rand-Rittler test
IBD	Identity-by-descent
INL	Inner nuclear layer
IPL	Inner plexiform layer
IS	Inner segments
ISCEV	International Society for Clinical Electrophysiology of Vision
LCA	Leber congenital amaurosis
LCR	Locus control region
NFL	Nerve fiber layer
NGS	Next-generation sequencing
NMD	Nonsense-mediated decay
NO	Nitric oxide
ONL	Outer nuclear layer
OPL	Outer plexiform layer
OS	Outer segments
PCR	Polymerase chain reaction
PDE	Phosphodiesterase

Protan	Red cone
PTC	Premature termination codon
ROC	Receiver operating characteristic
ROS	Reactive oxygen species
RP	Retinitis pigmentosa
RPE	Retinal pigment epithelium
SD	Standard deviation
SD-OCT	Spectral domain optical coherence tomography
SE	Standard error
SNP	Single nucleotide polymorphism
STGD	Stargardt disease
Tritan	Blue cone
VA	Visual acuity
XL	X-linked